REMARKS

I. Formal Matters

A. Status of Claims

Claims 20-23 are pending. Withdrawn claims 1-16 and 19 have been canceled without prejudice.

Original claims 17 and 18 have been replaced with new claims 20-23. Support for claims 20-23 is found, for example, in original claims 17-18, in the description from page 53 to page 55, line 4, and in the description at page 54, lines 12-16.

B. Information Disclosure Statements

The Examiner signed and returned the PTO forms SB/08 that accompanied the Information Disclosure Statements filed on October 26, 2004 and on February 1, 2006.

The Examiner indicated that U.S. Patent No. 6,365,365 was not considered due to a typographical error on the SB/08 form. The Examiner further indicated that for JP 2001-340080, only pages 6 and 7 were considered.

Submitted herewith is an IDS that correctly cites U.S. Patent No. 6,365,365 and that includes a machine-generated English translation of JP 2001-340080, for consideration by the Examiner.

C. Drawings

At page 4 of the Office Action, the Examiner objected to the Drawings because Figures 1A, 1B, 1C, 6A and 6B were not described in the specification. Corrected Drawing sheets, or alternatively amendments to the specification to add the reference characters to refer to Figures 1A, 1B, 1C, 6A and 6B, were required.

In response, the description of the figures in the specification has been amended. Support for the amendments is found in the Figures themselves.

D. Specification

The Examiner objected to the abstract of the disclosure for containing more than 150 words.

In response, Applicant submits a new abstract.

II. Detailed Action

A. Claim Objections

Claims 17 and 18 were objected to for the following reasons:

1. The Examiner asserted that use of the term "ameliorating" to describe an effect on insulin resistance is ambiguous, as it is unclear to the Examiner if "ameliorating" means preventing, curing or treating.

The new claims use the word treating, thus rendering this objection moot.

2. The Examiner asserted that the use of the term "represented" in claim 17 was unclear, since the term encompasses modified polynucleotides.

The Examiner's position is not entirely clear. However, the new claims do not use the language objected to. Rather the new claims recite that the promoter either "comprises" or "consists of" the nucleotide sequence of SEQ ID NO: 26.

Thus this objection is rendered moot.

3. The Examiner considered the phrase "transcription promoter activity" ambiguous in the context of claim 17, because it was not clear to the Examiner whether SEQ ID NO:26 has promoter activity, alters promoter activity, or is controlled by a promoter.

This phrase is not used in the new claims, thus rendering this objection moot.

B. Claim Rejections - 35 U.S.C. §112

1. Claims 17-18 were rejected under 35 U.S.C. §112, first paragraph, as failing to comply with the written description requirement.

Applicant understands the Examiner to be raising the following points.

(a) The Examiner asserted that there are no definitions for "deleted, substituted, inserted."

The words "deleted, substituted and/or inserted," are not in the new claims.

(b) The Examiner contended that the specification does not show definitively that SEQ ID NO:26 contains the promoter region for the FLJ13111 gene because of the low levels of luciferase activity that are allegedly shown in the specification for the reporter gene construct.

As explained in the Rule 132 declaration submitted herewith, the data in Fig. 9 was incorrectly labeled as representing the ratio of the luciferase activity divided by the β-galactosidase activity. However, in fact, Fig. 9 contains the raw data, i.e., the luciferase activity without being normalized by the β-galactosidase activity. Nonetheless, the data in Example 14 (and Fig. 9) still prove that SEQ ID NO:26 has a promoter for FLJ13111.

As explained by the declarant, the reason is as follows. The method utilized in Example 14 is a method for searching for and identifying a promoter region for a certain gene by comparing the case of a vector which is obtained by inserting the test DNA fragment (DNA fragment to be checked for existence of a promoter region) into pGL3 with the case of pGL3 (a vacant vector containing no DNA fragment) as a control. Such a method itself was well known at the time of filing this application, as is clear from the references (1) to (6), for example submitted with the declaration. In these references, a plasmid obtained by inserting a DNA fragment into pGL3 was prepared and the promoter activity was measured by using, as an index, the reporter activity in the case of the DNA fragment-inserted plasmid in comparison with the pGL3 (vacant vector). If the reporter activity in the case of the DNA fragment-inserted plasmid is higher than the reporter activity in the case of pGL3 (vacant vector), this means that the inserted DNA fragment has a promoter region.

The declarant further explains that it is also common to show the relative activity values (XX fold by taking the value in the case of the vacant vector to be "1") and not to show the raw data itself or the values obtained by dividing by the transfection efficiency (cf. references (2), (4)-(7) submitted with the declaration).

(1) Masumoto N, Chen J, Sirotnak FM.

Regulation of transcription of the murine gamma-glutamyl hydrolase gene.

Delineation of core promoter A and the role of LYF-1, E2F and ETS-1 in determining tumor-specific expression.

Gene. 2002 May 29;291(1-2):169-76.

(cf. page 170, left column, 2,1. Analysis of promoter activity, Fig. 1)

(2) Tzeng SJ, Huang JD.

Transcriptional regulation of the rat Mrp3 promoter in intestine cells.

Biochem Biophys Res Commun. 2002 Feb 22; 291(2):270-7.

(cf. Fig. 2)

(3) Liang L, Major T, Bocan T.

Characterization of the promoter of human extracellular matrix metalloproteinase inducer (EMMPRIN).

Gene. 2002 Jan 9;282(1-2):75-86.

(cf. Fig. 3)

(4) Human Molecular Genetics, 2001, Vol. 10 No. 26, 3101-3109

(5) Biochemical and Biophysical Research Communication 286, 381-387 (2001) (cf. Fig. 2B)

(6) Gene 275 (2001), 93-101

(cf. Fig, 3)

(7) Endocrinology 142(9); 3987-3995, 2001

(cf. Fig. 4)

The declarant goes on to state that Fig. 9 shows that the reporter vector having the sequence of SEQ ID NO: 26 showed about 29 times higher luciferase induction in comparison with the control reporter vector pGL3 having no promoter (please compare the lane 1 (left side) and lane 2 (second lane from the left side)). Accordingly, the luciferase activity induced by SEQ ID NO: 26 is not low. The difference between the control reporter vector pGL3 and the reporter vector having the sequence of SEQ ID NO: 26 is significant (the P value is 0.000930527; ** (double stars), when * (single star) is 0.05 or less and ** (double star) is 0.01 or less).

Further, according to the declarant, the promoter activity is different among different genes and among different types of cells. It is not common in the field of reporter assays to use a known reporter as a control. As shown in the above cited references, it is common to use the value in the case where the vacant vector (e.g., pGL3) is taken as the baseline control.

The declarant also points out that the luciferase activity differs depending on the retaining time of the vector in cells, type of cell, conditions of the measurement apparatus, etc. The fact that the value differs depending on the cell type is described in the Promega's web sites (Legend in Fig. 6). As described above, it is quite common to carry out comparison against the vacant in under the same experiment. The Examiner compares the values obtained in different experiments in the same way, which is meaningless. For example, it is meaningless to compare the value available on Promega's web site with the values of this experiment.

Furthermore, as established by the Rule 132 declaration, when the data in Fig. 9 is divided by the β-galactosidase activity, the results are almost unchanged. That is, it is still correct that the value of lane 2 (the case in which a vector having the sequence of SEQ ID NO: 26 was used) was about 29 fold when the value of the lane 1 (the case of vacant vector) is taken as "1" (1.6495/0.0561 is about 29 and 1030,94/35.06 is about 29).

Accordingly, Applicant submits that Fig. 9 does evidence that SEQ ID NO:26 does include a promoter region relating to FLJ1311 gene transcription.

(c) The Examiner also seemed to object to the fact that the claimed screening assay would identify potential drugs that operate upstream of the transcriptional activation at SEQ ID NO:26, and that the claims would encompass any downstream effect of the increased gene expression. That is, the claims are not limited to drugs that interact with the promoter region itself or the transcriptional factors described in the specification.

However, it is not necessary to specify in the claims the precise mechanism of action of a test compound that might be identified, as the Examiner's remarks seem to suggest. In fact, this is the value of performing screening assays using cellular systems, as opposed to purely *in vitro* reconstituted systems (i.e. other relevant factors are present in cellular systems making the results more biologically relevant).

The Examiner is confused about SEQ ID NO: 26 (FLJ13111 promoter) and FLJ13111 (coding region).

Example 11 shows a method for detection wherein FLJ13111 functions as a co-factor when the gene expression of PPARγ (a protein factor which responds to the upstream region of

the gene) is induced by rosiglitazone (a low molecular weight ligand). Example 12 (and Fig. 11) show a method wherein the same assay system as in Example 11 is carried out in the presence of a test compound for the purpose of screening for a substance that promotes PPARγ's transcription inducing activity by FLJ13111. On the other hand, Example 14 discloses a promoter assay system. Accordingly, it shows an assay system for screening for a substance that promotes the amount of expression of FLJ13111, using a promoter for FLJ13111 (SEQ ID NO: 26).

As described above, Examples 11 and 12 show assay systems that are quite different from the assay system of Example 14. The methods of Examples 11 and 12 do not use a promoter for FLJ13111 (SEQ ID N0:26). That is, Example 14 is a method according to claims 20-23. Examples 11 and 12 are not methods according to claims 20-23, and should not be relied upon as such.

Thus, claims 20-23 do not require transcription factor (PPARγ-GAL4).

Examples of the substances that can be used as the test substance are described in the specification (page 55, lines 6-18).

It had been known to one skilled in the art that β-galactosidase, alkaline phosphatase, etc. in addition to CAT, LUC, GFP (cf. pages 38-39), etc, may be used as a reporter gene.

See, for example, the following reference (submitted herewith) in which β-galactosidase is used as the reporter gene:

Infection and Immunity, 1999, Vol. 67, No. 7, p. 3227-3235

(cf. p. 3229, right column, β-galactosidase assays.).

Also see the following reference (submitted herewith) in which alkaline phosphatase is used a the reporter gene:

Molecular and Cellular Biology, 1995, Vol. 15, No. 12, p. 6710-6719

(cf. page 6711, right column, lines 8-10).

In view of the above remarks, evidence presented in the form of a Declaration under 37 CFR § 1.132, literature evidence and new claims, the Examiner is requested, respectfully, to reconsider and remove this rejection.

2. At pages 9-16, claims 17-18 were rejected under 35 U.S.C. §112, first paragraph, as failing to comply with the enablement requirement.

Applicant understands the Examiner to be making the following points.

The Examiner acknowledges that the specification is enabling for a method of screening thiazolidinedione derivatives, rosiglitazone, and piolitazone for alterations in PPARγ/GAL4 chimera transcription factor activity via SEQ ID NO:26.

However, the Examiner believes that all other subject matter is not enabled on the basis of the following:

(a) The claimed method includes the use of modified promoter sequences, which the Examiner believes are not enabled;

(b) The claimed method includes various signaling molecules and transcription factors as potential drug targets or effector molecules,

(c) The involvement of the CENP-T protein (encoded by the FLJ13111 gene) in insulin resistance is allegedly not supported by the prior art or the present specification,

(d) The specification does not conclusively establish that SEQ ID NO: 26 contains the FLJ13111 promoter, and

(e) The specification does not establish that compounds that increase expression via the promoter of SEQ ID NO: 26 would ameliorate insulin resistance.

For the following reasons, this rejection is traversed and/or overcome.

The new claims do not recite any variants.

Further, as explained above and in the Rule 132 declaration, SEQ ID NO: 26 has a promoter region which is responsible for the transcription of FLJ13111.

The new claims do not recite "a method for screening a substance that treats insulin resistance." Rather, the new claims recite "a method for screening for a substance that increases gene expression."

As explained above, it was known when the present application was filed that genes such as GFP, β-galactosidase, CAT, alkaline phosphatase, etc. may be used as a reporter gene. This is clear from the literature. Thus, one skilled in the art reading the specification of the present application could readily use reporter genes other than luciferase in the assay system of the screening method of the claims.

When a certain promoter region is found, it is sufficiently enabled by conducting screening of various compounds for a drug that controls the expression amount of the gene by utilizing a general promoter assay system. For example, U.S. Patent No. 5,744,310 (filed in

1996) and U.S. Patent No. 5,853,985 (filed in 1995) (copies of both are submitted herewith) have claims relating to a method for screening various compounds for a drug that controls the expression of a gene by using a promoter assay system similar to Example 14 of the present invention (i.e., the method of claims 20-23). Furthermore, in these U.S. patents, the promoter assay is merely described. Actual screening tests were not conducted but these cases were allowed. Moreover, the following reference (submitted herewith) shows screening using a promoter assay system similar to that of Example 14 and discloses that 35 compounds (primary hits) as the compound which controls the expression level of a gene could be selected among 2000 compounds. Thus, use of the promoter assay system for the purpose of screening various unspecified compounds as a test substance was sufficiently enabled for one skilled in the art.

Rapisarda A, Uranchimeg B, Scudiero DA, Selby M, Sausville EA, Shoemaker RH, Melillo G., Identification of small molecule inhibitors of hypoxia-inducible factor 1 transcriptional activation pathway, Cancer Res. 2002 Aug 1;62(15):4316-24

(cf. Abstract, p. 4318, right column, lines 8-11, lines 15-18)

In view of the above remarks, literature evidence and new claims, the Examiner is requested, respectfully, to reconsider and remove this rejection.

C. Claims Rejections - 35 U.S.C. §103

1. At pages 17-18 of the Office Action, claims 17 and 18 were rejected under 35 U.S.C. §103(a) as being obvious over Doebber et al. (U.S. Patent No. 5,847,008) and Shimkets and Leach (WO 00/58473).

Specifically, the Examiner contended that Doebber teaches methods of screening for antidiabetic compounds using a PPARγ responsive reporter construct.

The Examiner acknowledged that Doebber does not teach SEQ ID NO: 26.

However, the Examiner contended that Shimkets and Leach teach SEQ ID NO: 26, and the use of this polynucleotide ("ORFX") in screening assays for testing compounds. The Examiner further contended that Shimkets and Leach teach that such may be important in diabetes.

The Examiner reasoned that one of ordinary skill in the art would have been motivated to modify the assay of Doebber by using the sequences taught by Shimkets and Leach, because such would be expected to be useful for identifying compounds having antidiabetic properties. The Examiner further contended that modifying screening assays to use new and unknown sequences is a mere design choice.

2. At pages 18 and 19 of the Office Action, claims 17-18 were rejected under 35 U.S.C. §103(a) as being obvious over Taniguchi and Mizukami (EP 1 057 896 A1 or WO 99/10532) and Shimkets and Leach.

Specifically, with respect to claim 17, the Examiner contended that Taniguchi teaches methods of screening agonists or antagonists for PPAR, which may be used as treatments for diabetes.

The Examiner acknowledged that Taniguchi does not teach SEQ ID NO: 26.

However, the Examiner contended that Shimkets and Leach teach SEQ ID NO: 26 in screening assays for testing compounds and teach that ORFXs may be important in various diseases including diabetes.

The Examiner reasoned that one having ordinary skill in the art would have been motivated to use the assay of Taniguchi with new and unknown sequences, because in the Examiner's opinion, such would be a mere design choice.

For the following reasons, the rejections are traversed, respectfully.

Although the Examiner asserted that Shimkets and Leach teach use of SEQ ID NO: 26 (e.g., CENP-T, C16orf56, FLJ43376 or FLJ13111) and ORFX (e.g., SEQ ID NO: 26) in screening assays, Shimkets and Leach do not disclose the sequence of SEQ ID NO: 26.

In the Examiner's search strategy and results (06-22-2006) available through PAIR, sequence searches for SEQ ID NO: 26 are shown and no hit is found for a sequence identical to SEQ ID NO: 26.

Accordingly, even if the references were combined, the claimed screening method would not be obtained.

In view of the above remarks and new claims, the examiner is requested, respectfully, to reconsider and remove the rejections.

In view of the above, reconsideration and allowance of this application are now believed to be in order, and such actions are hereby solicited. If any points remain in issue which the Examiner feels may be best resolved through a personal or telephone interview, the Examiner is kindly requested to contact the undersigned at the telephone number listed below.

The USPTO is directed and authorized to charge all required fees, except for the Issue Fee and the Publication Fee, to Deposit Account No. 19-4880. Please also credit any overpayments to said Deposit Account.

Respectfully submitted,

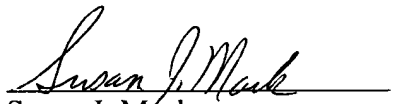

SUGHRUE MION, PLLC
Telephone: (202) 293-7060
Facsimile: (202) 293-7860

WASHINGTON OFFICE
23373
CUSTOMER NUMBER

Susan J. Mack
Registration No. 30,951

Date: December 1, 2006

INFECTION AND IMMUNITY, July 1999, p. 3227–3235 Vol. 67, No. 7
0019-9567/99/$04.00+0
Copyright © 1999, American Society for Microbiology. All Rights Reserved.

Promoter Architecture of the *Porphyromonas gingivalis* Fimbrillin Gene

HUA XIE* AND RICHARD J. LAMONT

Department of Oral Biology, University of Washington, Seattle, Washington 98195

Received 17 November 1998/Returned for modification 5 March 1999/Accepted 2 April 1999

Porphyromonas gingivalis **fimbriae can mediate adherence to many of the available substrates in the oral cavity. Expression of *P. gingivalis* fimbriae is regulated at the transcriptional level by environmental signals, such as temperature and hemin concentration. The arrangement of the upstream promoter and regulatory sequences required for transcription and control of the fimbrial structural gene (*fimA*) was investigated. Primer extension analysis demonstrated that the transcriptional start site of the *fimA* gene is located 41 bp upstream from the translational start codon. A region (*upf*) spanning 648 bp upstream of the start codon to 44 bp downstream of the translational start site was cloned upstream of a promoterless *lacZ* reporter gene. A series of deletion and base substitution mutations were then generated in the *upf* region. The constructs were introduced into the chromosome of *P. gingivalis*, and promoter activity measured by assaying levels of β-galactosidase. The results showed that *fimA* contains sequences resembling σ^{70} promoter consensus sequences, consisting of a −10 region (TATGAC) located at −18 to −23 and a −35 region (TTGTTG) located at −41 to −46 from the transcriptional start point. The AT-rich upstream sequences spanning bases −48 to −85 and bases −90 to −240 were required for full expression of the *fimA* gene, indicating the existence of positive regulation regions. Moreover, the −48 to −64 region may constitute an UP element, contributing to promoter activity in *P. gingivalis*. Thus, our data suggest that the *P. gingivalis fimA* gene has a transcription complex consisting of −10 and −35 sequences, an UP element, and additional AT-rich upstream regulatory sequences.**

Porphyromonas gingivalis is a primary causative agent in severe manifestations of periodontal disease, one of the most common bacterial infections in developed countries. Colonization of the periodontal area by *P. gingivalis* is facilitated by adherence to a variety of oral surfaces such as epithelial cells, extracellular matrix components, proline-rich proteins and statherin in enamel salivary pellicle, and antecedent plaque bacteria such as *Streptococcus gordonii* (9, 10, 12, 16). Fimbriae, which are among the major adhesins of *P. gingivalis*, are comprised of a major structural subunit protein with a molecular mass of approximately 43 kDa (fimbrillin, FimA). Much evidence suggesting an important role for *P. gingivalis* fimbrillin in pathogenicity has accumulated. In addition to directly mediating adhesion, fimbrillin-mediated attachment of *P. gingivalis* to gingival epithelial cells induces cytoskeletal rearrangements and modulates intracellular calcium-dependent signalling pathways, events that result in internalization of the bacteria within the epithelial cells (11, 15, 37). Fimbrillin has important immunomodulating properties and can stimulate the production of proinflammatory cytokines (such as interleukin-1, interleukin-6, and tumor necrosis factor alpha) in human monocytes and polymorphonuclear leukocytes (23, 24). Intracellular tyrosine phosphorylation-dependent signal transduction appears to be one of the targets of fimbrillin-induced cytokine production (21, 24). As a major surface protein, fimbrillin is strongly antigenic, and antifimbrillin immunoglobulin G titers are much higher in patients with adult periodontitis than in healthy individuals (25). The extent to which such antibodies contribute to protection or to antibody-mediated tissue destruction remains to be determined. Fimbriae are, therefore, considered pivotal in the multistep pathogenesis of periodontal disease. Indeed, insertional inactivation of the *fimA* gene, with concomitant loss of fimbrial production, results in a phenotype significantly less able to cause periodontal bone loss in the gnotobiotic rat model (18). Furthermore, immunization with purified fimbriae confers protection against periodontal destruction in gnotobiotic rats (7).

Many genes that are important for bacterial virulence are under tight transcriptional control and are regulated according to prevailing environmental conditions (6). Fimbrial genes from a variety of gram-negative bacteria are an illustrative model of how bacteria sense and respond to environmental cues. The fimbriae of *P. gingivalis*, however, lack any significant homology to fimbrial proteins from other bacteria and appear to constitute a unique class of gram-negative fimbriae (5). Despite the fact that the *fimA* gene was cloned more than a decade ago, little is known about gene expression and promoter architecture. Indeed, RNA polymerase binding sites and other regulatory sequences have not been functionally defined for any genes of this important oral anaerobe.

We have previously reported that expression of the *fimA* gene is regulated at the transcriptional level in *P. gingivalis*, as determined by analysis of a *fimA:lacZ* promoter-reporter fusion (38). Changes in environmental conditions, such as temperature and hemin concentration, were found to alter the level of *fimA* expression. Correspondingly, these small environmental fluctuations also modulated bacterial binding and invasive abilities. To further understand fimbrillin expression at the molecular level, we have generated a series of mutations in the *fimA* promoter region to determine specific DNA sequences recognized by the transcriptional machinery. In the study presented here, we demonstrate the characteristics and organization of the *P. gingivalis fimA* promoter. Our findings indicate that the *P. gingivalis fimA* gene contains both a σ^{70}-like promoter sequence that carries out basal-level transcription and *cis*-acting regulatory elements required for maximal transcription of the *fimA* gene.

* Corresponding author. Mailing address: Oral Biology, Box 357132, University of Washington, Seattle, WA 98195-7132. Phone: (206) 543-5477. Fax: (206) 685-3162. E-mail: hxie@u.washington.edu.

TABLE 1. Bacterial strains and plasmids used in this study

Strain or plasmid	Relevant characteristics[a]	Source or reference
Strains		
P. gingivalis		
33277	Type strain from ATCC	This laboratory
UPF	Derivative of 33277, *upf:lacZ* gene, Em^r	This study
MPF10	Derivative of 33277, *mpf10:lacZ* gene, Em^r	This study
MPS10	Derivative of 33277, *mps10:lacZ* gene, Em^r	This study
MPF35	Derivative of 33277, *mpf35:lacZ* gene, Em^r	This study
MPS35	Derivative of 33277, *mps35:lacZ* gene, Em^r	This study
MP58	Derivative of 33277, *mp58:lacZ* gene, Em^r	This study
MP150	Derivative of 33277, *mp150:lacZ* gene, Em^r	This study
MP60	Derivative of 33277, *mp60:lacZ* gene, Em^r	This study
MP59	Derivative of 33277, *mp59:lacZ* gene, Em^r	This study
E. coli DH5α	*endA1 hsdR17 supE44 thi-1 recA gyrA96 relA1* Δ(*lacZYA-argF*) *U169*λ-ϕ80 *dlacZ* Δ*M15*; recipient for recombinant plasmids	BRL
Cloning vectors		
pTZBg21.1	Containing a 2.5-kb *Sac*I DNA fragment with the *fimA* gene, Am^r	32
pUC19	*E. coli* cloning vector, Am^r	BRL
pDN19lac	Contains 3.6-kb *Bam*HI-*Sal*I fragment containing promoterless *lacZ* gene with ribosome binding site	35
pJRD215	Wide-host-range cosmid vector, Km^r Sm^r Mob^+, unable to replicate in *P. gingivalis*	28
pBF4	Contains 3.8-kb *Eco*RI fragment in Tn*4351* carrying two antibiotic resistance genes: Tc^r expressed in *E. coli* and Em^r expressed in *P. gingivalis*	33
R751	IncP plasmid used to mobilize vectors from *E. coli* to *Bacteroides* recipient, Tp^r Tra^+	28
pCR2.1-TOPO	Linearized plasmid with single 3′ dT residues, Km^r	Invitrogen
Recombinant plasmids		
pUPF1	*P. gingivalis fimA* promoter region (*upf*) containing sequence from −606 to +86 in plasmid pCR2.1-TOPO, Am^r Km^r	This study
pUPF5	*upf:lacZ* gene in pJRD215 with a 3.8-kb *Eco*RI fragment from Tn*4351*, Tc^r Km^r Sm^r	This study
pMPF101	*upf:lacZ* gene in pUC19 with 3-base change from TAT to CCG at positions −23 to −21 (*mpf10:lacZ*), Am^r	This study
pMPF103	*mpf10:lacZ* gene in pJRD215 with a 3.8-kb *Eco*RI fragment from Tn*4351*, Tc^r Km^r Sm^r	This study
pMPS101	*upf:lacZ* gene in pUC19 with 3-base change from TAA to GCC at positions −11 to −9 (*mps10:lacZ*), Am^r	This study
pMPS103	*mps10:lacZ* gene in pJRD215 with 3.8-kb *Eco*RI fragment from Tn*4351*, Tc^r Km^r Sm^r	This study
pMPF351	*upf:lacZ* gene in pUC19 with 3-base change from TTG to CCA at positions −46 to −44 (*mpf35:lacZ*), Am^r	This study
pMPF353	*mpf35:lacZ* gene in pJRD215 with 3.8-kb *Eco*RI fragment from Tn*4351*, Tc^r Km^r Sm^r	This study
pMPS351	*upf:lacZ* gene in pUC19 with 3-base change from TGG to CAC at positions −43 to −41 (*mps35:lacZ*), Am^r	This study
pMPS353	*mps35:lacZ* gene in pJRD215 with 3.8-kb *Eco*RI fragment from Tn*4351*, Tc^r Km^r Sm^r	This study
pMP1501	*upf:lacZ* gene in pCR2.1-TOPO with 150-bp deletion from −240 to −90 (*mp150:lacZ*), Am^r	This study
pMP1504	*mp150:lacZ*, gene in pJRD215 with 3.8-kb *Eco*RI fragment from Tn*4351*, Tc^r Km^r Sm^r	This study
pMP601	*mp150:lacZ* gene with 15-bp deletion from −85 to −71 (*mp60:lacZ*) in pUC19, Am^r	This study
pMP603	*mp60:lacZ* gene in pJRD215 with 3.8-kb *Eco*RI fragment from Tn*4351*, Tc^r Km^r Sm^r	This study
pMP591	pMP601 with 17-bp deletion from −64 to −48 (*mp59:lacZ*), Am^r	This study
pMP593	*mp59:lacZ* gene in pJRD215 with 3.8-kb *Eco*RI fragment from Tn*4351*, Tc^r Km^r Sm^r	This study
pMP581	*upf:lacZ* gene in pUC19 with 16-bp deletion from −23 to −8 (*mp58:lacZ*), Am^r	This study
pMP583	*mp58:lacZ* gene in pJRD215 with 3.8-kb *Eco*RI fragment from Tn*4351*, Tc^r Km^r Sm^r	This study

[a] Km^r, Sm^r, Tc^r, Em^r, Tp^r, and Am^r, resistance to kanamycin, streptomycin, tetracycline, erythromycin, trimethoprim, and ampicillin; Mob^+, can be mobilized; Tra^+, capable of self-transfer.

MATERIALS AND METHODS

Bacteria and plasmids. Bacterial strains and plasmids used in this study are listed in Table 1. *P. gingivalis* 33277 and its derivatives were grown in Trypticase soy broth (TSB; BBL, Cockeysville, Md.) or on 1.5% TSB agar plates, supplemented with yeast extract (Difco, Detroit, Mich.) (1 mg/ml), hemin (5 μg/ml), and menadione (1 μg/ml), at 37°C in an anaerobic (85% N_2, 10% H_2, 5% CO_2) chamber. All *P. gingivalis* strains harboring *fimA:lacZ* constructs were grown in TSB containing erythromycin (20 μg/ml). *Escherichia coli* DH5α was used as the host strain for recombinant plasmids and grown in L broth with appropriate antibiotics: ampicillin (100 μg/ml), kanamycin (50 μg/ml), trimethoprim (200 μg/ml), and tetracycline (10 μg/ml).

DNA and RNA manipulations. *P. gingivalis* chromosomal DNA was extracted by the procedure described by Sambrook et al. (31). All plasmid DNA was isolated by using a Promega miniprep kit and analyzed by 0.8% agarose gel electrophoresis. Restriction enzymes for DNA digestion were purchased from Gibco BRL (Grand Island, N.Y.). DNA fragments were purified from agarose gels by using a Geneclean kit (Bio 101, Inc., Vista, Calif.). *P. gingivalis* total RNA was isolated by using a TRIzol kit (Gibco BRL), and DNA contamination was eliminated following digestion with DNase I (Gibco BRL). RNA was visualized on 1.0% ethidium bromide-stained formaldehyde-agarose gels and quantitated spectrophotometrically.

DNA sequence analysis. DNA sequencing was conducted by the dideoxy-chain termination procedure using Sequenase version 2 (U.S. Biochemical Corp., Cleveland, Ohio). For determination of the upstream sequence of the *fimA* gene, the template was plasmid pTZBg21.1 containing a 2.5-kb *Sac*I *fimA* DNA fragment. For confirmation of the mutations in the *fimA* promoter region, the *upf:lacZ* fragment was subcloned into pUC19, and the recombinant plasmid was then used as the template. The synthetic oligonucleotide primers used in sequencing are described in Table 2.

TABLE 2. Synthetic oligonucleotide primers

Primer	Sequence (5′→3′)[a]	Position	Purpose
PE1	GCTGGTCCTCAATACCACGCTGATGGTGGC	+30 to +60	Primer extension
PE3	AGCATTATCTAGAACCTCCTTAGGATCCCG	*lacZ* gene	Primer extension
FS1	ATTGTGTTGTGCTCCGGGCTGGCCTTGCTG	−163 to −193	DNA sequencing
FS2	GATAGCTCTTGCGCTACGGGCTAAA	−422 to −446	DNA sequencing
FP1	GGAATTCCGAGCTATCGATGGCGGGTCTCT *Eco*RI	−605 to −628	Used with FP3 in PCR to obtain UPF fragment
FP3	CGGGATCCCGCCAACTCCAAAAGCACGATTCGA *Bam*HI	+87 to +61	Used with FP1 in PCR to obtain UPF fragment
MPF10	CTTGCTGCTCTTGC*CCG*GACAGCTTGTAAC	−36 to −6	Unique-site elimination mutagenesis
MPS10	GCTATGACAGCTTG*GCCC*AAAGACGGCGAGGC	−24 to +8	Same as above
MPF35	CAAAGTTTTTC*CCA*TTGGGACTTGCTGCTC	−55 to −25	Same as above
MPS35	CAAAGTTTTTCTTG*CAC*GGACTTGCTGCTC	−55 to −25	
MP58	GTTTTTCTTGTTGGGACTTGCTGCTCTTGCAAAGA CAACGAGGCAGAACCCGTTACAG	−51 to +20	Deletion from −22 to −7
MP59	GTTGTTGGGCTTGCATAATTCACCGAGATGCTTG TTGGGACTTGCTGCTCTTGCTATGA	−69 to −16	Deletion from −63 to −45
MP60	GGATGTTGTTGGGCTTGCATAATTCACCGAGATC AAAAAAACAAAGTTTTTCTTGTTGGG	−89 to −69	Deletion from −84 to −69
lacZ2	GAAAGGGGGATGTGCTGCAAGGCGATTAAG	Corresponding to *lacZ*	Testing primer
MPF3	TGTTGGGACTTGCTGCTCTTGCCCG		Testing primer for MPF10
MPS3	ACTTGCTGCTCTTGCTATGACAGCTTGGCC		Testing primer for MPS10
TMPF35	CAAAGTTTTTCCCAT		Testing primer for MPF35
TMPS35	AGTTTTTCTTGCACG		Testing primer for MPS35
MP16	CTTGCTGCTCTTGCAA		Testing primer for MP58
MP15	ATTCACCGAGATGCT		Testing primer for MP59
MP150	GCTTATGGATGTTGTTGGGCTTGCATATTCA		Testing primer for MP150
MP14	TGGGCTTGCATAATTCACCG		Testing primer for MP60

[a] Restriction sites are underlined; substituted nucleotides are italicized.

Primer extension analysis. The transcriptional start site was investigated by primer extension. The avian myeloblastosis virus reverse transcriptase primer extension system (Promega, Madison, Wis.) was used, with modifications. Primers PE1 and PE3 (Table 2) were 5′ end labeled with [γ-^{32}P]ATP (3,000 μCi/mmol; NEN, Boston, Mass.) with T4 polynucleotide kinase and annealed with approximately 50 μg of total RNA at 58°C for 20 min. The resulting heteroduplex was extended with avian myeloblastosis reverse transcriptase at 42 or 50°C for 30 min. The length of the extension was measured by polyacrylamide gel (8%) electrophoresis calibrated with a sequencing reaction using the same primer.

PCR and Southern blot analyses. PCR mixtures contained 10 pmol of template DNA, 30 pmol of each primer, 1.5 mM $MgCl_2$, 10 mM deoxynucleoside triphosphate, and 5 U of *Taq* DNA polymerase (Bethesda Research Laboratories [BRL]). The amplification was performed in a thermal cycler (Techne) at 94°C for 45 s, 42°C for 1 min, and 72°C for 1 min for a total 30 cycles, followed by 10 min of elongation at 72°C. Southern blotting was performed by using the PhotoGene detection system (BRL), with minor modifications. After UV cross-linking, the membrane was hybridized with the biotin-labeled 1.4-kb *fimA* fragment at 65°C overnight.

Construction of pUPF5 and derivatives carrying different mutations. Standard recombinant DNA techniques were used in all plasmid construction (31). The *fimA* upstream region (*upf*) between nucleotides −648 and +44 from the translational initiation codon was amplified by PCR using *P. gingivalis* chromosomal DNA as the template, FP1 as the forward primer, and FP3 as the reverse primer (Table 2). Primers were tagged with *Eco*RI and *Bam*HI restriction sites, respectively. The PCR product was cloned into pCR2.1-TOPO as instructed by the manufacturer (Invitrogen), creating pUPF1. To generate the *upf:lacZ* gene fusion, the *upf* fragment was cloned into plasmid pDN19lac (35), which contains a promoterless *lacZ* gene. A 4.3-kb *Eco*RI and *Bam*HI *upf:lacZ* fragment of the resulting plasmid pUPF2 was cloned into the broad-host-range vector pJRD215 to generate pUPF4. A 3.8-kb *Eco*RI fragment of Tn*4351* with Tc^r and Em^r genes was then cloned into pUPF4 to create pUPF5. For pUPF5 derivatives (with the exception of pMP1504), the *upf:lacZ* fragment from pUPF2 was cloned into pUC19 to generate pUPF3 and a series of site-specific mutations was generated (see below) prior to cloning into pJRD215.

Site-specific mutagenesis. An 150-bp deletion mutation (MP150 [Fig. 2B]) was generated by exploiting unique restriction sites in pUPF1. After digestion with *Nde*I and *Ssp*I, the linearized plasmid with an *Nde*I overhang was blunt ended by the large fragment of DNA polymerase I and religated with T4 DNA ligase. Site-specific small deletion and base substitution mutations were generated by using a unique-site elimination mutagenesis kit (Pharmacia Biotech, Piscataway, N.J.). The general procedure was to use a pair of primers for each mutation; one was to introduce the desired mutation, and the other was a selection primer which could change a unique *Sca*I site to *Mlu*I in pUPF3. When both primers annealed to the same strand of the denatured pUPF3, a new strand was synthesized and selected by digestion of reaction mixture with *Sca*I. The authenticity of the mutated sequence was verified by DNA sequencing and PCR analysis. To identify mutations by using PCR, specific pairs of primers for each mutation were designed. The forward primer corresponded to the *fimA* promoter sequence except for the last two or three nucleotides at the 3′ end matching the mutated bases; the reverse primer was complementary to the *lacZ* gene. The results from both DNA sequencing and PCR analyses were always consistent.

Introduction of the *upf:lacZ* fusion and its derivatives into *P. gingivalis*. The *upf:lacZ* fusion was introduced into *P. gingivalis* by conjugal transfer of the suicide plasmid pUPF5 from *E. coli*, resulting in integration of the fusion construct into the chromosome by a Campbell insertion. The conjugation experiments were performed with *E. coli* DH5α containing plasmids pUPF5 (or derivatives) and R751 as the donor and with *P. gingivalis* as the recipient. Briefly, *E. coli* DH5α containing pUPF5 and R751 was cultured aerobically in L broth for 2 to 4 h to an A_{600} of 0.2, and *P. gingivalis* was grown anaerobically in TSB medium for 8 h to an A_{600} of 0.3 (early logarithmic growth). The conjugation mixture had a donor-to-recipient ratio of 0.2 and was spotted onto a 0.45-μm-pore-size HAWP filter (Millipore, Bedford, Mass.). The mating was performed aerobically on TSB sheep blood plates for 16 h and then anaerobically in TSB for 8 h. Transconjugants were selected on TSB blood plates containing gentamicin (100 μg/ml) and erythromycin (20 μg/ml). Since *P. gingivalis* is naturally resistant to this concentration of gentamicin and *E. coli* is naturally sensitive to gentamicin, colonies growing on the antibiotic plates were *P. gingivalis* with pUPF5 integrated into the chromosomal DNA.

To confirm that the *P. gingivalis* transconjugants possessed a chromosomal integration of pUPF5 immediately upstream of the *fimA* gene, a Southern blot analysis was performed. *P. gingivalis* chromosomal DNA was digested with *Bam*HI and analyzed by Southern hybridization with a 1.4-kb *fimA* fragment (generated by PCR and labeled with biotin) as the probe. The hybridized probe was detected by the Photogene nucleic acid detection system (BRL).

β-Galactosidase assays. Expression of the *lacZ* gene under control of the *fimA* promoter was measured by a spectrophotometric β-galactosidase assay with *o*-nitrophenyl galactosidase as the substrate, according to the standard protocol of Miller (19) as described previously (38). The recombinant strains of *P. gingivalis* were cultured anaerobically in TSB under a variety of defined conditions. Bacteria were recovered from late log phase (except where noted) and tested at an optical density at 600 nm of 0.4 to 0.6. Since *P. gingivalis* does not normally ferment lactose or other sugars, background levels of enzyme activity were low.

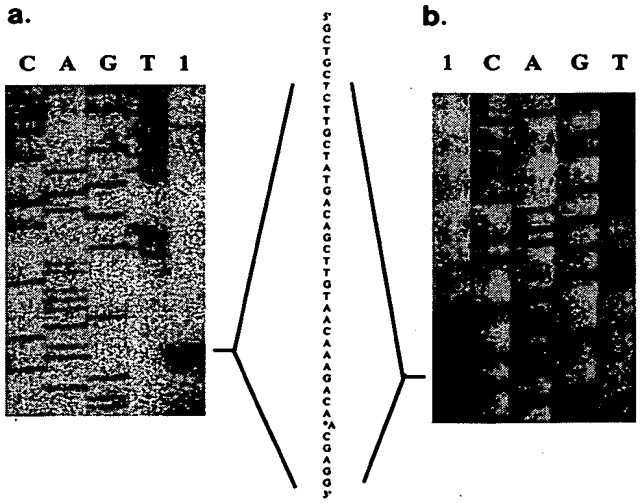

FIG. 1. Transcriptional start site mapping of *P. gingivalis fimA*, using primers PE1 (a) and PE3 (b) Lanes: 1, primer extension with *P. gingivalis* 33277 (a) and *P. gingivalis* UPF (b) RNAs as templates; G, T, C, and A, nucleotide-specific sequencing reactions.

To ensure that any differences in β-galactosidase activity were not the result of a spontaneous chromosomal mutation, assays were performed on at least two independent isolates of each strain.

Mobility shift DNA-binding assay. A 280-bp DNA fragment containing the wild-type *fimA* promoter (−44 to +236) was used as the probe and prepared by PCR. *E. coli* RNA polymerase (holoenzyme) saturated with σ^{70} was purchased from Epicentre Technologies (Madison, Wis.). The experiments were conducted with a Bandshift kit (Pharmacia Biotech). Briefly, the DNA fragment was digested with *Eco*RI and labeled with [α-^{32}P]dATP (3,000 μCi/mmol; NEN), using Klenow enzyme. For the protein-DNA reaction, 1 μg of ^{32}P-labeled DNA, 0.5 μg of RNA polymerase, and 3 μg of unrelated DNA (calf thymus DNA) were mixed and incubated at room temperature for 20 min; the mixture was then loaded onto a 5% nondenaturing polyacrylamide gel and electrophoresed in 0.5× Tris-borate-EDTA buffer at 10 V/cm. Finally, the gel was dried and exposed to X-ray film at −70°C.

RESULTS

Determination of the transcriptional start site. The transcription initiation site of the *fimA* gene was investigated by primer extension analysis. RNA isolated from *P. gingivalis* 33277 was analyzed with primer PE1, and RNA from the *upf:lacZ*-containing strain UPF was analyzed with primer PE3 (corresponding to sequence of the *lacZ* gene) (Table 2); two identical extension products were detected (Fig. 1). Therefore, the transcriptional start site was mapped to an A residue 41 bp upstream of the translational initiation codon. Examination of the upstream sequence revealed potential sequences recognized by σ^{70}-dependent RNA polymerase (−10 sequences TATGAC and TAACAA; −35 sequence TTGTTG). The functionality of these sequences was examined by site-specific mutagenesis (see below).

Development of promoter fusion reporters. We have previously demonstrated (38) that sequences required for the promotion of transcription of the *fimA* gene reside within 236 bp upstream of the translational start site. However, to facilitate integration of mutated *fimA:lacZ* constructs (especially the deletion mutations) into *P. gingivalis* chromosomal DNA and to investigate the presence of additional upstream regulatory sequences, a longer upstream region was used in this study. As shown in Fig. 2A and 3, a 692-bp *Eco*RI and *Bam*HI fragment was amplified by PCR, fused to a promoterless *lacZ* gene, and integrated into *P. gingivalis* chromosomal DNA. The *fimA* promoter region used in this study thus spanned 648 bp upstream to 44 bp downstream of the translational start codon. This DNA fragment was designated *upf* and contained sufficient homologous sequence to permit integration into the chromosome of *P. gingivalis*.

Construction of *upf:lacZ* and its derivatives. The strategy for identification of *cis*-acting regulatory elements of the *fimA* gene was to define the affect of DNA sequence alteration on *fimA* promoter activity in *P. gingivalis*. For this purpose, the

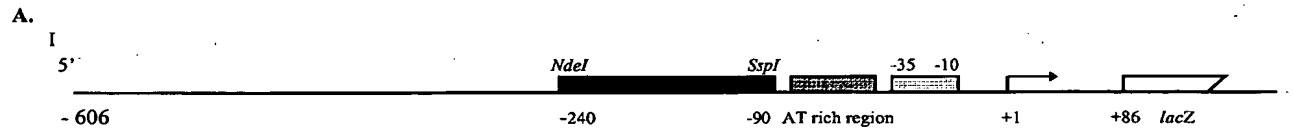

B.

Promoter and its derivatives

	-90 -84 -46 -23 -11 +1
UPF	TTAGAAAACAATATTCACCTTTTAAAACAAAAACGAGATGAAAAAAACAAAGTTTTTCTTGTTGGGACTTGCTGCTCTTGCTATGACAGCTTGTAACAAAGACAACG
MPF10	TTAGAAAACAATATTCACCTTTTAAAACAAAAACGAGATGAAAAAAACAAAGTTTTTCTTGTTGGGACTTGCTGCTCTTGCCCGGACAGCTTGTAACAAAGACAACG
MPS10	TTAGAAAACAATATTCACCTTTTAAAACAAAAACGAGATGAAAAAAACAAAGTTTTTCTTGTTGGGACTTGCTGCTCTTGCTATGACAGCTTGGCCCAAAGACAACG
MPF35	TTAGAAAACAATATTCACCTTTTAAAACAAAAACGAGATGAAAAAAACAAAGTTTTTCCCATTGGGACTTGCTGCTCTTGCTATGACAGCTTGTAACAAAGACAACG
MPS35	TTAGAAAACAATATTCACCTTTTAAAACAAAAACGAGATGAAAAAAACAAAGTTTTTCTTGCACGGACTTGCTGCTCTTGCTATGACAGCTTGTAACAAAGACAACG
MP58	TTAGAAAACAATATTCACCTTTTAAAACAAAAACGAGATGAAAAAAACAAAGTTTTTCTTGTTGGGACTTGCTGCTCTTGC —— Δ_{16} —— AAAGACAACG
	-240 -90
MP150	TA — Δ_{150} — ATTCACCTTTTAAAACAAAAACGAGATGAAAAAAACAAAGTTTTTCTTGTTGGGACTTGCTGCTCTTGCTATGACAGCTTGTAACAAAGACAACG
MP60	TA — Δ_{150} — ATTCACC —— Δ_{15} —— GAGATGAAAAAAACAAAGTTTTTCTTGTTGGGACTTGCTGCTCTTGCTATGACAGCTTGTAACAAAGACAACG
MP59	TA — Δ_{150} — ATTCACC —— Δ_{15} —— GAGATG —— Δ_{17} —— CTTGTTGGGACTTGCTGCTCTTGCTATGACAGCTTGTAACAAAGACAACG

FIG. 2. Core promoter region of the *fimA* gene. (A) Schematic map of the *fimA* promoter region fused with the *lacZ* reporter gene. (B) Sequences of the core promoter region of *fimA* with and without mutations. UPF represents wild-type promoter sequence; the sequences subsequently mutated are underlined and in boldface. The sequences of eight mutated promoters are also shown. Base substitutions are represented by underlined and bolded letters and deletion mutations are shown by the symbol Δ, with the number representing deleted base pairs.

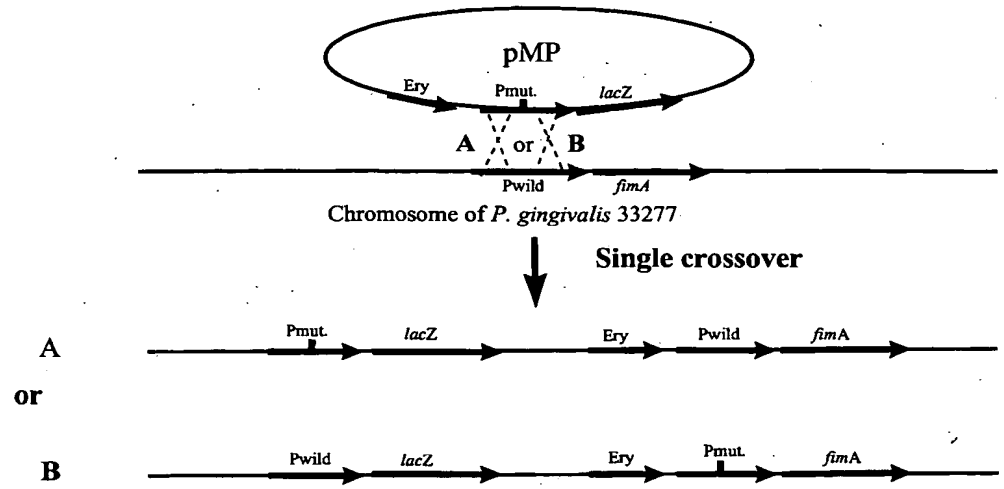

FIG. 3. Homologous recombination between pUPF5 or its derivatives (pMP) and the *P. gingivalis* chromosome. The thicker lines represent the DNA fragment containing the *fimA* gene, *fimA* promoter region, *lacZ* gene, and erythromycin resistance gene (Ery). (A) The homologous recombination occurs upstream of the mutation. (B) The recombination occurs downstream of the mutation. Pmut. and Pwild, mutant and wild-type promoters, respectively.

fimA upstream region (*upf*) and its eight derivatives (Fig. 2B) with mutations generated in *upf* were individually fused with a promoterless *lacZ* gene and returned to *P. gingivalis*. The upstream region of the transcriptional start site determined by primer extension possesses potential −10 sequences centered at −8/−9 (TAACAA), −11/−12 (TTGTAA) or −20/−21 (TA TGAC) and −35 sequences centered at −33/−34 (TTGCTG) or −43/−44 (TTGTTG). Thus, primers MPF10 and MPS10 were used in site-specific mutagenesis to generate two modified *fimA* promoters: one with a conversion of TAT to CCG at positions −23 to −21, and one with a conversion of TAA to GCC at −11 to −9. For delimiting the −35 sequence, primers MPF35 and MPS35 were designed to convert TTG at −46 to −44 to CCA and TTG at −43 to −41 to CAC, respectively. In each case, the impact of the mutations on *lacZ* expression would depend on the requirement of sequence for full promoter activity. A deletion mutation was also generated with the removal of bases −23 to −8 (MP58). This deletion mutation would decrease *fimA* promoter activity only partially, if additional upstream promoters were present.

We also constructed a series of upstream deletion mutations in order to detect any regulatory sequence(s) that contributes to *fimA* expression. The first large deletion mutation (MP150) entailed removal of 150 bp from −240 to −90. An AT-rich sequence located between −85 to −48 was also selected as a candidate regulatory region. Further deletions in this AT-rich sequence resulted in a double (MP60)- and triple (MP59)-deletion mutations in the *upf* region.

Selection of *P. gingivalis* strains with fused genes. The *upf*:*lacZ* gene and its derivatives were introduced into *P. gingivalis* by conjugation between *E. coli* DH5α and *P. gingivalis* 33277. Plasmid pJRD215 carrying the *upf*:*lacZ* gene (pUPF5) or its derivatives cannot replicate in *P. gingivalis* due to the lack of a functional origin of replication. Southern blot analysis confirmed the integration of pUPF5 and its derivatives. Single crossover of pUPF5 could result in two genomic configurations (depicted in Fig. 3), depending on whether the crossover occurs proximal or distal to the mutation. If recombination occurs upstream of the mutation, the mutated *fimA* promoter would drive the *lacZ* gene (Fig. 3A). In contrast, the *lacZ* gene would be under control of the intact wild-type *fimA* promoter, leaving the mutated *fimA* promoter with the *fimA* structure gene, if recombination occurred downstream of the mutation (Fig. 3B). For the purpose of this study, *P. gingivalis* strains with the promoterless *lacZ* gene under control of the mutated *fimA* promoter (Fig. 3A) were required. Selection for the desired isolates was accomplished by PCR with a forward primer corresponding to the mutated promoter and a reverse primer (lacZ2) corresponding to the *lacZ* gene. A PCR product of the correct size could be obtained only when the mutated *fimA* promoter was directly upstream of the *lacZ* gene. The PCR results were confirmed by Southern blot analysis for the large deletion mutation, as shown in Fig. 4 for *P. gingivalis* MP150. The chromosomal DNAs from three isolates of *P. gingivalis* MP150 were used as templates, and FP1 (forward primer) and laCZ2 (reverse primer) were used for PCR analysis. Agarose gel electrophoresis shows two sizes of PCR products (Fig. 4a). The size (about 800 bp) of the larger product (lanes 2 and 4) indicated that the *lacZ* gene had a wild-type *fimA* promoter region, whereas the smaller fragment (lane 3) of 650 bp resulted from a 150-bp deletion. Thus, the DNA template used in lane 3 was from the mutant strain, and this was used in sub-

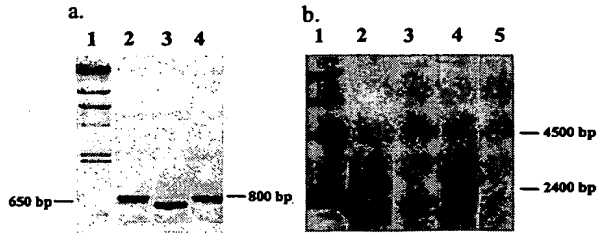

FIG. 4. PCR and Southern blot analyses of *P. gingivalis* MP150. (A) Chromosomal DNAs from three isolates of *P. gingivalis* MP150 analyzed by PCR with forward primer FP1 and reverse primer lacZ2. Lanes: 1, DNA standard; 2 to 4, isolates of *P. gingivalis* MP150. (B) DNA samples analyzed by Southern blotting. DNA was digested with *Ssp*I and *Hin*dIII and probed with a 1.4-bp *fimA* fragment. Lanes: 1, DNA standard; 2, UPF; 3 to 5, isolates of MP150.

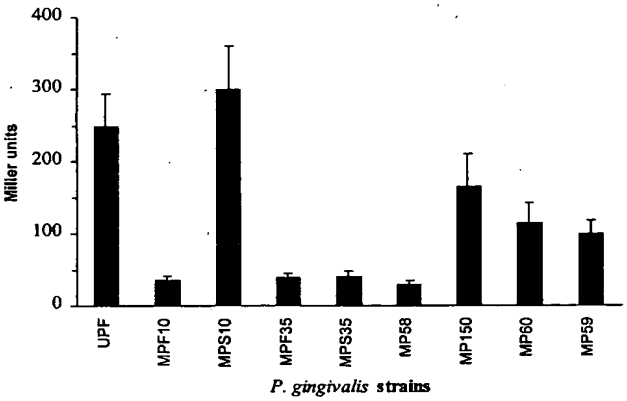

FIG. 5. Effects of *fimA* mutations in the promoter region on transcriptional activity. See Fig. 2 for depiction of mutations. β-Galactosidase level is presented in Miller units as described in the text. Data represent the means and standard errors obtained from at least three independent experiments.

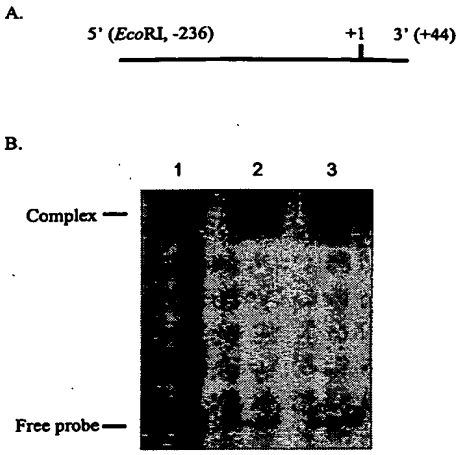

FIG. 6. RNA polymerase (σ^{70})-*fimA* interaction. (A) DNA used in the mobility shift DNA binding assay. The region 5' of the DNA fragment was tagged with an *Eco*RI site, and +1 corresponds to the transcriptional start site of the *fimA* gene. (B) Mobility shift DNA binding assay. Lanes: 1, *fimA* promoter fragment only; 2, *fimA* promoter fragment and *E. coli* RNA holoenzyme; 3, *fimA* promoter, RNA holoenzyme, and calf thymus DNA.

sequent experiments for β-galactosidase activity. The results from Southern blotting also showed two different-size bands when the same *P. gingivalis* MP150 isolates were examined (Fig. 4b). Blotting was performed by digesting chromosomal DNA with *Ssp*I and *Hin*dIII and probing with 1.4 bp of the *fimA* gene. Since *Ssp*I was a unique restriction site in the *fimA* promoter that was lost during the deletion procedure (digestion and religation), the larger bands (lanes 3 and 5) indicated that the mutated *fimA* promoter was associated with the *fimA* gene. The small band (lane 4) indicated that the *lacZ* gene was associated with the mutated *fimA* promoter (*mp*150). A similar PCR analysis was performed for each small deletion or base pair substitution mutation.

Characterization of the *fimA* promoter. The effects of a series of mutations on *fimA* promoter activity in *P. gingivalis* are shown in Fig. 5. A 16-bp deletion from positions −23 to −8, which encompasses the putative −10 sequences (MP58), almost completely abolished *fimA* promoter activity. The contribution of the individual −10 consensus sequences was determined by using strains MPF10 and MPS10. The replacement of TAT with CGG at positions −23 to −21 (MPF10) decreased the level of *fimA* promoter activity dramatically. Moreover, the enzymatic activity of LacZ remained constant when *P. gingivalis* MPF10 was tested over a 50-h period, showing that the promoter deficiency is stable and not controlled by growth phase. In contrast, *P. gingivalis* MPS10, in which the mutation is in the −11 to −9 region (TAA replaced with GCC), did not show a reduction of *fimA* promoter activity; instead, we observed a slight increase in expression, most marked at 34°C. Thus, the −18 to −23 (TATGAC) region appears to be a σ^{70} functional site.

Further evidence that the *fimA* gene is controlled by a σ^{70}-dependent promoter was provided by the results obtained with mutations in the putative −35 region and mobility shift DNA binding assay. Strains MPF35 (replacement of TTG at −44 to −46 with CAA) and MPS35 (replacement of TTG at −41 to −43 with CAC) showed a significant loss of promoter activity (Fig. 5). Moreover, as shown in Fig. 6, RNA holoenzyme containing σ^{70} was able to bind the *fimA* promoter (lane 2). This reaction showed specificity, since unrelated DNA (calf thymus DNA) was unable to compete with the *fimA* promoter region for enzyme binding (lane 3). These results strongly suggested that the *fimA* gene has a σ^{70}-recognized promoter with a −10 sequence of TATGAC centered at −20/−21, and a −35 sequence of TTGTTG centered at −43/−44, from the transcriptional start site. The spacing between these two hexamers is 17 bp.

***fimA* upstream regulatory sequences.** *P. gingivalis* MP150, MP60, and MP59, which contained deletions upstream of the *fimA* promoter region (Fig. 2B), displayed only 66 to 40% of the total promoter activity displayed by the full-length *fimA* promoter (*upf*) (Table 3). AT-rich tracts in the region between −48 and −240 thus appear to be important for full expression of the *fimA* gene. These data support the concept that regulatory nucleotide sequences are involved in the control of *fimA* expression. Furthermore, the AT-rich −48 to −64 area, which begins 2 bp distal to the −35 region, may represent an UP element that interacts with the α subunit of RNA polymerase (Fig. 7).

Activity of the *fimA* promoter increases as temperature decreases, being >4-fold greater at 34°C than at 39°C (Table 3). Upstream deletion mutants MP150, MP60, and MP59 responded similarly to culture temperature; however, a trend toward proportionally greater activity at 34°C was observed. Whereas the ratio of activity at 34°C to that at 37°C was 2.3 for strain UPF, ratios for mutants MP59 and MP60 were 3.75 and 3.9, respectively. This finding indicates that the AT-rich region

TABLE 3. Effects of mutations upstream of the *fimA* −35 region on promoter activity.

P. gingivalis strain	Relative % β-galactosidase level[a]			Ratio[b]		
	34°C	37°C	39°C	34°C	37°C	39°C
UPF	230	100	53	2.3	1	0.5
MP150	200	66	37	3	1	0.56
MP60	180	46	37	3.9	1	0.8
MP59	150	40	32	3.75	1	0.8

[a] The 100% activity is 250 ± 60 Miller units of β-galactosidase, which was obtained as *P. gingivalis* UPF grew at 37°C to log-phase growth.

[b] Ratio of *fimA* promoter activity following growth at 34 or 39°C compared to that at 37°C.

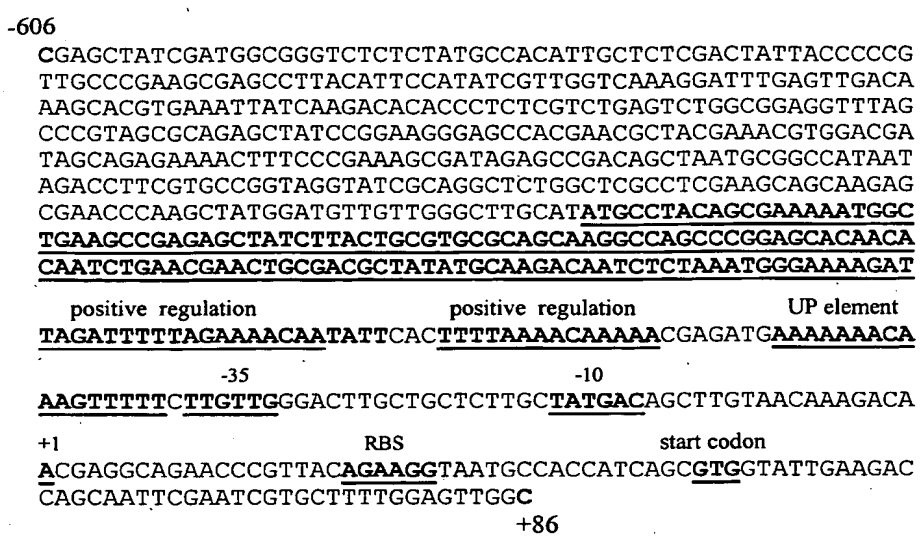

FIG. 7. Nucleotide sequence of the *fimA* promoter region. The underlined and boldface sequences represent −10, −35, UP element, and transcriptional start site regions. The −71 to −240 region contains positive regulatory sequences. RBS, ribosome binding site.

spanning residues −71 to −85 may be involved in temperature control.

Interestingly, all of the *fimA* derivatives retained functional activity when they were expressed in *E. coli*. Moreover, *E. coli* RNA polymerase causes a mobility shift of the mutated constructs. This observation indicates that *E. coli* sigma factors can recognize alternative sequences in the *fimA* upstream region.

DISCUSSION

The ability of many pathogenic bacteria to sense important environmental cues and respond by regulating gene expression at the transcriptional level is well established. Previous reports show that expression of *P. gingivalis* fimbrillin, an important virulence factor, is regulated at the transcriptional level by certain nutritional and environmental signals (1, 38). It was proposed (38) that *P. gingivalis* optimizes expression of fimbrillin in the early stages of colonization to facilitate adherence and invasion and subsequently represses fimbrillin production to diminish the severity of the host immune response. In general, there are two major participants in the control of gene expression: *trans*-acting elements, including RNA polymerase and other protein regulators; and *cis*-acting elements, namely, specific DNA sequences involved in *trans* factor recognition and activity. The contribution of these elements to the control of virulence gene expression in *P. gingivalis* is not known. The putative promoter regions of many of the virulence genes of *P. gingivalis* that have been cloned and sequenced are deduced on the basis of DNA sequence (5, 13, 22, 29). Genes including those for fimbrillin (*fimA*), superoxide dismutase (*sod*), hemagglutinin A (*hagA*), and various proteases (*prtR*, *prtRI*, *prtH*, and *dppIV*) possess sequences for conventional σ^{70} recognition. The location of the promoter for the *tpr* gene was inferred on the basis of deletion mutational analysis (17); however, the RNA polymerase binding site was not resolved. Therefore, to date, functional definition of *P. gingivalis* promoters has not been established.

Promoter recognition for bacterial fimbrial genes can involve σ^{70} recognition (for example *E. coli* Pap and type 1 fimbriae [20]) or recognition by the alternative sigma factor σ^{54} (for example, the type 4 fimbrial family [34]). The upstream region of the *P. gingivalis fimA* gene has three potential −10 and two potential −35 σ^{70} recognition sequences partially matching the *E. coli* consensus sequences. By utilizing a specific mutagenesis scheme in combination with a transcriptional gene fusion assay in a *P. gingivalis* host, the functional promoter sequences were determined to be the hexamers centered around bases −20 and −21 (−10 region) and −43 and −44 (−35 region), as shown in Fig. 7. Although this −10 sequence is further upstream from the transcriptional initiation site than is commonly observed, there are additional features of this promoter arrangement that are consistent with σ^{70}-dependent transcriptional promotion. The transcriptional start site is an adenine residue that was centered in AAC, a common start point for σ^{70} promoters. Furthermore, the spacing between the −10 and −35 regions, 17 bp, is optimal for *E. coli* σ^{70} promoters (8). Although the expression of the *E. coli*, Pap, and type 1 fimbriae is also under the control of the σ^{70} factor, differences in gene organization, regulation, and amino acid sequence tend to exclude *P. gingivalis* fimbriae from this grouping.

Deletion and base change mutations that reduced promoter activity in *P. gingivalis* had no effect on activity in *E. coli*. The transcriptional machinery in *E. coli* can, therefore, apparently recognize alternative sequences in the AT-rich *fimA* upstream region. These results may partially explain the observations of Onoe et al. (26), who reported that an *E. coli* recombinant strain containing the *fimA* gene and upstream sequences produced a prefimbrillin with an extremely long leader peptide (46 amino acids). This led to the proposal that the *fimA* promoter region is further upstream than the region we have defined. Evidence presented in this report, however, suggests that the extended prefimbrillin leader sequence observed in *E. coli* may be a consequence of promiscuous recognition of *P. gingivalis* sequences by *E. coli* RNA polymerases. Similarly, Boyd and Lory (2) demonstrated that *Pseudomonas aeruginosa* sequences are not faithfully recognized in *E. coli*. These findings emphasize the importance of performing promoter definition studies with the organism under investigation, rather than extrapolating from data obtained for *E. coli*. Such analyses have been problematic in studies of *P. gingivalis* due to the lack of

the requisite genetic tools; thus, the genetic systems developed for this study may find utility in the investigation of other *P. gingivalis* promoters and regulatory mechanisms.

Since *fimA* expression is regulated in response to environmental conditions, it is likely that gene expression involves a regulatory DNA sequence(s). This concept is supported by the results of the deletion mutation analysis. Unlike promoter elements, regulatory sequences do not act without a promoter, nor does their loss completely abolish promoter activity (14). *P. gingivalis* MP150, bearing a large deletion from −240 to −90, showed a decrease in *fimA* promoter activity of approximately 35% at 37°C, suggesting that this 150-bp region contains a positive regulatory sequence. Such AT-rich regions are frequently involved in positive regulation of gene expression (27, 30). Additional AT-rich sequences in the −85 to −48 region also appeared to be involved in positive regulation at 37°C. Moreover, the −48 to −64 area may correspond to an UP element. This element is believed to be part of the promoter that interacts with C-termini of the α subunit of RNA polymerase (3). UP elements increase the strength of the overall RNA polymerase binding and thus enhance transcription. This may be important for *fimA* expression, as the −10 and −35 regions match the consensus sequences in only four and three of six bases, respectively.

Temperature fluctuation has been found to be a significant regulatory factor for *fimA* promoter activity, with expression increasing as temperature declines from 39 to 34°C (38). Although the −71 to −85 area may be involved in temperature-dependent control, the results did not allow a precise delineation of the elements of thermoregulation. It is possible, therefore, that more than one regulatory pathway is involved in *fimA* expression. For example, bacterial DNA supercoiling increases with increasing growth temperature (36). Changes in supercoiling can, in turn, affect the stability of binding between RNA polymerase and its promoter and thus modulate gene transcription. DNA topology-dependent control may be important in the thermoregulation of the *P. gingivalis fimA* gene.

In conclusion, transcription of the *fimA* gene in *P. gingivalis* is promoted by σ^{70}-recognized sequences, including −10, −35, and UP elements (Fig. 7). AT-rich upstream regulatory sequences are required for full expression of *fimA* in *P. gingivalis*. More than one control pathway appears to be involved in environmental regulation of *fimA* expression.

ACKNOWLEDGMENTS

We thank Steve Lory and Yoonsuk Park for much helpful advice and for provision of plasmids.

The support of the NIDR (grants DE11111 and DE00401) is gratefully acknowledged.

REFERENCES

1. **Amano, A., A. Sharma, H. K. Kuramitsu, and R. J. Genco.** 1994. Effects of temperature stress on expression of fimbriae and superoxide dismutase by *Porphyromonas gingivalis*. Infect. Immun. **62**:4682–4685.
2. **Boyd, J. M., and S. Lory.** 1996. Dual function of PilS during transcriptional activation of the *Pseudomonas aeruginosa* pilin subunit gene. J. Bacteriol. **178**:831–839.
3. **Busby, S., and R. H. Ebright.** 1994. Promoter structure, promoter recognition, and transcription activity in prokaryotes. Cell **79**:743–746.
4. **Cutler, C. W., J. R. Kalmar, and C. A. Genco.** 1995. Pathogenic strategies of the oral anaerobe, *Porphyromonas gingivalis*. Trends Microbiol. **3**:45–51.
5. **Dickinson, D., M. A. Kubiniec, F. Yoshimura, and R. J. Genco.** 1988. Molecular cloning and sequencing of the gene encoding the fimbrial subunit protein of *Bacteroides gingivalis*. J. Bacteriol. **170**:1658–1665.
6. **DiRita, J., and J. J. Mekalanos.** 1989. Genetic regulation of bacterial virulence. Annu. Rev. Genet. **23**:455–482.
7. **Evans, R. T., B. Klausen, H. T. Sojar, G. S. Bedi, C. Sfintescu, N. S. Ramamurthy, L. M. Golub, and R. J. Genco.** 1992. Immunization with *Porphyromonas gingivalis* fimbriae protects against periodontal destruction. Infect. Immun. **60**:2926–2935.
8. **Hawley, D. K., and W. R. McClure.** 1983. Compilation and analysis of *Escherichia coli* promoter DNA sequences. Nucleic Acids Res. **11**:2237–2255.
9. **Hideki, N., A. Sharma, H. T. Sojar, A. Amano, M. I. Levine, and R. J. Genco.** 1997. Role of the carboxyl-terminal region of *Porphyromonas gingivalis* fimbrillin in binding to salivary proteins. Infect. Immun. **65**:422–427.
10. **Hirose, K., E. Isogai, H. Mizugai, and I. Ueda.** 1996. Adhesion of *Porphyromonas gingivalis* fimbriae to human gingival cell line Ca9-22. Oral Microbiol. Immunol. **11**:402–406.
11. **Izutsu, K. T., C. M. Belton, A. Chan, S. Fatherazi, J. P. Kanter, Y. Park, and R. J. Lamont.** 1996. Involvement of calcium in interactions between gingival epithelial cells and *Porphyromonas gingivalis*. FEMS Microbiol. Lett. **144**: 145–150.
12. **Kontani, M., S. Kimura, I. Nakagawa, and S. Hamada.** 1997. Adherence of *Porphyromonas gingivalis* to matrix proteins via a fimbrial cryptic receptor exposed by its own arginine-specific protease. Mol. Microbiol. **24**:1179–1187.
13. **Kuramitsu, H. K., M. Yoneda, and T. Madden.** 1995. Proteases and collagenases of *Porphyromonas gingivalis*. Adv. Dent. Res. **9**:37–40.
14. **Kustu, S., A. K. North, and D. S. Weiss.** 1991. Prokaryotic transcriptional enhancers and enhancer-binding proteins. Trends Biochem. Sci. **16**:397–402.
15. **Lamont, R. J., A. Chan, C. M. Belton, K. T. Izutsu, D. Vasel, and A. Weinberg.** 1995. *Porphyromonas gingivalis* invasion of gingival epithelial cells. Infect. Immun. **63**:3878–3885.
16. **Lamont, R. J., C. A. Bevan, S. Gil, R. E. Persson, and B. Rosan.** 1993. Involvement of *Porphyromonas gingivalis* fimbriae in adherence to *Streptococcus gordonii*. Oral Microbiol. Immunol. **8**:272–276.
17. **Lu, B., and B. C. McBride.** 1998. Expression of the *trp* protease gene of *Porphyromonas gingivalis* is regulated by peptide nutrients. Infect. Immun. **66**:5147–5156.
18. **Malek, R., J. G. Fisher, A. Caleca, M. Stinson, C. J. Oss, J. Y. Lee, M. I. Cho, R. J. Genco, R. T. Evans, and D. W. Dyer.** 1994. Inactivation of the *Porphyromonas gingivalis fimA* gene blocks periodontal damage in gnotobiotic rats. J. Bacteriol. **176**:1052–1059.
19. **Miller, J.** 1972. Experiments in molecular genetics. Cold Spring Harbor Laboratory, Cold Spring Harbor, N.Y.
20. **Mol, O., and B. Oudega.** 1996. Molecular and structural aspects of fimbriae biosynthesis and assembly in *Escherichia coli*. FEMS Microbiol. Res. **19**: 25–52.
21. **Murakami, Y., S. Hanazawa, A. Watanabe, K. Naganuma, H. Iwasaka, K. Kawakami, and S. Kitano.** 1994. *Porphyromonas gingivalis* fimbriae induce a 68-kilodalton phosphorylated protein in macrophages. Infect. Immun. **62**: 5242–5246.
22. **Nakayama, K.** 1994. Rapid viability loss on exposure to air in a superoxide dismutase-deficient mutant of *Porphyromonas gingivalis*. J. Bacteriol. **176**: 1939–1943.
23. **Ogawa, T., and H. Uchida.** 1993. A peptide, ALTTE, within the fimbrial subunit protein from *Porphyromonas gingivalis*, induces production of interleukin 6, gene expression and protein phosphorylation in human peripheral blood mononuclear cells. FEMS Immunol. Med. Microbiol. **11**:197–206.
24. **Ogawa, T., H. Uchida, and S. Hamada.** 1994. *Porphyromonas gingivalis* fimbriae and their synthetic peptides induce proinflammatory cytokines in human peripheral blood monocyte cultures. FEMS Microbiol. Lett. **116**:237–242.
25. **Ogawa, T., Y. Kono, M. L. McGhee, J. R. McGhee, J. E. Roberts, S. Hamada, and H. Kiyono.** 1991. *Porphyromonas gingivalis*-specific serum IgG and IgA antibodies originated from immunoglobulin-secreting cells in inflamed gingiva. Clin. Exp. Immunol. **83**:237–244.
26. **Onoe, T., C. I. Hoover, K. Nakayama, T. Ideka, H. Nakamura, and F. Yoshimura.** 1995. Identification of *Porphyromonas gingivalis* prefimbrillin possessing a long leader peptide: possible involvement of trypsin-like protease in fimbrillin maturation. Microb. Pathog. **19**:351–364.
27. **Owen-Huphes, T. A., G. D. Pavitt, D. S. Santos, J. M. Sidebotham, C. S. Hulton, J. C. Hinton, and C. F. Higgins.** 1992. The chromatin-associated protein H-NS-interacts with curved DNA topology and gene expression. Cell **71**:255–265.
28. **Park, Y., and B. C. McBride.** 1993. Characterization of the *tpr* gene product and isolation of a specific protease-deficient mutant of *Porphyromonas gingivalis* W83. Infect. Immun. **61**:4139–4146.
29. **Progulske-Fox, A., T. Tumwasorn, and S. C. Holt.** 1989. The expression and function of *Bacteroides gingivalis* hemagglutinin gene in *Escherichia coli*. Oral Microbiol. Immunol. **4**:121–131.
30. **Puente, J. L., D. Bieber, S. W. Ramer, W. Murray, and K. Schoolnik.** 1996. The bundle-forming pili of enteropathogenic *Escherichia coli*: transcriptional regulation by environmental signals. Mol. Microbiol. **20**:87–100.
31. **Sambrook, J., E. F. Fritsch, and T. Maniatis.** 1989. Molecular cloning: a laboratory manual, 2nd ed. Cold Spring Harbor Laboratory, Cold Spring Harbor, N.Y.
32. **Sharma, A., J. Y. Lee, G. S. Bedi, and R. J. Genco.** 1992. PCR amplification

and cloning of the *Porphyromonas gingivalis* fimbrillin gene. J. Dent. Res. **71:** 293.
33. **Shoemaker, N. B., C. Getty, J. F. Gardner, and A. A. Salyers.** 1986. Tn*4351* transposes in *Bacteroides* spp. and mediates the integration of plasmid R751 into the *Bacteroides* chromosome. J. Bacteriol. **165:**929–936.
34. **Strom, M. S., and S. Lory.** 1993. Structure-function and biogenesis of the type IV pili. Annu. Rev. Microbiol. **47:**565–596.
35. **Totten, P. A., and S. Lory.** 1990. Characterization of the type a flagellin gene from *Pseudomonas aeruginosa* PAK. J. Bacteriol. **172:**7188–7199.
36. **Tse-Dinh, Y. C., H. Qi, and R. Menzel.** 1997. DNA supercoiling and bacterial adaptation: thermotolerance and thermoresistance. Trends Microbiol. **5:** 323–326.
37. **Weinberg, A., C. M. Belton, Y. Park, and R. J. Lamont.** 1997. Role of fimbriae in *Porphyromonas gingivalis* invasion of gingival epithelial cells. Infect. Immun. **65:**313–316.
38. **Xie, H., S. Cai, and R. J. Lamont.** 1997. Environmental regulation of fimbrial gene expression in *Porphyromonas gingivalis*. Infect. Immun. **65:**2265–2271.

Editor: J. R. McGhee

MOLECULAR AND CELLULAR BIOLOGY, Dec. 1995, p. 6710–6719
0270-7306/95/$04.00+0
Copyright © 1995, American Society for Microbiology
Vol. 15, No. 12

Molecular Mechanism of Inhibition of Estrogen-Induced Cathepsin D Gene Expression by 2,3,7,8-Tetrachlorodibenzo-*p*-Dioxin (TCDD) in MCF-7 Cells

VENKATESH KRISHNAN, WESTON PORTER, MICHAEL SANTOSTEFANO, XIAHONG WANG, AND STEPHEN SAFE*

Department of Veterinary Physiology and Pharmacology and Department of Biochemistry and Biophysics, Texas A&M University, College Station, Texas

Received 6 June 1995/Returned for modification 5 July 1995/Accepted 20 September 1995

17β-Estradiol (E2) induces cathepsin D mRNA levels and intracellular levels of immunoreactive protein in MCF-7 human breast cancer cells. 2,3,7,8-Tetrachlorodibenzo-*p*-dioxin (TCDD) alone does not affect cathepsin D gene expression in this cell line; however, in cells cotreated with TCDD and E2, TCDD inhibited E2-induced cathepsin D mRNA levels, the rate of gene transcription, and levels of immunoreactive protein. The inhibitory responses were observed within 30 to 120 min after the cells were treated with TCDD. TCDD also inhibited E2-induced secreted alkaline phosphatase activity in aryl hydrocarbon (Ah)-responsive MCF-7 and wild-type mouse Hepa 1c1c7 cells cotransfected with the human estrogen receptor (hER) and the pBC12/S1/pac plasmid, which contains the 5′ promoter region (−296/+57) of the cathepsin D gene and an alkaline phosphatase reporter gene. The E2-responsive ER/Sp1 sequence (−199 to −165) in the cathepsin D 5′ region contains an imperfect GTGCGTG (−175/−181) xenobiotic responsive element (XRE); the role of this sequence in Ah responsiveness was investigated in gel electrophoretic mobility shift assays and with plasmid constructs containing a wild-type ER/Sp1 oligonucleotide or a mutant ER/Sp1-"*XRE*" oligonucleotide containing two C→A mutations in the XRE sequence (antisense strand). In plasmid constructs which contained a chloramphenicol acetyltransferase reporter gene and the wild-type ER/Sp1 promoter sequence, E2-induced chloramphenicol acetyltransferase activity and mRNA levels were inhibited by TCDD whereas no inhibition was observed with the mutant ER/Sp1-"*XRE*" plasmids. Electrophoretic mobility shift assays showed that the nuclear or transformed cytosolic Ah receptor complex blocked formation of the ER-Sp1 complex with the wild-type but not the ER/Sp1 mutant oligonucleotide. Moreover, incubation of the wild-type bromodeoxyuridine-substituted ER/Sp1 oligonucleotide with the nuclear Ah receptor complex gave a specifically bound cross-linked 200-kDa band. These data demonstrate that Ah receptor-mediated inhibition of E2-induced cathepsin D gene expression is due to disruption of the ER-Sp1 complex by targeted interaction with an overlapping XRE.

The aryl hydrocarbon (Ah) receptor protein is expressed in laboratory animals and humans and in mammalian cells in culture (54, 65). Although the endogenous ligand(s) for this receptor has not been identified, several different classes of compounds reversibly bind the Ah receptor, and these include the polynuclear and polyhalogenated aromatic hydrocarbons (42, 54, 57, 59, 65, 67). 3-Methylcholanthrene and 2,3,7,8-tetrachlorodibenzo-*p*-dioxin (TCDD) are prototypical aromatic hydrocarbons which exhibit high-affinity binding ($K_d \leq 1$ nM) for the Ah receptor (44, 58) and have been utilized for characterizing Ah receptor-mediated responses.

TCDD induces a broad spectrum of biochemical and toxic responses including a wasting syndrome, immune suppression, hepatotoxicity, developmental and reproductive toxicity, carcinogenicity, dermal toxicity, alteration of endocrine response pathways, and modulation of diverse enzyme activities (26, 29, 59, 73, 82). The induction of *CYP1A1* gene expression by TCDD and 3-methylcholanthrene has been extensively investigated, and the results indicate that the Ah receptor acts as a nuclear ligand-induced transcription factor (13, 29, 73, 82). After treatment of animals or cells with TCDD, there is a rapid formation of a heterodimeric nuclear Ah receptor complex (19) which consists of the ligand-binding protein (7) and the Ah receptor nuclear translocator (Arnt) protein (31). The unbound Ah receptor is associated with heat shock protein 90 (48, 55, 60, 61), and the subcellular distribution of these proteins in the absence of ligand is currently being investigated (60, 61). The nuclear Ah receptor complex interacts with cognate genomic sequences (dioxin or xenobiotic responsive elements [DREs and XREs, respectively]) in the 5′-promoter region of the *CYP1A1* gene and transactivates *CYP1A1* gene expression (15–17, 27, 34, 70, 83). There is evidence that this transactivation process is comparable for induction of *CYP1A1* gene expression and induction of the expression of other members of the Ah gene battery, namely CYP1A2, glucuronosyl transferase, aldehyde-3-dehydrogenase, glutathione *S*-transferase *Ya* gene, and NAD(P)H:menadione oxidoreductase (1, 35, 53, 56, 62, 64). Other studies also report that enhanced expression of other genes by TCDD is due to posttranscriptional processes (20).

TCDD also decreases gene expression and/or the respective activities of the encoded proteins. Phosphoenolpyruvate carboxy kinase, glucose-6-phosphatase, and tryptophan 2,3-dioxygenase activities and mRNA levels are decreased in rats treated with an acutely toxic dose (125 μg/kg of body weight) of TCDD (72). Rat uterine c-*fos* and epidermal growth factor

* Corresponding author. Mailing address: Department of Veterinary Physiology and Pharmacology, Texas A&M University, College Station, TX 77843-4466. Phone: (409) 845-5988. Fax: (409) 862-4949. Electronic mail address: ssafe@vetmed.tamu.edu.

receptor mRNA levels are also decreased (2, 3), and decreased epidermal growth factor receptor mRNA levels or binding activity has been observed in several animal species and mammalian cells (33, 36, 43). TCDD inhibits several estrogen (E2)-induced responses in the rodent uterus (21, 66) and mammary gland including the development and formation of mammary tumors in female Sprague-Dawley rats and B6D2 mice (22, 32, 38). The antiestrogenic effects of TCDD and related compounds have also been reported in Ah-responsive MCF-7 human breast cancer cells (22–25, 30, 40). TCDD and related compounds inhibit E2-induced cell proliferation, progesterone receptor protein and mRNA levels, postconfluent focus production and extracellular tissue plasminogen activator activity, procathepsin D, and cathepsin D. This study will utilize the E2-regulated cathepsin D gene as a model for investigating the mechanism of action of TCDD as an antiestrogen.

Cathepsin D is expressed in human mammary cancer cells and tumors, and levels of this protein are used as a negative prognostic indicator for disease-free survival for women with breast cancer (71, 74, 75). Treatment of MCF-7 cells with E2 results in the induction of cathepsin D gene expression and increased intra- and extracellular levels of procathepsin D and cathepsin D (8–11, 47, 52, 76, 79–81). Cavailles et al. (10) have reported that cathepsin D gene transcription is initiated at five start sites (I to V); E2 induces transcription from start site I, and this response is dependent on an intact TATA sequence between −40 to −44. The 5′-proximal flanking region of the cathepsin D gene does not contain a classical palindromic estrogen-responsive element (ERE); however, deletion analysis experiments show that a promoter fragment from −365 to −122 was required for E2 responsiveness (4, 9, 10). More recent data confirmed the importance of this sequence and suggested that E2 regulation of this promoter sequence was complex and appeared to require cooperative interactions with other *trans*-acting nuclear factors such as Sp1 (4). An imperfect ERE half-site and an Sp1 binding site were identified in the cathepsin D promoter between −199 to −165 (41), and this site was protected in DNase I footprinting assays using E2-induced nuclear extracts (4). Research in this laboratory showed that incubation of nuclear extracts from E2-treated MCF-7 cells with a synthetic [^{32}P]ER/Sp1 oligonucleotide (−199 to −165) resulted in formation of an ER-Sp1 complex which could be detected by gel electrophoretic mobility shift assays. Subsequent studies with wild-type and mutant ER/Sp1 oligonucleotides in electrophoretic mobility shift and transient transfection assays showed that formation of an ER-Sp1 complex was required for the E2-induced response (41). The results reported in this study demonstrate that TCDD inhibits E2-induced cathepsin D gene expression and chloramphenicol acetyltransferase (CAT) activity in MCF-7 cells transiently transfected with an ER/Sp1-tk-CAT construct. The data indicate that the inhibitory effects of TCDD are associated with direct interaction of the nuclear Ah receptor complex with an XRE strategically located between the ER and Sp1 response elements. Thus, the nuclear Ah receptor complex acts as a negative transcriptional factor, and the results illustrate a molecular model for interaction between the Ah receptor- and ER-mediated endocrine pathways.

MATERIALS AND METHODS

Chemicals, biochemicals, cells, oligonucleotides, and plasmids. TCDD, [^{3}H]TCDD (32 Ci/mmol), and 2,3,7,8-tetrachlorodibenzofuran (TCDF) were synthesized in this laboratory (>98%). RPMI 1640, DME-F12 (2906), controlled processed serum replacement (CPSR-2), transferrin, bovine serum albumin, antibiotic-antimycotic solution, and E2 were purchased from Sigma Chemical Co. (St. Louis, Mo.). Fetal calf serum was obtained from JRH Biosciences (Kansas City, Mo.). An ELSA cath-D radioimmunoassay (RIA) kit was purchased from CIS-US Inc. (Bedford, Mass.). α-Naphthoflavone (αNF) was purchased from the Aldrich Chemical Co. (Milwaukee, Wis.). [γ-^{32}P]ATP (3,000 Ci/mmol), [^{3}H]17β-estradiol (130 Ci/mmol), and [α-^{32}P]UTP (800 Ci/mmol) were obtained from New England Nuclear (Boston, Mass.). All other chemicals and biochemicals were of the highest purity available from commercial sources.

The human estrogen receptor (hER) expression plasmid was provided by Ming-Jer Tsai (Baylor College of Medicine, Houston, Tex.). The pB12/pL/pac (Seap-pac) plasmid containing the cathepsin D promoter (−296/+57) fused to an alkaline phosphatase gene was used to study the promoter activity (63). The pBC12/S1/pac (S1) plasmid containing no promoter and the pBC12/RSV/pac (RSV) plasmid containing a Rous sarcoma virus promoter fused to the alkaline phosphatase gene were used as negative and positive controls, respectively. The above plasmids were generous gifts from Andrej Hasilik, Münster, Germany (with permission from B. R. Cullen, Duke University, Durham, N.C.). A 2.6-kb *Bam*HI fragment containing the entire *arnt* cDNA was isolated from the pMB5/NEO-M1-1 expression vector (kindly supplied by O. Hankinson, University of California at Los Angeles) and religated in the pcDNA1/NEO expression vector (Invitrogen). The direction of the *arnt* cDNA was confirmed by *Pvu*II restriction mapping. The correct bacterial clone was amplified, and the plasmid containing antisense *arnt* cDNA was purified and used in the experiment. The MCF-7 cells were purchased from the American Type Culture Collection (Rockville, Md.); the wild-type and class II mutant Hepa 1c1c7 cells were kindly provided by J. P. Whitlock, Jr. (Stanford University). This mutant cell line expresses the cytosolic Ah receptor, but TCDD does not induce formation of the nuclear Ah receptor complex (50).

The ER/Sp1 and ER/Sp1-"*XRE*" oligonucleotides were synthesized by DNA Technologies Laboratory, Texas A&M University. The complementary strands were annealed, and the 5′ overhangs were used for cloning into the thymidine kinase-CAT vector (37). Ligation products were transformed into *Escherichia coli* DH5α cells, and clones obtained were verified by restriction mapping. Plasmids containing cDNA probes for Northern (RNA) analysis of cathepsin D and β-tubulin mRNA levels were obtained from the American Type Culture Collection. A cDNA for CAT mRNA was kindly provided by D. O. Peterson (Texas A&M University). Quantitation of radiolabeled bands after separation by electrophoretic and chromatographic assays was determined with a Betagen Betascope 603 blot analyzer. The following oligonucleotides were synthesized and used in this study: ER/Sp1 oligonucleotide (antisense strand), 5′-GATCCTGGG CGGGGCAACCTCGGGCACGCACAGCGCCCGGGCGGGGGGCGGG GA-3′; ER/Sp1-"*XRE*" oligonucleotide (antisense strand), 5′-GATCCTGGGC GGGGCAACCTCGGGCAAGAACAGCGCCCGGGCGGGGGGCGGGA-3′; DRE, 5′-GATCTGGCTCTTCTCACGCAACTCCG-3′; DRE′ (mutant), 5′-GA TCCCAGGCTCTTCTACATCAACTCCGGGGC-3′; and cross-linking primer sequence, TCCCCGCCCCCCGCC.

RIA for cathepsin D. The commercially available ELSA cath-D kit consisted of ELSA tubes coated with the anti-cathepsin-D monoclonal antibody (8, 39); 300 μl of monoclonal ^{125}I-labeled anti-cathepsin-D antibody and then 50 μl of sample (medium or cytosolic extract) were added to each tube. This mixture was then incubated at 25°C with shaking in an incubator shaker for 3 h. The tubes were then washed three times with 3 ml of Tween 20 solution after the contents in the tube were removed by aspiration. The tubes were then measured for bound ^{125}I in a Packard gamma scintillation counter. Quantitation of cathepsin D in the samples was based on a standard curve obtained as outlined in the instructions provided in the kit.

Northern blot analysis of cathepsin D mRNA. Cathepsin D mRNA levels were measured by using a 1.2-kb *Eco*RI fragment of the human cathepsin D cDNA. β-Tubulin mRNA levels were measured by using a 1.1-kb *Eco*RI fragment of human β-tubulin cDNA. Total RNA was isolated by the guanidinium isothiocyanate-acid phenol extraction method (12). Total RNA (20 μg) was separated in a 1.2% agarose–1 M formaldehyde gel in 20 mM sodium phosphate–2 mM EDTA, transferred onto a nylon membrane by capillary action, and bound to the membrane by UV cross-linking. The cDNAs were labeled with [α-^{32}P]dCTP by using a Random Primers DNA labeling system (Bethesda Research Laboratories) and added at 1×10^6 to 5×10^6 cpm/ml of hybridization solution (5× SSPE [1× SSPE is 0.15 M NaCl, 10 mM NaH_2PO_4, 1 mM EDTA; pH 7.4], 1% sodium dodecyl sulfate [SDS], 10% dextran sulfate, 5× Denhardt's solution). Hybridizations were performed in roller bottles at 65°C for 24 h. Nonspecifically-bound probe was removed by two 15-min washes at 20°C in 1× SSPE, two 45-min washes at 65°C in 0.1× SSPE–1% SDS, and one 20-min wash at 20°C in 1× SSPE. Membranes were stripped of probe by boiling for 20 min in 0.01× SSPE–0.5% SDS. Bands were quantitated with a Betagen Betascope 603 blot analyzer imaging system. Four separate experiments were carried out for each treatment group, and the results are expressed as means ± standard deviations (SD).

Nuclear run-on assays. MCF-7 cells (5×10^7) were harvested, resuspended in 5 ml of 1.5 M sucrose buffer plus 0.1% Brij 58, and homogenized with 10 to 20 strokes in a Dounce homogenizer. The homogenate was diluted to 15 ml with 1.5 M sucrose and centrifuged at 10,000 rpm for 20 min at 4°C. The nuclear pellet was resuspended in 0.5 ml of nucleus storage buffer (20 mM HEPES [*N*-2-hydroxyethylpiperazine-*N*′-2-ethanesulfonic acid; pH 8.3], 75 mM NaCl, 0.5 mM EDTA, 0.85 mM dithiothreitol, 0.125 mM phenylmethylsulfonyl fluoride, 50% glycerol). The concentration of nuclei was determined by diluting an aliquot in 0.5% (wt/vol) trypan blue and counting with a hemocytometer. Aliquots of 2 ×

10^6 nuclei were then stored in liquid nitrogen until the transcription elongation assay was performed. The nuclear transcription run-on assay was performed essentially as described elsewhere (45). Briefly, nuclei were isolated at the appropriate times after treatment with TCDD and incubated with [α-^{32}P]UTP (200 μCi) and unlabeled ATP, CTP, and GTP (0.5 mM for each nucleotide). The radiolabeled RNA transcripts were isolated and hybridized to excess (10 μg) of denatured cDNA immobilized onto a nylon membrane by using a slot blot apparatus (Hoefer PR600). The membranes were exposed for 5 weeks, visualized by autoradiography, and quantitated by a Molecular Dynamics 300A scanning laser densitometer.

Preparation and transformation of cytosolic extracts. MCF-7 cells were grown in DME-F12 medium supplemented with 10% fetal bovine serum (2× dextran-coated charcoal). Cells were harvested and washed with Hanks solution. Cells were washed in HEDG buffer (25 mM HEPES, 1.5 mM EDTA, 1 mM dithiothreitol, 10% glycerol [pH 7.6]) and incubated in HED buffer (HEDG buffer without glycerol) for 10 min at 4°C. The cells were then centrifuged at 800 × *g* for 10 min, followed by homogenization using a Teflon pestle-drill apparatus in 1 ml of HEDG buffer. The cell suspension was centrifuged at 1,000 × *g* for 10 min at 4°C. The supernatant was subjected to ultracentrifugation at 4,000 × *g* for 30 min at 4°C. Supernatant was obtained and protein content was quantitated by the Bradford assay (6). Cytosolic extract (1 mg of protein per ml) was incubated with 20 nM TCDD for 2 h at 25°C. Transformed cytosol (100 μl) was incubated with nuclear extracts from MCF-7 cells and analyzed by electrophoretic mobility shift assays using ER/Sp1 and ER/Sp1-"*XRE*" oligonucleotides.

Electrophoretic mobility shift assays. Complementary strands of the synthetic ER/Sp1 and mutated ER/Sp1-"*XRE*" oligonucleotides were labeled at the 5′ end by using T4 polynucleotide kinase and [γ-^{32}P]ATP (68). Nuclear extracts (5 μg) from MCF-7 and HeLa cells treated with dimethyl sulfoxide (DMSO) (<0.1%) and other appropriate chemicals were incubated in TEGD buffer with 1 μg of poly(dI-dC) for 15 min at 20°C to bind nonspecific DNA-binding proteins. Following addition of 1 nM ^{32}P-labeled specific oligonucleotide, the mixture was incubated for 15 min at 20°C. For competition with specific unlabeled oligonucleotides, the unlabeled oligonucleotide in appropriate excess was incubated for 5 min prior to the addition of the labeled oligonucleotide. Reaction mixtures were loaded onto a 5% polyacrylamide gel (acrylamide/bisacrylamide ratio, 30:0.8) and run at 110 V in 0.09 M Tris–0.09 M borate–2 mM EDTA, pH 8.3. The relative intensities of the retarded complexes were quantitated by the Betagen Betascope 603 blot analyzer imaging system, visualized by autoradiography, and also quantitated with a model 300A scanning laser densitometer (Molecular Dynamics).

Cloning, transient transfection, CAT, and alkaline phosphatase assays. Cloning of the ER/Sp1 and the mutant ER/Sp1-"*XRE*" oligonucleotides into the thymidine kinase-CAT vector at the *Bam*HI and *Hin*dIII sites was carried out as previously described (37, 41). Transient transfection of the CAT plasmids and the Seap-pac, S1, RSV, and hER plasmids was carried out essentially as described elsewhere (37, 41). MCF-7 cells were cotransfected with a Polybrene (200-μg/ml) solution containing 5 to 20 μg of appropriate plasmid DNA and the hER plasmid. After 6 h, the cells were shocked with 15% glycerol in Hanks solution for 75 s, washed twice with the same solution, and grown in DME-F12 (without phenol red)–5% stripped fetal bovine serum. Cells were dosed 12 h after being shocked with appropriate chemicals dissolved in DMSO; control cells were treated with DMSO alone (<0.1%). Two days later the cells were removed by manual scraping, cell extracts were obtained, and 100 μg of protein extract was used to determine CAT activity as previously described (28, 37). Levels of acetylated product were quantitated by a Betagen Betascope 603 blot analyzer imaging system and visualized by autoradiography. Secreted alkaline phosphatase activity was determined essentially as described elsewhere (5, 63). One milliliter of medium was obtained at the appropriate times and incubated for 10 min at 65°C. The medium was then centrifuged at 10,000 × *g* for 5 min, and 900 μl of the supernatant was mixed with an equal amount of Seap buffer (5). This mixture was then warmed in a 37°C water bath separately, along with freshly prepared substrate (120 mM *p*-nitrophenyl phosphate). The two solutions were mixed with constant vortexing and incubated in the 37°C water bath for 6 h. The product of the alkaline phosphatase reaction was quantitated with a spectrophotometer at an optical density at 405 nM. The activity from each sample was compared with the standard curve obtained by using a serial dilution of alkaline phosphatase enzyme activity (5).

Cross-linking studies. For cross-linking studies, 10 pmol of the synthetic oligonucleotide ER/Sp1 was annealed to 10 pmol of a cross-linked primer sequence. The annealed template was end filled with the Klenow fragment of DNA polymerase in the presence of 0.1 μM dGTP, dATP, and bromodeoxyuridine (BrdU) and 1 μM [^{32}P]dCTP (68) and was designated the BrdU-substituted DRE oligonucleotide. Nuclear extracts (10 μg) from MCF-7 cells treated with appropriate chemicals (i.e., E2, E2 plus TCDD, or [^{3}H]TCDD) were incubated with the BrdU-substituted ^{32}P-labeled DRE for 15 min at 20°C following a 15-min incubation at 20°C with 400 ng of poly(dI-dC) in HEGD buffer or for 10 min followed by a 5-min incubation at 20°C with unlabeled excess competitor. The incubation mixtures were irradiated by using a FOTODYNE UV transilluminator at >205 nm for 30 min at 20°C. Samples were then mixed with 20 μl of an SDS loading buffer, heated to 95°C for 5 min, and then subjected to electrophoresis on SDS–6% polyacrylamide gels. ^{32}P-labeled ligand-Ah receptor-DRE complexes were resolved by autoradiography of the dried gel. When 10 nM [^{3}H]TCDD (±2 μM TCDF) was used in the experiments, the resulting gels were cut into eight (1.2-cm) slices and extracted with Solvable (Dupont, Boston, Mass.) and radioactivity was determined by liquid scintillation counting. Molecular weights of UV cross-linked nuclear and transformed ligand-Ah receptor-ER/Sp1 complexes were calculated from ^{14}C-methylated protein standards obtained from Amersham Corp. (Arlington Heights, Ill.).

Electrophoretic mobility shift assays using in vitro-translated proteins. Plasmids containing the full-length Ah receptor and Arnt cDNAs were used to in vitro transcribe and translate the corresponding proteins in a rabbit reticulocyte lysate kit (Promega, Madison, Wis.). DNA binding assays were performed by assembling the appropriate in vitro-translated proteins in 20 mM HEPES–5% glycerol–100 mM potassium chloride–5 mM magnesium chloride–0.5 mM dithiothreitol–1 mM ethylene diaminetetraacetic acid in a final volume of 25 μl. The labeled oligonucleotides (30,000 cpm) were then added to the reaction mixtures in the presence of 1 μg of poly(dI-dC), and the mixtures were incubated for 15 min at 25°C. Reaction mixtures were immediately analyzed by gel electrophoretic mobility shift assays as described above. Gels were dried, and protein-DNA binding was visualized by autoradiography.

Statistical analysis. All the experiments were carried out at least in triplicate, and the results were expressed as means ± SD. Statistical significance was determined by analysis of variance using Scheffe's post hoc test.

RESULTS

Effects of TCDD on E2-induced cytosolic immunoreactive cathepsin D. MCF-7 cells were treated with 1 nM E2 alone for 24 h; cotreated cells were also treated with 1 nM E2 for 24 h, and 1 nM TCDD was added 2, 4, 6, and 12 h prior to harvesting of the cells and isolation of cytosolic extracts. Extracts were analyzed for immunoreactive cathepsin D by using a commercially available RIA kit to detect and quantitate intracellular levels of cathepsin D as previously described (39). The results in Fig. 1 (top) illustrate that E2 alone induced cathepsin D levels (1.8-fold); TCDD alone also slightly increased levels of this protein compared with control (DMSO-treated) cells. In cells cotreated with 1 nM E2 for 24 h and TCDD for 2, 4, 6, or 12 h, there was a significant decrease in immunoreactive cathepsin D at the earliest time point.

Effects of TCDD on E2-induced cathepsin D mRNA levels and rate of transcription. The results in Fig. 1 summarize the time-dependent decrease in E2-induced cathepsin D mRNA levels by TCDD. Treatment of MCF-7 cells for 24 h with 10 nM E2 resulted in a threefold increase in cathepsin D mRNA levels. In cells cotreated with 10 nM E2 for 24 h and 10 nM TCDD for 1, 2, 4, 8, or 12 h, there was significant decrease in cathepsin D mRNA levels at the earliest time point. TCDD alone caused some initial increase in cathepsin D mRNA levels. The results in Fig. 2 summarize the effects of E2 and TCDD plus E2 on the rate of cathepsin D gene transcription in nuclear run-on assays. E2 caused a 6.8-fold increase in cathepsin D mRNA levels, whereas in cells cotreated with E2 plus TCDD a significant decrease in E2-induced mRNA levels was observed 30 or 60 min after addition of TCDD. A Northern blot of cathepsin D mRNA levels after treatment with DMSO, E2, or TCDD plus E2 is shown in Fig. 2C. These data demonstrate the E2 inducibility of cathepsin D gene expression as previously reported (11, 41, 47, 76, 80). Moreover, like ICI 164,384, an antiestrogen which blocks formation of the ER homodimer (14), TCDD also inhibits E2-induced cathepsin D gene expression. However, the inhibitory effects of TCDD in the nuclear run-on assay were observed within 30 min (Fig. 2), whereas the effects of ICI 164,384 occurred 2 to 4 h after treatment (41).

Inhibition of E2-induced cathepsin D promoter activity in MCF-7, wild-type, and mutant mouse Hepa 1c1c7 cells. The effects of TCDD on cathepsin D promoter activity were determined in MCF-7 human breast cancer cells and wild-type and mutant mouse Hepa 1c1c7 cells cotransfected with the Seap-pac and hER plasmids and treated with E2, TCDD, or E2 plus TCDD (Table 1). Because of the relatively high expression of

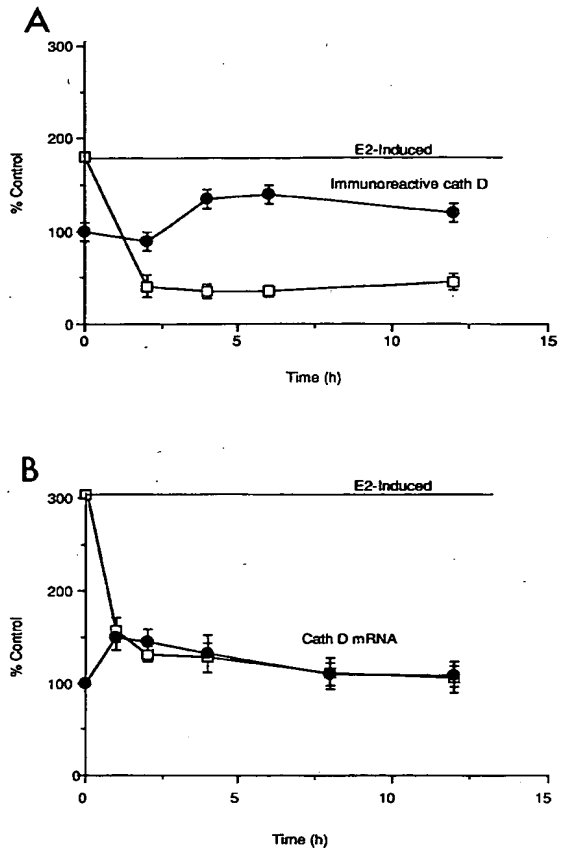

FIG. 1. RIA of immunoreactive cathepsin D (cath-D) using cytosolic cathepsin D levels (top) and cathepsin D mRNA levels (bottom) in MCF-7 cells. Levels of immunoreactive cathepsin D (A) were determined after treatment of cells with 1 nM E2 alone for 24 h and after treatment with 1 nM TCDD alone (●) for 2, 4, 6, and 12 h. The effect of cotreatment on immunoreactive cathepsin D was determined in cells treated with 1 nM E2 for 24 h and TCDD for 1, 2, 4, 6, and 12 h (□). The amount of immunoreactive cathepsin D in control cells was determined after treatment with DMSO (vehicle control) for 24 h and was assigned a value of 100%. The amount of protein in femtomoles per milligram was determined by plotting a standard curve as indicated in the instructions for the RIA kit. The results are expressed as means ± SD for at least three determinations for each time point. E2 significantly induced cathepsin D levels at all time points ($P < 0.05$), and TCDD significantly inhibited the E2-induced response at all time points ($P < 0.05$). Cathepsin D mRNA levels (B) were determined in cells treated with 1 nM E2 alone for 24 h and with 10 nM TCDD alone (●) for 1, 2, 4, 8, and 12 h. Cathepsin D mRNA levels were also determined in MCF-7 cells cotreated with 10 nM E2 for 24 h plus 10 nM TCDD (□) for 1, 2, 4, 8, and 12 h. Treatment of cells with DMSO for 24 h gave control cathepsin D mRNA levels, which were assigned a value of 100%. Cathepsin D mRNA was isolated, visualized by Northern blot analysis, and quantitated by a Betagen Betascope 603 blot analyzer as described in Materials and Methods. Cathepsin D mRNA levels were normalized relative to β-tubulin mRNA for each treatment group.

the recombinant plasmid, cotransfection of the hER expression plasmid was required for E2 responsiveness. Cotransfection of the hER plasmid has previously been reported with plasmid constructs derived from 5′-promoter sequences of the cathepsin D, pS2, and progesterone receptor genes (9, 10, 41, 69, 85). In MCF-7, wild-type, and mutant Hepa 1c1c7 cells cotransfected with the Seap-pac and hER plasmids, 10 nM E2 induced an 8.4-, a 6.9-, and a 6.4-fold increases in secreted alkaline phosphatase activity, respectively. For cells cotreated with 10 nM E2 for 48 h plus 10 nM TCDD for different periods, TCDD caused a time-dependent decrease in secreted alkaline phosphatase activity in MCF-7 and wild-type Hepa 1c1c7 cells whereas no inhibitory effects were observed in class II mutant Hepa 1c1c7 cells. In MCF-7 cells treated with 10 nM TCDD alone and transfected with the Seap-pac plasmid, alkaline phosphatase activity was not significantly induced. Ten nanomolar TCDD was the optimum concentration for inhibition of E2-induced activity in all the transient transfection studies, and this concentration was not cytotoxic or growth inhibitory. Ten nanomolar E2 was also the optimal concentration which was used in all the transient transfection studies.

CAT assays and CAT mRNA levels. An ER/Sp1 sequence in the cathepsin D promoter (−199 to −165) has been cloned into a thymidine kinase-CAT plasmid (41), and the effects of E2, TCDD, and E2 plus TCDD on CAT activity in MCF-7 cells transiently cotransfected with this plasmid and the hER plasmid were determined (Fig. 3). The results show that E2 induced CAT activity (lane 2) and TCDD inhibited the E2-induced response (lane 3). In addition, cotreatment of MCF-7 cells with αNF (lanes 5 and 6), an Ah receptor antagonist, or cotransfection with a plasmid expressing antisense Arnt (lanes 7 through 10) resulted in reversal of the TCDD-mediated decrease in E2-induced CAT activity (lanes 5 and 9, respectively). TCDD inhibits E2-induced ER/Sp1 binding (lanes 2 and 3), and αNF reverses this inhibitory effect (lane 5). A plasmid containing mutations in the XRE (ER/Sp1-"*XRE*"-tk-CAT) was utilized to determine the role of this sequence in mediating the effects of TCDD (lanes 11 through 14). E2 induced CAT activity in the transient transfection assay using the mutant ER/Sp1-"*XRE*"-tk-CAT plasmid (lane 12), but TCDD did not significantly inhibit E2-induced CAT activity (lane 13) with this plasmid. These results show that the mutant ER/Sp1-"*XRE*"-tk-CAT plasmid retains E2 responsiveness; however, TCDD did not inhibit E2-induced CAT activity. These data indicate that an intact XRE is required for TCDD responsiveness.

In parallel experiments with MCF-7 cells, the effects of 10 nM TCDD on E2-induced CAT mRNA levels were also determined by Northern blot analysis (Table 2). The cells were treated with 10 nM E2 for 24 h and 10 nM TCDD for 2 h. The results show that in cells transiently transfected with the wild-type ER/Sp1-tk-CAT plasmid, E2 induced CAT mRNA levels and TCDD inhibited the E2-induced response. E2 also induced CAT activity in cells transiently transfected with the mutant ER/Sp1-"*XRE*"-tk-CAT plasmid; however, TCDD did not inhibit the hormone-induced response. These data also demonstrate that the plasmid-containing mutants with mutations in the XRE are not responsive to the effects of TCDD.

Electrophoretic mobility shift assays of nuclear extracts, transformed cytosol from MCF-7 cells, and in vitro-translated proteins using wild-type and mutant ER/Sp1 oligonucleotides. The results in Fig. 4 illustrate the pattern of retarded bands in electrophoretic mobility shift assays using the wild-type ER/Sp1 and the mutant ER/Sp1-"*XRE*" oligonucleotides in a titration experiment using TCDD (20 nM)- or DMSO-transformed cytosol from MCF-7 cells as previously reported (51). Incubation of wild-type [^{32}P]ER/Sp1 oligonucleotide (Fig. 4) with nuclear extracts from MCF-7 cells treated with DMSO, 10 nM E2, 10 nM TCDD alone, or 10 nM E2 (24 h) plus 10 nM TCDD for 1 h showed that relatively low levels of ER/Sp1 binding were observed in cells treated with DMSO and TCDD whereas E2 induced ER/Sp1 binding and TCDD rapidly inhibited the E2-induced response. In cells cotreated with E2, TCDD, and 1 μM αNF, the effects of TCDD on formation of

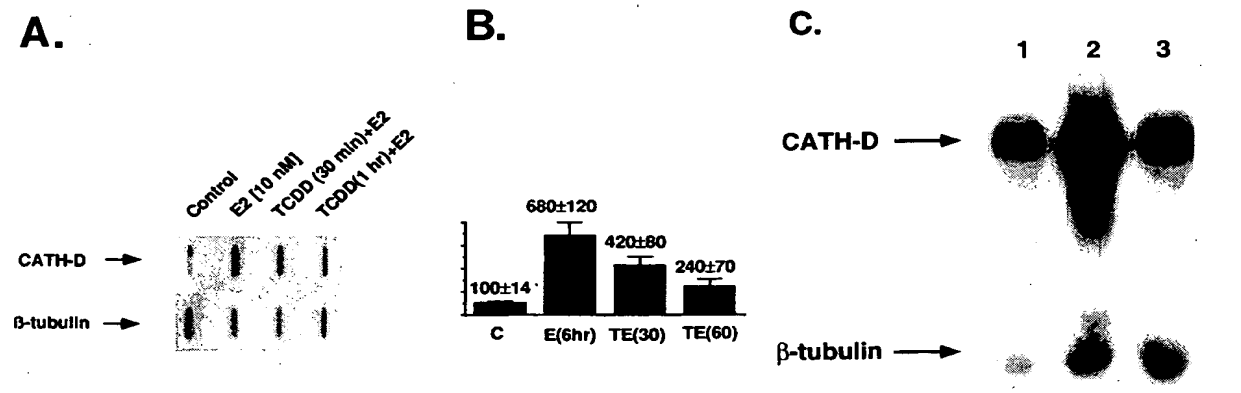

FIG. 2. Effect of 10 nM TCDD on the rate of E2-mediated cathepsin D (CATH-D) gene expression. (A) MCF-7 cells were treated with DMSO (control), 10 nM E2 (24 h), 10 nM TCDD (30 min) plus 10 nM E2, or 10 nM TCDD (1 h) plus 10 nM E2. Cotreated cells were treated with E2 for 24 h, and TCDD was added 30 min or 1 h prior to the end of this period. Cells in the various treatment groups were harvested at appropriate times, and nuclei were obtained and subjected to the nuclear run-on assay as described in Materials and Methods. The amount of newly transcribed mRNA was quantitated by slot blot analysis using a scanning laser densitometer. (B) Cathepsin D mRNA levels were normalized relative to β-tubulin in mRNA and expressed as means ± SD for three separate determinations. Cathepsin D mRNA levels in the different treatment groups were compared with levels in control cells, which were assigned a value of 100%. E2 significantly induced cathepsin D gene transcription after treatment for 6 h; TCDD significantly inhibited the E2-induced response within 30 [TE(30)] or 60 [TE(60)] min after addition ($P < 0.05$). (C) RNA was isolated from MCF-7 cells treated with DMSO (lane 1), 10 nM E2 alone for 24 h (lane 2), or 10 nM E2 for 24 h plus 10 nM TCDD for 1 h (lane 3). The Northern blot was visualized by autoradiography and quantitated by a Betagen Betascope blot analyzer as described for Fig. 1. Cathepsin D mRNA levels were normalized to β-tubulin mRNA for each treatment group, and the relative cathepsin D mRNA levels were 100 ± 12 (lane 1), 301 = 60 (lane 2), and 158 ± 16 (lane 3). The levels in cells treated with 10 nM TCDD alone were 156 ± 14 (data not shown). The results are expressed as means ± SD for three separate determinations. There was a significant decrease ($P < 0.05$) in cathepsin D mRNA levels in the cotreated cells compared with those treated with E2 alone.

the ER/Sp1 retarded band were reversed (data not shown). Coincubation of nuclear extracts from E2-induced MCF-7 cells with cytosol from MCF-7 cells transformed with DMSO resulted in minimal effects on ER/Sp1 binding, whereas coincubation with cytosol transformed with 20 nM TCDD resulted in a significant loss of ER/Sp1 binding. The same experiment was repeated with the mutated ER/Sp1-"*XRE*" oligonucleotide (Fig. 4), and the binding of nuclear extracts from E2-treated cells was not decreased after coincubation with DMSO- or TCDD-transformed cytosol; the intensities of the retarded ER-Sp1 complex were comparable after the mutant ER/Sp1-"*XRE*" was incubated with nuclear extracts from MCF-7 cells treated with 10 nM E2 or 10 nM E2 plus 10 nM TCDD for 1 h. These results demonstrate that the transformed or nuclear Ah receptor complexes blocked formation of the ER-Sp1 complex and this inhibitory response was dependent on an intact XRE sequence.

TABLE 1. Inhibition of E2-induced alkaline phosphatase activity by TCDD in MCF-7 and Hepa 1c1c7 cells transfected with the Seap-pac and hER plasmids[a]

Treatment (h)	Alkaline phosphatase activity (% of control)		
	MCF-7	Wild-type Hepa 1c1c7	Class II mutants
DMSO (48)	100 ± 1	100 ± 9	100 ± 14
E2 (48)	845 ± 89	690 ± 30	640 ± 100
E2 (48) + TCDD (1)	782 ± 87		
E2 (48) + TCDD (2)	629 ± 30[b]	435 ± 51[b]	501 ± 70
E2 (48) + TCDD (4)	515 ± 47[b]		
E2 (48) + TCDD (6)	311 ± 30[b]	316 ± 38[b]	657 ± 47
E2 (48) + TCDD (12)	245 ± 28[b]	268 ± 9[b]	595 ± 72
E2 (48) + TCDD (24)	153 ± 13[b]	115 ± 16[b]	601 ± 99
S1[c]	53 ± 13	37 ± 3	22 ± 14
RSV[d]	1,533 ± 240	1,250 ± 17	860 ± 72

[a] Cells were treated with 10 nM E2 alone for 48 h, and, in the cotreatment group, cells were treated with 10 nM E2 for 48 h and 10 nM TCDD was added at different time points prior to the end of the 48-h period. The cells were cotransfected with the Seap-pac and hER plasmids, and secreted alkaline phosphatase activity was determined as described in Materials and Methods. Treatment of cells with 10 nM TCDD alone for 12 h and the Seap-pac plasmid did not result in increased alkaline phosphatase activity compared with DMSO treatment; however, in cells transfected with the hER and Seap-pac plasmids and treated with 10 nM TCDD, there was a significant increase in alkaline phosphatase activity in MCF-7, wild-type, and mutant Hepa 1c1c7 cells (data not shown). The Ah receptor-independent responses were not further investigated.
[b] Significantly lower ($P < 0.05$) than the value for cells treated with E2 alone.
[c] Negative control.
[d] Positive control.

Figure 5A illustrates the results of SDS-polyacrylamide gel electrophoresis (SDS-PAGE) of nuclear extracts from MCF-7 cells cross-linked to a BrdU-ER/Sp1 oligonucleotide. Nuclear extracts from DMSO-treated cells did not form a cross-linked band (lane 2); incubation of nuclear extracts from cells treated with 10 nM TCDD plus 10 nM E2 and [^{32}P]BrdU-ER/Sp1 gave a 200-kDa cross-linked band (lane 3), and coincubation with a 100-fold excess of unlabeled DRE (lane 4) resulted in decreased formation of this band. Competition with a mutated DRE oligonucleotide (lane 5) did not decrease the intensity of the cross-linked band. Only weak, specifically bound cross-linked bands were observed with extracts from cells treated with 10 nM E2 or 10 nM TCDD alone (data not shown). In parallel experiments, cells were treated with 10 nM E2 and 10 nM [^{3}H]TCDD in the presence or absence of a 200-fold excess of unlabeled TCDF. After cross-linking and photoaffinity labeling followed by SDS-PAGE, the gels were sliced, and the specifically-bound radioactivity (^{3}H) was localized in the 200-kDa cross-linked band (Fig. 5B).

The binding of the Ah receptor complex to the ER/Sp1 oligonucleotide was further investigated with an Ah receptor complex formed by reconstituting the Ah receptor and Arnt proteins expressed in vitro by using the rabbit reticulocyte lysate system (Fig. 6). Direct binding of the reconstituted Ah receptor complex to [^{32}P]ER/Sp1 was not detected (data not

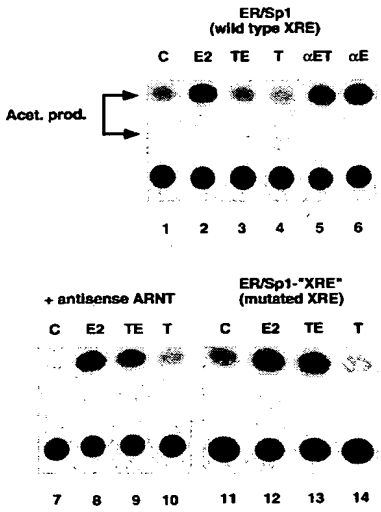

FIG. 3. Effects of TCDD, αNF, and antisense Arnt on E2-induced ER/Sp1-tk-CAT activity: requirement for a functional nuclear Ah receptor-Arnt complex and intact XRE sequence. MCF-7 cells were transiently transfected as described in Materials and Methods. Briefly, cells were seeded in DME-F12 media containing fetal bovine serum stripped twice, and were grown to 60% confluency. ER/Sp1-tk-CAT plasmids (10 μg) along with the hER plasmid (5 μg) or Arnt antisense plasmid (10 μg) were mixed in a solution containing Polybrene and added to the media. Cells were shocked after 12 h by using 15% glycerol in Hanks solution and dosed with DMSO (C), 10 nM E2, 10 nM TCDD plus 10 nM E2 (TE), 10 nM TCDD alone (T), 10 nM E2 plus 1 μM α-NF (αE), or 10 nM TCDD plus 10 nM E2 plus 1 μM α-NF (αET). After 48 h, cells were harvested and assayed for CAT (Acet.) activity. CAT activities relative to that for the control (lane 1, 100% ± 9%) were as follows: lane 2, 364 ± 29; lane 3, 102 ± 14; lane 4, 95 ± 12; lane 5, 372 ± 40; lane 6, 375 ± 35; lane 7, 100 ± 14; lane 8, 405 ± 28; lane 9, 325 ± 30; lane 10, 132 ± 12. Lanes 7 through 10, cells transfected with both the wild-type ER/Sp1-tk-CAT plasmid and the antisense Arnt expression plasmid. In a separate experiment, the mutant ER/Sp1-"*XRE*"-tk-CAT plasmid was utilized as described above, and relative CAT activities in cells treated with DMSO (assigned a value of 100%), E2, TCDD plus E2, and TCDD alone were 100 ± 14, 298 ± 30, 302 ± 42, and 95 ± 14, respectively (lanes 11 through 14). CAT activities in experiments using antisense Arnt DNA or 1 μM αNF were not significantly different from control values (data not shown). Results are expressed as means ± SD for three separate experiments.

FIG. 4. Effect of TCDD on ER/Sp1 binding: role of the XRE. Nuclear extracts from MCF-7 cells treated with DMSO (lanes C), 10 nM E2 alone for 24 h (lanes E), 10 nM TCDD for 1 h plus 10 nM E2 for 24 h (lanes TE1), or 10 nM TCDD alone for 1 h (lanes T) were isolated, incubated with the mutant [^{32}P]ER/Sp1-"*XRE*" or wild-type [^{32}P]ER/Sp1 oligonucleotide, and analyzed by electrophoretic mobility shift assays as described in Materials and Methods. Cytosolic extracts were obtained from MCF-7 cells and transformed in vitro with 20 nM TCDD or DMSO for 2 h at 25°C as previously described (51). Cytosol (100 μl) transformed with TCDD (lanes TE) or DMSO (lanes DE) was incubated with nuclear extracts from E2-treated cells plus [^{32}P]ER/Sp1 or mutant [^{32}P]ER/Sp1 oligonucleotide and analyzed by electrophoretic mobility shift assay. The retarded ER/Sp1 bands (arrow) were visualized by autoradiography and quantitated by a Molecular Dynamics 300A laser densitometer. The intensity values in lanes 2 through 12 relative to the control band (lane 1, 100% ± 15%) were 510 ± 42, 525 ± 30, 470 ± 22, 440 ± 35, 50 ± 7, 90 ± 9, 444 ± 42, 65 ± 17, 330 ± 23, 95 ± 11, and 80 ± 10 (means ± SD for three separate determinations), respectively. The intensities of the ER-Sp1 complexes in lanes 6, 7, 9, 11, and 12 were all significantly lower ($P < 0.05$) than that observed for complexes with extracts from E2-treated cells and the mutant (lane 2) or wild-type (lane 8) ER/Sp1 oligonucleotide. Previous studies have determined the binding specificity of the ER/Sp1 band (41).

shown), but a specifically bound complex was formed after incubation with [^{32}P]DRE (lane 1). The intensity of this retarded band was not decreased after coincubation with a 100-fold excess of ERE (lane 3), 100- or 400-fold excess of ER/Sp1-"*XRE*" (lanes 6 and 7), or 100-fold excess of mutated DRE (data not shown). In contrast, competition with 100-fold excess DRE (lane 2) or 100- or 400-fold excess of ER/Sp1 (lanes 4 and 5) decreased formation of the specifically bound DRE-Ah receptor complex retarded band. These results with in vitro-expressed Ah receptor and Arnt proteins confirm the interaction of the Ah receptor-Arnt heterodimer with the XRE sequence located within the cathepsin D ER/Sp1 oligonucleotide.

TABLE 2. Inhibition of E2-induced CAT mRNA levels by TCDD in MCF-7 cells transiently cotransfected with the hER and ER/Sp1-tk-CAT or ER/Sp1-"*XRE*"-tk-CAT plasmids[a]

Treatment (h)	Relative % CAT mRNA	
	ER/Sp1-tk-CAT	ER/Sp1-"*XRE*"-tk-CAT
DMSO	100 ± 20	100 ± 15
E2 (10)	278 ± 30	327 ± 21
TCDD (2)	120 ± 12	114 ± 15
E2 (10) + TCDD (2)	95 ± 19[b]	348 ± 31

[a] Cells were cotransfected with the hER and ER/Sp1-tk-CAT or mutant ER/Sp1-"*XRE*"-tk-CAT plasmids and treated with 10 nM E2 for 10 h and 10 nM TCDD for 2 h prior to the end of the 10-h incubation period as described in Materials and Methods. CAT mRNA levels were determined by Northern blot analysis (standardized relative to β-tubulin mRNA), and the relative CAT mRNA levels are given as means ± SD for three separate determinations.

[b] Significantly lower ($P < 0.05$) than the value for cells treated with E2 alone.

DISCUSSION

Several studies report that TCDD and related compounds inhibit a number of E2-induced responses (2, 3, 22–25, 30, 32, 38, 40, 66, 84a, 85) including secretion of procathepsin D and cathepsin D in MCF-7 cells. Studies using wild-type Ah-responsive and mutant Ah-nonresponsive MCF-7 cells showed that formation of a transcriptionally active nuclear Ah receptor was required for inhibition of E2-induced secretion of procathepsin D by TCDD (51). Moreover, there was a good correlation between the structure-Ah receptor binding affinities for several Ah receptor agonists and their structure-dependent inhibition of this E2-induced secretory protein (40). This study further investigates the molecular mechanism of action of

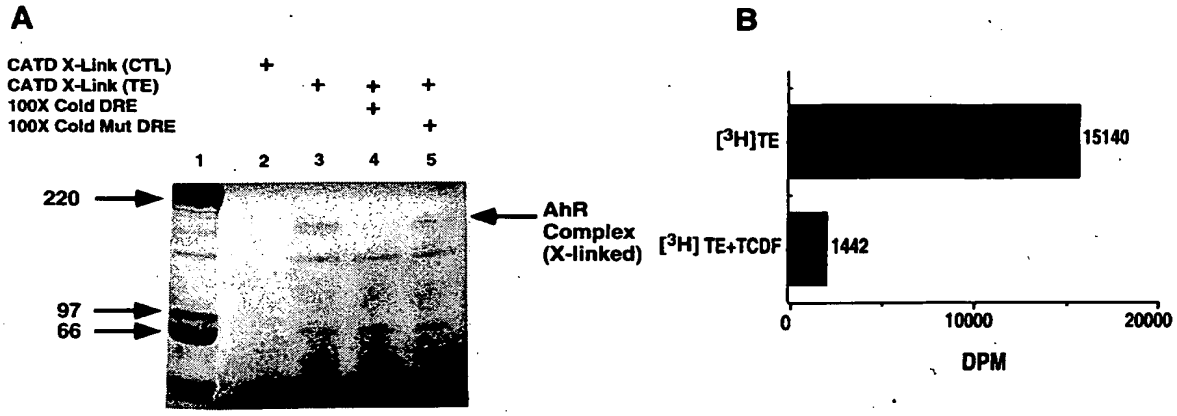

FIG. 5. Cross-linking of the nuclear Ah receptor complex with BrdU-ER/Sp1. (A) The BrdU-ER/Sp1 oligonucleotide was incubated with nuclear extracts from cells treated with DMSO (control [CTL]) (lane 2), TCDD plus E2 (TE) (lane 3), or TCDD plus E2 in the presence of 100-fold excess of unlabeled wild-type DRE (lane 4) or mutant (Mut) DRE (lane 5). Incubation, cross-linking, and electrophoresis of the cross-linked complexes were carried out as described in Materials and Methods. The 200-kDa cross-linked (X-linked) Ah receptor complexes (arrow) were visualized by autoradiography and quantitated by using a Sharp SX-330 scanner and Scanalytics (Billerica, Mass.) ZERO-Dscan software. Molecular weights were determined with ^{14}C-labeled protein standards purchased from Amersham Corp. (lane 1). The band intensity values in lanes 3 to 5 relative to the control (lane 2, 100% ± 37%) were 404 ± 14, 121 ± 2, and 346 ± 5, respectively; the results are means ± SD for three determinations. CATD, cathepsin D. (B) Nuclear extracts were obtained as described in Materials and Methods from MCF-7 cells treated with 10 nM [^{3}H]TCDD plus 10 nM E2 alone or in combination with a 200-fold excess of TCDF. Incubation, cross-linking, and electrophoresis were carried out, and the regions corresponding to the cross-linked complex were excised for the two treatment groups, extracted with Solvable (Dupont), and counted in a liquid scintillation counter. The values obtained were 15,140 dpm ([^{3}H]TCDD plus E2) and 1,442 dpm ([^{3}H]TCDD plus E2 plus TCDF). Background levels (520 dpm) were subtracted to give the net dpm values for the 200-kDa band. The only radioactive (^{3}H) band on the gel was associated with the photoaffinity-labeled 200-kDa cross-linked band.

TCDD as an antiestrogen and utilizes the E2-responsive cathepsin D gene as a model.

The results summarized in Fig. 1 and 2 demonstrate that E2 induced intracellular immunoreactive cathepsin D levels, cathepsin D mRNA levels, and the rate of cathepsin D gene transcription in nuclear run-on assays. In cells cotreated with E2 plus TCDD, all of the induced responses were significantly inhibited within 0.2 to 2 h after treatment with TCDD, suggesting that TCDD induces an early gene product which affects cathepsin D gene transcription at some level or there is a direct interaction of the nuclear Ah receptor complex with protein and/or DNA elements involved in transactivation of this gene.

Deletion analysis of the 5′-flanking region of the cathepsin D gene identified several nonconsensus ERE sequences and an E2-responsive region from −252 to −124 (4). The Seap-pac plasmid containing the −296/+59 5′-flanking sequence from the cathepsin D gene (63) was used to determine the effects of TCDD on E2-induced secreted alkaline phosphatase activity in cells transiently transfected with this plasmid (Table 1). In Ah-responsive human MCF-7 and wild-type mouse Hepa 1c1c7 cells transiently transfected with the Seap-pac and hER plasmids, E2 induces secreted alkaline phosphatase activity and TCDD inhibited the induced response within 2 h after treatment. In contrast, TCDD did not inhibit E2-induced alkaline phosphatase activity in the class II mutant Hepa 1c1c7 cell line, which expresses the Ah receptor but does not form transcriptionally active nuclear Ah receptor complexes (50). These results confirm that the antiestrogenic response requires a functional nuclear Ah receptor complex and genomic sequences within the −296/+59 region are sufficient for mediating the TCDD-induced inhibitory response.

Results of previous studies suggest that formation of ER-Sp1 complexes regulates E2-induced transactivation of the *c-myc*, creatine kinase B, and cathepsin D genes (18, 41, 84). An ER-Sp1 complex, GGGCGGn_{23}ACGGG, was previously identified (−199 to −165) in the cathepsin D promoter (41), and further analysis of this sequence has identified an XRE, namely

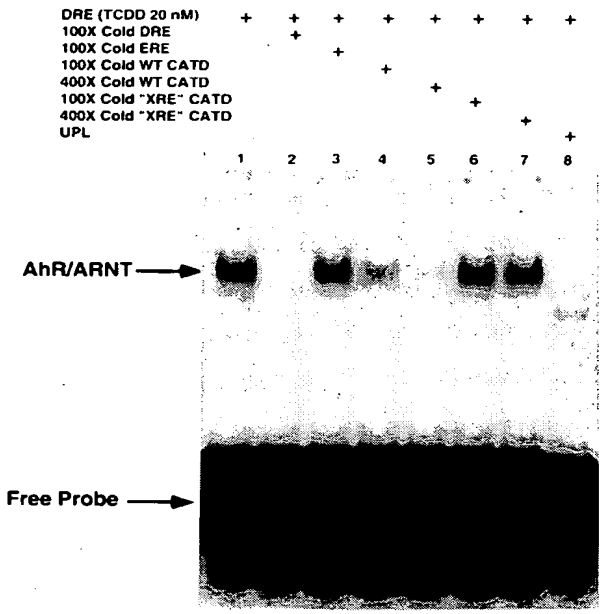

FIG. 6. Electrophoretic mobility shift assays using in vitro-translated Ah receptor and Arnt. In vitro-translated proteins were obtained as described in Materials and Methods. Ah receptor (3 μl) and Arnt (3 μl) or unprogrammed rabbit reticulocyte lysate (UPL) (6 μl) were incubated in the presence of 20 nM TCDD for 2 h at 25°C. The preincubated proteins were then subjected to gel electrophoretic mobility shift assay using a ^{32}P-labeled DRE oligonucleotide. The retarded band (lane 1) (arrow) was blocked with a 100-fold excess of an unlabeled DRE oligonucleotide (lane 2), 100-fold excess of an unlabeled ERE oligonucleotide (lane 3), 100- or 400-fold excess of an unlabeled ER/Sp1 (wild-type cathepsin D [WT CATD]) oligonucleotide (lanes 4 and 5), or 100- or 400-fold excess of an unlabeled ER/Sp1-*"XRE"* ("XRE" CATD) oligonucleotide (lanes 6 and 7). In the absence of ligand, a specifically bound, but less intense, retarded band (20 to 25% the intensity of the band in lane 1) was observed (data not shown).

GTGCGTG (−175/−181), located between the genomic sequences which bind the ER and Sp1 proteins. The potential role of this XRE as a critical target site for mediating the antiestrogenic effects of TCDD was therefore investigated by utilizing the wild-type ER/Sp1 and a mutant ER/Sp1-"*XRE*" oligonucleotide in electrophoretic mobility shift assays and in transient transfection assays in which these oligonucleotides were cloned into plasmids with a thymidine kinase promoter and a CAT reporter gene. The results in Fig. 4 illustrate that nuclear extracts from MCF-7 cells treated with 10 nM E2 formed a retarded ER-Sp1 complex with both wild-type ER/Sp1 (lane 8) and mutant ER/Sp1-"*XRE*" (lane 2) oligonucleotides. Electrophoretic mobility shift assays of nuclear extracts from cells treated with 10 nM E2 (24 h) plus 10 nM TCDD for 1 h showed that TCDD blocked formation of a retarded band with the wild-type ER/Sp1 (Fig. 4, lane 12) but not the mutant ER/Sp1-"*XRE*" (Fig. 4, lane 5) oligonucleotide. The role of the Ah receptor heterodimer in destabilizing formation of the ER-Sp1 complex was further investigated by incubating nuclear extracts from E2-treated MCF-7 cells with cytosolic extracts treated with DMSO or 20 nM TCDD, which transforms the cytosolic Ah receptor to an XRE-binding form indistinguishable from the nuclear Ah receptor complex (51). The transformed cytosolic Ah receptor decreased formation of the ER-Sp1 complex (Fig. 4, lane 11), whereas formation of the ER-Sp1 complex was not affected by addition of transformed Ah receptor complex using the mutant ER/Sp1-"*XRE*" oligonucleotide (Fig. 4, lane 4). Thus, disruption of the ER-Sp1 complex requires (i) the intact XRE sequence located between the ER and Sp1 genomic binding sites in the cathepsin D promoter and (ii) the presence of transformed or nuclear Ah receptor complex (T and TE1 lanes, respectively, with the ER/Sp1 oligonucleotide; Fig. 4).

The results of the gel electrophoretic mobility shift assays did not show a retarded band associated with direct binding of the transformed or nuclear Ah receptor complex with the wild-type ER/Sp1 oligonucleotide (Fig. 4). This may be due to increased protein-DNA dissociation which can result in loss of a retarded band in the assay system. Therefore, two additional experiments were performed to investigate binding of the Ah receptor complex to the DRE located within the ER/Sp1 oligonucleotide (Fig. 5 and 6). Cross-linking experiments with the BrdU-ER/Sp1 oligonucleotide showed that a specifically bound TCDD-induced 200-kDa cross-linked complex was formed only with nuclear extracts from MCF-7 cells treated with E2 plus TCDD (Fig. 5A, lane 3). Competition with excess unlabeled DRE oligonucleotide decreased formation of the cross-linked band (lane 4), whereas competition with mutant DRE had minimal effect (lane 5). In this study, only one major specifically bound cross-linked 200-kDa band was observed, and this was consistent with results obtained with MCF-7 and T47D breast cancer cells (78). Previous studies have demonstrated that UV irradiation of the nuclear Ah receptor complex bound with [^{3}H]TCDD results in photoaffinity labeling of the Ah receptor (77). In parallel cross-linking experiments using the BrdU-ER/Sp1 oligonucleotide and nuclear extracts from cells treated with [^{3}H]TCDD plus E2, the specifically bound radioactivity (^{3}H) was localized in the 200-kDa band (Fig. 5B). Thus, formation of the cross-linked complex (Fig. 5A) was induced by TCDD only in cells cotreated with E2, suggesting that E2-induced formation of the ER-Sp1 complex is required to facilitate accessibility and interaction of the Ah receptor complex with the XRE site; these data are consistent with results showing that disruption of the retarded ER-Sp1 band (Fig. 4) by the nuclear Ah receptor complex required an intact XRE and occurred only in extracts from cells cotreated with TCDD plus E2.

The data in Fig. 6 also confirm competitive binding of the reconstituted Ah receptor-Arnt heterodimer with in vitro-translated proteins. Unlabeled DRE (lane 2) and unlabeled ER/Sp1 (lanes 4 and 5) oligonucleotides competitively decrease formation of the retarded [^{32}P]DRE-Ah receptor complex. In contrast, competition with the ER/Sp1-"*XRE*" oligonucleotide (lanes 6 and 7), which contains mutations in the XRE sequence, does not decrease formation of the retarded band. Thus, in competitive binding studies, wild-type ER/Sp1 competitively decreased formation of the DRE-Ah receptor complex retarded band, confirming the competitive binding affinity of the ER/Sp1 oligonucleotide with the Ah receptor/Arnt heterodimer.

The results obtained in transient transfection studies using the wild-type ER/Sp1-tk-CAT and mutant ER/Sp1-"*XRE*"-tk-CAT plasmids (Fig. 3) complement the results of electrophoretic mobility shift assays and confirm that the antiestrogenic activity of TCDD requires a nuclear Ah receptor complex and an intact XRE sequence within the ER/Sp1 oligonucleotide. TCDD inhibited E2-induced CAT activity and mRNA levels (Table 2) in MCF-7 cells transiently transfected with the ER/Sp1-tk-CAT construct (Fig. 3, lane 3), whereas no inhibition of CAT activity or mRNA levels was observed with the mutant ER/Sp1-"*XRE*"-tk-CAT construct (Fig. 3, lane 13) containing C→A mutations in the XRE (antisense strand). In addition, αNF, an Ah receptor antagonist which inhibits formation of the nuclear Ah receptor complex (49) (Fig. 3, lane 5) and expression of antisense Arnt mRNA (Fig. 3, lane 9), blocked the antiestrogenic activity of TCDD.

In summary, the results of in vitro binding and induction assays using wild-type and mutated 5′-flanking ER/Sp1 sequences indicate that the core XRE sequence located between the ER and Sp1 genomic binding sites in the cathepsin D promoter is required for disruption of the E2-induced ER-Sp1 complex by TCDD. These data demonstrate a unique Ah receptor-mediated mechanism of action in which direct interaction of the nuclear Ah receptor complex with a strategically located XRE results in decreased transcription of an E2-induced gene. Binding to an XRE sequence may also be important for inhibition of E2-induced pS2 gene expression by TCDD (84a), and it is possible that similar mechanisms may play a role in cell-specific inhibition of other genes by Ah receptor agonists (82). The mechanisms associated with inhibition of other E2- and mitogen-induced genes by TCDD in breast cancer cell lines are unknown and are currently being investigated in this laboratory.

ACKNOWLEDGMENTS

The financial assistance of the National Institutes of Health (grant ES04176) is gratefully acknowledged. S. Safe is a Sid Kyle Endowed Professor.

REFERENCES

1. **Asman, D. C., K. Takimoto, H. C. Pitot, T. J. Dunn, and R. Lindahl.** 1993. Organization and characterization of the rat class 3 aldehyde dehydrogenase gene. J. Biol. Chem. 268:12530–12536.
2. **Astroff, B., B. Eldridge, and S. Safe.** 1991. Inhibition of 17β-estradiol-induced and constitutive expression of the cellular protooncogene c-*fos* by 2,3,7,8-tetrachlorodibenzo-*p*-dioxin (TCDD) in the female uterus. Toxicol. Lett. 56:305–315.
3. **Astroff, B., C. Rowlands, R. Dickerson, and S. Safe.** 1990. 2,3,7,8-Tetrachlorodibenzo-*p*-dioxin inhibition of 17β-estradiol-induced increases in rat uterine EGF receptor binding activity and gene expression. Mol. Cell. Endocrinol. 72:247–252.

4. **Augereau, P., F. Miralles, V. Cavailles, and C. Gaudelet.** 1994. Characterization of the proximal estrogen-responsive element of human cathepsin D gene. Mol. Endocrinol. **8**:693–703.
5. **Berger, J., J. Hauber, R. Gieger, and B. R. Cullen.** 1988. Secreted alkaline phosphatase: a novel reporter gene with unique applications. Gene **66**:1–10.
6. **Bradford, M. M.** 1976. A rapid and sensitive method for the quantitation of microgram quantities of protein utilizing the principle of protein-dye binding. Anal. Biochem. **72**:248–254.
7. **Burbach, K. M., A. B. Poland, and C. A. Bradfield.** 1992. Cloning of the Ah-receptor cDNA reveals a distinctive ligand-activated transcription factor. Proc. Natl. Acad. Sci. USA **89**:8185–8189.
8. **Cavailles, V., P. Augereau, M. Garcia, and H. Rochefort.** 1988. Estrogens and growth factors induce mRNA of the 52K-pro-cathepsin-D secreted by breast cancer cells. Nucleic Acids Res. **16**:1903–1919.
9. **Cavailles, V., P. Augereau, and H. Rochefort.** 1991. Cathepsin D gene of human MCF-7 cells contains estrogen-responsive sequences in its 5′-proximal flanking region. Biochem. Biophys. Res. Commun. **174**:816–824.
10. **Cavailles, V., P. Augereau, and H. Rochefort.** 1993. Cathepsin D gene is controlled by a mixed promoter, and estrogens stimulate only TATA-dependent transcription. Proc. Natl. Acad. Sci. USA **90**:203–207.
11. **Cavailles, V., M. Garcia, and H. Rochefort.** 1989. Regulation of cathepsin D and pS2 gene expression by growth factors in MCF-7 human breast cancer cells. Mol. Endocrinol. **3**:552–558.
12. **Chomczynski, P., and N. Sacchi.** 1987. Single step method of RNA isolation by acid guanidium thiocyanatephenol-chloroform extraction. Anal. Biochem. **162**:156–159.
13. **Cuthill, S., A. Wilhelmsson, and L. Poellinger.** 1991. Role of the ligand in intracellular receptor function: receptor affinity determines activation in vitro of the latent dioxin receptor to a DNA-binding form. Mol. Cell. Biol. **11**:401–411.
14. **Dauvois, S., P. S. Danielian, R. White, and M. G. Parker.** 1992. Antiestrogen ICI 164,384 reduces cellular estrogen receptor content by increasing its turnover. Proc. Natl. Acad. Sci. USA **89**:4037–4041.
15. **Denison, M. S., J. M. Fisher, and J. P. Whitlock, Jr.** 1988. Inducible, receptor-dependent protein-DNA interactions at a dioxin-responsive transcriptional enhancer. Proc. Natl. Acad. Sci. USA **85**:2528–2532.
16. **Denison, M. S., J. M. Fisher, and J. P. Whitlock, Jr.** 1988. The DNA recognition site for the dioxin-Ah receptor complex. J. Biol. Chem. **263**: 17221–17224.
17. **Denison, M. S., H. I. Swanson, P. A. Bank, and E. V. Yao.** 1994. Interaction of transformed Ah receptor complex with a dioxin-responsive element and modulation of gene expression. Toxicologist **14**:238.
18. **Dubik, D., and R. P. C. Shiu.** 1992. Mechanism of estrogen activation of c-*myc* oncogene expression. Oncogene **7**:1587–1594.
19. **Elferink, C. J., T. A. Gasiewicz, and J. P. Whitlock, Jr.** 1990. Protein-DNA interactions at a dioxin-responsive enhancer. Evidence that the transformed Ah receptor is heteromeric. J. Biol. Chem. **265**:20708–20712.
20. **Gaido, K. W., S. C. Maness, L. S. Leonard, and W. F. Greenlee.** 1992. 2,3,7,8-Tetrachlorodibenzo-*p*-dioxin-dependent regulation of transforming growth factors-α and β_2 expression in a human keratinocyte cell line involves both transcriptional and post-transcriptional control. J. Biol. Chem. **267**: 24591–24595.
21. **Gallo, M. A., E. J. Hesse, G. J. MacDonald, and T. H. Umbreit.** 1986. Interactive effects of estradiol and 2,3,7,8-tetrachlorodibenzo-*p*-dioxin on hepatic cytochrome P-450 and mouse uterus. Toxicol. Lett. **32**:123–132.
22. **Gierthy, J. F., J. A. Bennett, L. M. Bradley, and D. S. Cutler.** 1993. Correlation of *in vitro* and *in vivo* growth suppression of MCF-7 human breast cancer by 2,3,7,8-tetrachlorodibenzo-*p*-dioxin. Cancer Res. **53**:3149–3153.
23. **Gierthy, J. F., and D. W. Lincoln.** 1988. Inhibition of postconfluent focus production in cultures of MCF-7 breast cancer cells by 2,3,7,8-tetrachlorodibenzo-*p*-dioxin. Breast Cancer Res. **12**:227–233.
24. **Gierthy, J. F., D. W. Lincoln, M. B. Gillespie, J. I. Seeger, H. L. Martinez, H. W. Dickerman, and S. A. Kumar.** 1987. Suppression of estrogen-regulated extracellular plasminogen activator activity of MCF-7 cells by 2,3,7,8-tetrachlorodibenzo-*p*-dioxin. Cancer Res. **47**:6198–6203.
25. **Gierthy, J. F., D. W. Lincoln, K. E. Roth, S. S. Bowser, J. A. Bennett, L. Bradley, and H. W. Dickerman.** 1991. Estrogen-stimulation of postconfluent cell accumulation and foci formation of human MCF-7 breast cancer cells. J. Cell. Biochem. **45**:177–187.
26. **Goldstein, J. A., and S. Safe.** 1989. Mechanism of action and structure-activity relationships for the chlorinated dibenzo-*p*-dioxins and related compounds, p. 239–293. *In* R. D. Kimbrough and A. A. Jensen (ed.), Halogenated biphenyls, naphthalenes, dibenzodioxins and related compounds. Elsevier-North Holland, Amsterdam.
27. **Gonzalez, F. J., and D. W. Nebert.** 1985. Autoregulation plus upstream positive and negative control regions associated with transcriptional activation of the mouse cytochrome P_1-450 gene. Nucleic Acids Res. **13**:7269–7288.
28. **Gorman, C. M., L. F. Moffat, and B. H. Howard.** 1982. Recombinant genomes which express chloramphenicol acetyltransferase in mammalian cells. Mol. Cell. Biol. **2**:1044–1051.
29. **Hankinson, O.** 1993. Perspectives in biochemistry and biophysics: research on the aryl hydrocarbon (dioxin) receptor is primed to take off. Arch. Biochem. Biophys. **300**:1–5.
30. **Harper, N., X. Wang, H. Liu, and S. Safe.** 1994. Inhibition of estrogen-induced progesterone receptor in MCF-7 human breast cancer cells by aryl hydrocarbon (Ah) receptor agonists. Mol. Cell. Endocrinol. **104**:47–55.
31. **Hoffman, E. C., H. Reyes, F. Chu, F. Sander, L. H. Conley, B. A. Brooks, and O. Hankinson.** 1991. Cloning of a factor required for activity of the Ah (dioxin) receptor. Science **252**:954–958.
32. **Holcomb, M., and S. Safe.** 1994. Inhibition of 7,12-dimethylbenzanthracene-induced rat mammary tumor growth by 2,3,7,8-tetrachlorodibenzo-*p*-dioxin. Cancer Lett. **82**:43–47.
33. **Hudson, L. G., W. A. Toscano, Jr., and W. F. Greenlee.** 1985. Regulation of epidermal growth factor binding in a human keratinocyte cell line by 2,3,7,8-tetrachlorodibenzo-*p*-dioxin. Toxicol. Appl. Pharmacol. **77**:251–259.
34. **Israel, D. I., and J. P. Whitlock, Jr.** 1984. Regulation of cytochrome P_1-450 gene transcription by 2,3,7,8-tetrachlorodibenzo-*p*-dioxin in wild type and variant mouse hepatoma cells. J. Biol. Chem. **259**:5400–5402.
35. **Jaiswal, A. K.** 1994. Human NAD(P)H:quinone oxidoreductase: gene structure, activity and tissue-specific expression. J. Biol. Chem. **269**:14502–14508.
36. **Kärenlampi, S. O., H. J. Eisen, O. Hankinson, and D. W. Nebert.** 1983. Effects of cytochrome P_1-450 inducers on the cell-surface receptors for epidermal growth factor, phorbol 12,13-dibutyrate, or insulin of cultured mouse hepatoma cells. J. Biol. Chem. **258**:10378–10383.
37. **Klein-Hitpass, L., M. Schorpp, U. Wagner, and G. U. Ryffel.** 1986. An estrogen-responsive element derived from the 5′-flanking region of the xenopus vitellogenin A2 gene functions in transfected human cells. Cell **46**: 1053–1061.
38. **Kociba, R. J., D. G. Keyes, J. E. Beger, R. M. Carreon, C. E. Wade, D. A. Dittenber, R. P. Kalnins, L. E. Frauson, C. L. Park, S. D. Barnard, R. A. Hummel, and C. G. Humiston.** 1978. Results of a 2-year chronic toxicity and oncogenicity study of 2,3,7,8-tetrachlorodibenzo-*p*-dioxin (TCDD) in rats. Toxicol. Appl. Pharmacol. **46**:279–303.
39. **Krishnan, V., T. R. Narasimhan, and S. Safe.** 1992. Development of gel staining techniques for detecting the secretion of procathepsin D (52-kDa protein) in MCF-7 human breast cancer cells. Anal. Biochem. **204**:137–142.
40. **Krishnan, V., and S. Safe.** 1993. Polychlorinated biphenyls (PCBs), dibenzo-*p*-dioxins (PCDDs) and dibenzofurans (PCDFs) as antiestrogens in MCF-7 human breast cancer cells: quantitative structure-activity relationships. Toxicol. Appl. Pharmacol. **120**:55–61.
41. **Krishnan, V., X. Wang, and S. Safe.** 1994. ER/Sp1 complexes mediate estrogen-induced cathepsin D gene expression in MCF-7 human breast cancer cells. J. Biol. Chem. **269**:15912–15917.
42. **Landers, J. P., and N. J. Bunce.** 1991. The Ah receptor and the mechanism of dioxin toxicity. Biochem. J. **276**:273–287.
43. **Madhukar, B. V., D. W. Brewster, and F. Matsumura.** 1984. Effects of *in vivo*-administered 2,3,7,8-tetrachlorodibenzo-*p*-dioxin on receptor binding of epidermal growth factor in the hepatic plasma membrane of rat, guinea pig, mouse, and hamster. Proc. Natl. Acad. Sci. USA **81**:7407–7411.
44. **Manchester, D. K., S. K. Gordon, C. L. Golas, E. A. Roberts, and A. B. Okey.** 1987. Ah receptor in human placenta: stabilization by molybdate and characterization of binding of 2,3,7,8-tetrachlorodibenzo-*p*-dioxin, 3-methylcholanthrene, and benzo[a]pyrene. Cancer Res. **47**:4861–4868.
45. **Marzluff, W. F.** 1978. Transcription of RNA in isolated nuclei. Methods Cell Biol. **19**:317–331.
46. **May, F. E. B., D. J. Smith, and B. R. Westley.** 1993. The human cathepsin D-encoding gene is transcribed from an estrogen-regulated and a constitutive start point. Gene **134**:277–282.
47. **May, F. E. B., and B. R. Westley.** 1987. Effects of tamoxifen and 4-hydroxytamoxifen on the pNR-1 and pNR-2 estrogen regulated RNAs in human breast cancer cells. J. Biol. Chem. **262**:15894–15899.
48. **McGuire, J., M. L. Whitelaw, I. Pongratz, J.-Å. Gustafsson, and L. Poellinger.** 1994. A cellular factor stimulates ligand-dependent release of hsp90 from the basic helix-loop-helix dioxin receptor. Mol. Cell. Biol. **14**:2438–2446.
49. **Merchant, M., V. Krishnan, and S. Safe.** 1993. Mechanism of action of α-naphthoflavone as an Ah receptor antagonist in MCF-7 human breast cancer cells. Toxicol. Appl. Pharmacol. **120**:179–185.
50. **Miller, A. G., D. Israel, and J. P. Whitlock, Jr.** 1983. Biochemical and genetic analysis of variant mouse hepatoma cells defective in the induction of benzo[a]pyrene-metabolizing enzyme activity. J. Biol. Chem. **258**:3523–3527.
51. **Moore, M., X. Wang, Y. Lu, M. Wormke, A. Craig, J. Gerlach, R. Burghardt, and S. Safe.** 1994. Benzo[a]pyrene resistant (BaP^R) human breast cancer cells: a unique aryl hydrocarbon (Ah)-nonresponsive clone. J. Biol. Chem. **269**:11751–11759.
52. **Morisset, M., F. Capony, and H. Rochefort.** 1986. Processing and estrogen regulation of the 52-kDa protein inside MCF-7 breast cancer cells. Endocrinology **119**:2773–2782.
53. **Nebert, D. W., D. D. Petersen, and A. Puga.** 1991. Human *AH* locus polymorphism and cancer: inducibility of *CYP1A1* and other genes by combustion products and dioxin. Pharmacogenetics **1**:68–78.
54. **Okey, A. B., D. S. Riddick, and P. A. Harper.** 1994. The Ah receptor: mediator of the toxicity of 2,3,7,8-tetrachlorodibenzo-*p*-dioxin (TCDD) and

related compounds. Toxicol. Lett. 70:1–22.
55. **Perdew, G. H.** 1988. Association of the Ah receptor with the 90-kDa heat shock protein. J. Biol. Chem. 263:13802–13805.
56. **Pimental, R. A., B. Liang, G. K. Yee, A. Wilhelmsson, L. Poellinger, and K. E. Paulson.** 1993. Dioxin receptor and C/EBP regulate the function of the glutathione *S*-transferase Ya gene xenobiotic response element. Mol. Cell. Biol. 13:4365–4373.
57. **Piskorska-Pliszczynska, J., B. Keys, S. Safe, and M. S. Newman.** 1986. The cytosolic receptor binding affinities and AHH induction potencies of 29 polynuclear aromatic hydrocarbons. Toxicol. Lett. 34:67–74.
58. **Poland, A., E. Glover, and A. S. Kende.** 1976. Stereospecific, high affinity binding of 2,3,7,8-tetrachlorodibenzo-*p*-dioxin by hepatic cytosol: evidence that the binding species is receptor for induction of aryl hydrocarbon hydroxylase. J. Biol. Chem. 251:4936–4946.
59. **Poland, A., and J. C. Knutson.** 1982. 2,3,7,8-Tetrachlorodibenzo-*p*-dioxin and related halogenated aromatic hydrocarbons. Examinations of the mechanism of toxicity. Annu. Rev. Pharmacol. Toxicol. 22:517–554.
60. **Pongratz, I., G. G. F. Mason, and L. Poellinger.** 1992. Dual roles of the 90 kDa heat shock protein Hsp 90 in modulating functional activities of the dioxin receptor. J. Biol. Chem. 267:13728–13734.
61. **Probst, M. R., S. Reisz-Porszasz, R. V. Agbunag, M. S. Ong, and O. Hankinson.** 1993. Role of the aryl hydrocarbon receptor nuclear translocation protein in aryl hydrocarbon (dioxin) receptor action. Mol. Pharmacol. 44:511–518.
62. **Quattrochi, L. C., and R. H. Tukey.** 1989. The human cytochrome *CYP1A2* gene contains regulatory elements responsive to 3-methylcholanthrene. Mol. Pharmacol. 36:66–71.
63. **Redecker, B., B. Heckendorf, H. Grosch, G. Mersmann, and A. Hasilik.** 1991. Molecular organization of the human cathepsin D gene. DNA Cell Biol. 10:423–431.
64. **Rushmore, T. H., R. G. King, K. E. Paulson, and C. B. Pickett.** 1990. Regulation of glutathione S-transferase Ya subunit gene expression: identification of a unique xenobiotic-responsive element controlling inductible expression by planar aromatic compounds. Proc. Natl. Acad. Sci. USA 87: 3826–3830.
65. **Safe, S.** 1988. The aryl hydrocarbon (Ah) receptor. ISI atlas of science. Pharmacology 2:78–83.
66. **Safe, S., B. Astroff, M. Harris, T. Zacharewski, R. Dickerson, M. Romkes, and L. Biegel.** 1991. 2,3,7,8-Tetrachlorodibenzo-*p*-dioxin (TCDD) and related compounds as antiestrogens: characterization and mechanism of action. Pharmacol. Toxicol. 69:400–409.
67. **Safe, S., S. Bandiera, T. Sawyer, B. Zmudzka, G. Mason, M. Romkes, M. A. Denomme, J. Sparling, A. B. Okey, and T. Fujita.** 1985. Effects of structure on binding to the 2,3,7,8-TCDD receptor protein and AHH induction—halogenated biphenyls. Environ. Health Perspect. 61:21–33.
68. **Sambrook, J., E. F. Fritsch, and T. Maniatis.** 1989. Molecular cloning: a laboratory manual, 2nd ed. Cold Spring Harbor Laboratory Press, Cold Spring Harbor, N.Y.
69. **Savouret, J. F., A. Bailly, M. Misrahi, C. Rarch, G. Redeuilh, A. Chaucherau, and E. Milgram.** 1991. Characterization of the hormone responsive element involved in the regulation of the progesterone receptor gene. EMBO J. 10:1875–1883.
70. **Sogawa, K., A. Fujisawa-Sehara, M. Yamane, and Y. Fujii-Kuriyama.** 1986. Location of regulatory elements responsible for drug induction in the rat cytochrome P-450c gene. Proc. Natl. Acad. Sci. USA 83:8044–8048.
71. **Spyratos, R., J. Brouillet, A. DeFrenne, K. Hacene, J. Rouesse, T. Maudelande, M. Brunet, C. Andrieu, A. Desplaces, and H. Rochefort.** 1989. Cathepsin D: an independent prognostic factor for metastasis of breast cancer. Lancet ii:115–118.
72. **Stahl, B. U., D. G. Beer, L. W. D. Weber, and K. Rozman.** 1993. Reduction of hepatic phosphoenolpyruvate carboxykinase (PEPCK) activity by 2,3,7,8-tetrachlorodibenzo-*p*-dioxin (TCDD) is due to decreased mRNA levels. Toxicology 79:81–95.
73. **Swanson, H. I., and C. A. Bradfield.** 1993. The Ah-receptor: genetics, structure and function. Pharmacogenetics 3:213–223.
74. **Tandon, A. K., G. M. Clark, G. C. Chamness, J. M. Chirgwin, and W. L. McGuire.** 1990. Cathepsin D and prognosis in breast cancer. N. Engl. J. Med. 322:297–302.
75. **Thorpe, S. M., H. Rochefort, M. Garcia, G. Freiss, I. J. Christensen, S. Khalaf, F. Paolucci, B. Pau, R. B. Rasmussen, and C. Rose.** 1989. Association between high concentration of Mr 52,000 cathepsin D and poor prognosis in primary human breast cancer. Cancer Res. 49:6008–6014.
76. **Wakeling, A. E.** 1991. Steroidal pure antiestrogens, p. 239–257. *In* M. E. Lippman and R. B. Dickson (ed.), Regulatory mechanisms in breast cancer. Kluwer, Boston.
77. **Wang, X., T. R. Narasimhan, V. Morrison, and S. Safe.** 1991. *In situ* and *in vitro* photoaffinity labeling of the nuclear aryl hydrocarbon (Ah) receptor from transformed rodent and human cell lines. Arch. Biochem. Biophys. 287:186–194.
78. **Wang, X., J. S. Thomsen, M. Santostefano, R. Rosengren, S. Safe, and G. H. Perdew.** Comparative properties of the nuclear Ah receptor complex from several human cell lines. Eur. J. Pharmacol., in press.
79. **Westley, B., F. E. B. May, A. M. C. Brown, A. Krust, P. Chambon, M. E. Lippman, and H. Rochefort.** 1984. Effects of antiestrogens on the estrogen regulated pS2 RNA, 51 and 160 K proteins in MCF-7 and two tamoxifen-resistant sublines. J. Biol. Chem. 259:10030–10035.
80. **Westley, B. R., F. Holzel, and F. E. B. May.** 1989. Effects of oestrogen and the antioestrogens tamoxifen and LY117018 on four oestrogen-regulated RNAs in the EFM-19 breast cancer cell line. J. Steroid Biochem. 32:365–372.
81. **Westley, B. R., and F. E. B. May.** 1987. Oestrogen regulates cathepsin D mRNA levels in oestrogen responsive human breast cancer cells. Nucleic Acids Res. 15:3773–3780.
82. **Whitlock, J. P., Jr.** 1993. Mechanistic aspects of dioxin action. Chem. Res. Toxicol. 6:754–763.
83. **Whitlock, J. P., Jr., M. S. Denison, L. K. Durrin, J. M. Fisher, D. R. Galeazzi, and P. B. C. Jones.** 1989. Regulation of cytochrome P_1-450 gene expression in mouse hepatoma cells by 2,3,7,8-tetrachlorodibenzo-*p*-dioxin. Drug Metab. Rev. 20:839–846.
84. **Wu-Peng, X. S., T. E. Pugliese, H. W. Dickerson, and B. T. Pentecost.** 1992. Delineation of sites mediating estrogen regulation of the rat creatine kinase B gene. Mol. Endocrinol. 6:231–240.
84a. **Zacharewski, T.** Personal communication.
85. **Zacharewski, T., K. Bondy, P. McDonell, and Z. F. Wu.** 1994. Antiestrogenic effects of 2,3,7,8-tetrachlorodibenzo-*p*-dioxin on 17β-estradiol-induced pS2 expression. Cancer Res. 54:2707–2713.

[CANCER RESEARCH 62, 4316–4324, August 1, 2002]

Identification of Small Molecule Inhibitors of Hypoxia-inducible Factor 1 Transcriptional Activation Pathway[1]

Annamaria Rapisarda,[2] Badarch Uranchimeg,[2] Dominic A. Scudiero, Mike Selby, Edward A. Sausville, Robert H. Shoemaker, and Giovanni Melillo[3]

Developmental Therapeutics Program-Tumor Hypoxia Laboratory [A. R., B. U., G. M.], Science Applications International Corporation-Frederick, Inc. [D. A. S., M. S.], and Developmental Therapeutics Program, National Cancer Institute at Frederick [E. A. S., R. H. S.], Frederick, Maryland 21702-1201

ABSTRACT

Hypoxia-inducible factor 1 (HIF-1) is a master regulator of the transcriptional response to oxygen deprivation. HIF-1 has been implicated in the regulation of genes involved in angiogenesis [*e.g.*, vascular endothelial growth factor (VEGF) and inducible nitric oxide synthase] and anaerobic metabolism (*e.g.*, glycolytic enzymes). HIF-1 is essential for angiogenesis and is associated with tumor progression. In addition, overexpression of HIF-1α has been demonstrated in many common human cancers. Therefore, HIF-1 is an attractive molecular target for development of novel cancer therapeutics. We have developed a cell-based high-throughput screen for the identification of small molecule inhibitors of the HIF-1 pathway. We have genetically engineered U251 human glioma cells to stably express a recombinant vector in which the luciferase reporter gene is under control of three copies of a canonical hypoxia-responsive element (U251-HRE). U251-HRE cells consistently expressed luciferase in a hypoxia- and HIF-1-dependent fashion. We now report the results of a pilot screen of the National Cancer Institute "Diversity Set," a collection of approximately 2000 compounds selected to represent the greater chemical diversity of the National Cancer Institute chemical repository. We found four compounds that specifically inhibited HIF-1-dependent induction of luciferase but not luciferase expression driven by a constitutive promoter. In addition, these compounds inhibited hypoxic induction of VEGF mRNA and protein expression in U251 cells. Interestingly, three compounds are closely related camptothecin analogues and topoisomerase (Topo)-I inhibitors. We show that concomitant with HIF-1 and VEGF inhibition, the activity of the Topo-I inhibitors tested is associated with induction of cyclooxygenase 2 mRNA expression. The luciferase-based high-throughput screen is a feasible tool for the identification of small molecule inhibitors of HIF-1 transcriptional activation. In addition, our results suggest that altered Topo-I function may be associated with repression of HIF-1-dependent induction of gene expression.

INTRODUCTION

Hypoxia, a decrease in O_2 levels, triggers adaptive responses in solid tumors that include induction of angiogenesis and a switch to anaerobic metabolism (1).

HIF-1[4] is a basic helix-loop-helix Per-Arnt-Sim transcription factor composed of two subunits, HIF-1α and HIF-1β (2). Two other homologues of the α subunit have been cloned (HIF-2α or EPAS-1 and HIF-3α), but there appears to be little redundancy in the hypoxic response. HIF-1β, also known as aryl hydrocarbon receptor nuclear translocator, is constitutively present in normoxic cells. In contrast, HIF-1α levels are primarily dependent on the intracellular oxygen concentration (3). Under nonhypoxic conditions, HIF-1α protein is rapidly and continuously degraded by ubiquitination and proteosomal degradation. Degradation of HIF-1α is dependent on binding with Von Hippel-Lindau and hydroxylation of Pro-564 via an enzymatic process that requires O_2 and iron (4, 5). However, under hypoxic conditions, HIF-1α protein accumulates and translocates to the nucleus, where it forms an active complex with HIF-1β and activates transcription of target genes by binding to the DNA consensus sequence 5′-RCGTG-3′. Besides physiological hypoxia, genetic abnormalities frequently detected in human cancers, including loss of function mutations (*i.e.*, Von Hippel-Lindau, p53, and PTEN), are associated with induction of HIF-1α activity and expression of HIF-1-inducible genes including but not limited to VEGF production (6–9).

HIF-1α plays a critical role in embryonic development. Indeed, genetic deletion of the HIF-1α subunit in mouse embryos resulted in developmental arrest and vascular abnormalities with embryonic lethality by embryon day 11 (10–12). HIF-1 is also essential for angiogenesis and tumor progression "*in vivo*," as indicated by experiments in which tumor xenografts of HIF-1β-deficient hepatoma cells (13), HIF-1α-deficient H-ras-transformed cell lines (14), or embryonic stem cells from HIF-1$\alpha^{-/-}$ mice (11) showed decreased growth rate and vascularization relative to wild-type cells. More importantly, overexpression of HIF-1α protein has been demonstrated in many common human cancers (15) including prostate and breast cancer, in which HIF-1α levels were associated with increased vascularity and tumor progression (16). Finally, disruption of HIF-1α transcriptional activity, using a peptide that interferes with the interaction between HIF-1α and the coactivator p300/CREB-binding protein, has shown therapeutic activity in xenograft models of colon carcinoma and breast cancer (17), providing "proof of principle" that HIF-1 is a promising molecular target for development of cancer therapeutics.

We have developed a cell-based HTS to identify small molecule inhibitors of the HIF-1 pathway, which may have antiangiogenic and anticancer activities. U251 human glioma cells were genetically engineered to stably express a recombinant vector in which the luciferase reporter gene is under control of three copies of a canonical HRE. We now report the results of a pilot HTS of the NCI "Diversity Set," a collection of approximately 2000 compounds generated to maximally represent the three-dimensional chemical diversity in the whole NCI library (18). We identified four compounds that specifically inhibited luciferase expression driven by a HIF-1-inducible promoter but not by a constitutively active promoter. In addition, these compounds also inhibited in a dose-dependent fashion hypoxic induction of VEGF mRNA and protein expression in U251 cells. Interestingly, three compounds are closely related CPT analogues and Topo-I inhibitors (NSC-609699, NSC-606985, and NSC-639174).

In conclusion, we have developed a molecular targeted HTS that coherently identifies small molecule inhibitors of HIF-1 transcriptional activity and VEGF expression. Screening of larger chemical

Received 1/28/02; accepted 6/18/02.

The costs of publication of this article were defrayed in part by the payment of page charges. This article must therefore be hereby marked *advertisement* in accordance with 18 U.S.C. Section 1734 solely to indicate this fact.

[1] Funded in whole or in part with federal funds from the National Cancer Institute, NIH, under Contract NO1-CO-56000.

[2] A. R. and B. U. contributed equally to this work.

[3] To whom requests for reprints should be addressed, at DTP-Tumor Hypoxia Laboratory, Building 432, Room 218, National Cancer Institute at Frederick, Frederick, MD 21702. Phone: (301) 846-5050; Fax: (301) 846-6081; E-mail: melillo@dtpax2.ncifcrf.gov.

[4] The abbreviations used are: HIF, hypoxia-inducible factor; HRE, hypoxia-responsive element; VEGF, vascular endothelial growth factor; COX-2, cyclooxygenase 2; GLUT-3, glucose transporter type 3; HTS, high-throughput screen; PTEN, phosphatase and tensin homologue; DFX, desferrioxamine; SRB, sulforhodamine B; SI, specificity index; Topo, topoisomerase; CPT, camptothecin; NCI, National Cancer Institute; ActD, actinomycin D; TK, thymidine kinase; RT-PCR, reverse transcription-PCR; NF-κB, nuclear factor κB.

libraries may lead to the identification of active compounds that could find interesting applications in anticancer treatment.

MATERIALS AND METHODS

Cell Lines and Reagents. We routinely maintained U251 human glioma cells in RPMI 1640 (Whittacker Bioproducts, Walkersville, MD) supplemented with 5% heat-inactivated fetal bovine serum (Whittacker Bioproducts), penicillin (50 IU/ml), streptomycin (50 μg/ml) and 2 mM glutamine (all purchased from Invitrogen-Life Technologies, Inc., Carlsbad, CA). Cells were maintained at 37°C in a humidified incubator containing 21% O_2, 5% CO_2 in air (referred to as normoxic conditions). Hypoxia treatment was performed by placing cells in a modular incubator chamber (Billupus-Rothemberg Inc., Del Mar, CA) and then flushing with a mixture of 1% O_2, 5% CO_2, and 94% nitrogen for 20 min. The chamber was then placed at 37°C. DFX was purchased from Sigma (St. Louis, MO), and ActD was purchased from Calbiochem (La Jolla, CA). Drugs from the NCI Training and Diversity Set (described elsewhere[5]) were initially dissolved in DMSO (Sigma) and diluted into complete medium for assay.

Plasmids. We generated pGL2-TK promoter plasmid by replacing the SV40 promoter of pGL2 promoter (Promega) with the herpes simplex virus TK promoter fragment (from −105 to +51).

The pGL2-TK-HRE plasmid was generated by subcloning three copies of the HRE (5′-GTGACTACGTGCTGCCTAG-3′) from the inducible nitric oxide synthase promoter into the pGL2-TK promoter vector (19). Plasmids were sequenced at the Molecular Technology Laboratory, Science Applications International Corporation-Frederick, Inc.

pGL3-control (Promega) contains the firefly luciferase coding sequence under control of the SV40 promoter and enhancer sequences.

Plasmid p7, containing the VEGF 5′-flanking sequence (−1005 to +306) upstream of the luciferase reporter gene, and p11WT, encompassing the HIF-1-binding site of VEGF promoter at position −985 and −939, were generous gifts from Dr. Gregg Semenza (20).

Stable Transfection and Engineered Cell Lines. DNA plasmids were prepared using a commercially available kit (Endofree Maxi-Prep; Qiagen, Inc., Valencia, CA). Transfections were performed using Effectene Transfection Reagents (Qiagen, Inc.) according to the manufacturer's instructions. Stably transfected cells (U251-HRE, U251-TK, U251-pGL3, U251-p7, and U251-p11) were generated by cotransfection of the specific reporter plasmid (pGL2-TK-HRE, pGL2-TK promoter, pGL3-control, VEGF-p7, or VEGF-p11WT, respectively) with an expression vector carrying the neomycin resistance gene for selection in mammalian cells (ratio, 100:1). Twenty-four h after transfection, reagents were removed, and cells were allowed to recover for 24 h before the addition of selection medium containing the antibiotic G418 at 500 μg/ml (Invitrogen-Life Technologies, Inc.). Stably transfected cells were seeded at a concentration of 1×10^4 cells/well in 96-well optiplates the day before treatment and routinely treated for 16–24 h.

Luciferase reporter assays were performed in 96-well optiplates (Packard Instrument, Inc., Meriden, CT) using Bright Glo luciferase assay reagents (Promega, Inc., Madison, WI).

Nuclear Extract Preparation and Immunoblotting (Western Blot). Cells were collected and washed twice with ice-cold Dulbecco's PBS 1× (PBS) and pelleted by centrifugation at 1,200 rpm. The cell pellet was subsequently washed once in a hypotonic buffer [10 mM Tris-HCl (pH 7.5), 1.5 mM $MgCl_2$, 10 mM KCl, 2 mM DTT, 1 mM Pefabloc, 2 mM sodium vanadate, 4 μg/ml pepstatin, 4 μg/ml leupeptin, and 4 μg/ml aprotinin], resuspended in the same buffer, and incubated for 10 min on ice. The cell suspension was homogenized with 18–20 strokes in a glass Dounce homogenizer. The nuclear pellet was obtained after centrifugation at 1,000 × *g* at 4°C for 10 min and resuspended in a hypertonic buffer [20 mM Tris-HCl (pH 7.5), 1.5 mM $MgCl_2$, 0.42 M KCl, 20% glycerol, 2 mM DTT, 1 mM Pefabloc, 2 mM sodium vanadate, 4 μg/ml pepstatin, 4 μg/ml leupeptin, and 4 μg/ml aprotinin] to obtain nuclear extracts. The nuclear suspension was rotated at 4°C for 30 min, and nuclear debris were pelleted by centrifugation at 15,000 × *g* for 30 min at 4°C.

Typically, 50 μg of protein were separated on an 8% Tris-glycine gel (Invitrogen Corp., Carlsbad, CA) and electroblotted on an Immobilon-P membrane (Invitrogen Corp.). Membranes were blocked for 1 h at room temperature with blocking buffer A (1× PBS, 0.1% Tween 20, and 4% BSA) to detect HIF-1α and blocked with blocking buffer B (1× PBS, 0.1% Tween 20, and 5% nonfat dry milk) to detect HIF-1β before incubation with primary antibodies (1 h at room temperature) in dilution buffer (1× PBS, 0.1% Tween 20, and 0.4% BSA). Monoclonal anti-HIF-1α (clone H1α67) and monoclonal anti-HIF-1β (clone H1B234) antibodies were purchased from Novus Biologicals (Littleton, CO). HIF-1α was detected using a 1:1000 dilution of the specific antibody, whereas HIF-1β antibody was diluted 1:1500. After washing three times in washing buffer (1× PBS and 0.1% Tween 20), membranes were incubated for 30 min at room temperature with a peroxidase-conjugated sheep antimouse antibody (diluted 1:20000 in dilution buffer) for both HIF-1α and HIF-1β (Amersham Pharmacia Biotech, Inc., Piscataway, NJ). Membranes were then washed three times in washing buffer, and chemiluminescence detection was performed using an enhanced chemiluminescence kit according to the manufacturer's protocol (Amersham Pharmacia Biotech, Inc.).

Electrophoretic Mobility Shift Assay. Nuclear extracts, prepared as described previously, were dialyzed against one change of dialysis buffer [25 mM Tris-HCl (pH 7.5), 0.2 mM EDTA, 0.1 M KCl, 20% glycerol, 1 mM DTT, 0.2 mM Pefabloc, and 0.5 mM sodium vanadate]. The double-stranded oligonucleotide AB.2 (5′-GTGCTACGTGCTGCCTAG-3′) encompassing the HIF-1 binding site was labeled with [^{32}P]dCTP using the Klenow enzyme (Invitrogen-Life Technologies, Inc.). To perform the binding reaction, 5 μg of nuclear protein were incubated on ice in binding buffer [25 mM Tris-HCl (pH 7.5), 0.2 mM EDTA, 0.1 M KCl, 20% glycerol, and 0.4 μg of denatured calf thymus DNA] in the presence or absence of antibodies for HIF-1α for 30 min. Probe (1×10^4 cpm) was added, and the samples were incubated for an additional 20 min on ice. Samples were subjected to a 5% nondenaturing polyacrylamide gel, and electrophoresis was performed at 180 V in 0.3× Tris-borate EDTA at 4°C. Gel was allowed to dry using HydroTech gel drying system (Bio-Rad Laboratories, Hercules, CA) before being autoradiographed using Kodak XAR-5 film and intensifying screens at −80°C.

HTS Assay. U251-HRE cells were inoculated into 384 well white flat-bottomed plates (Costar catalogue number 3704) at 3000 cells/well with a Beckman Biomek 2000 Laboratory Automation Workstation in a volume of 25 μl and incubated for 24 h at 37°C, 5% CO_2, and ambient O_2. Experimental agents at the appropriate concentrations were added in a volume of 25 μl using the Biomek 2000, and after a 20-h incubation in a hypoxia chamber (Billups Rothenberg, MIC 101) at 37°C, 5% CO_2, and 1% O_2, the plates were removed and incubated at room temperature, 5% CO_2, and ambient O_2 for 1.5 h. Forty μl of Bright Glo luciferase reagent (Promega catalogue number E26500) were added with the Biomek 2000, and after 3 min, luminescence was measured using a Tecan Ultra Multifunction Plate Reader in luminescence mode. Appropriate control cells were treated identically, except that they were treated at 37°C, 5% CO_2, and ambient O_2. Compound toxicity was assayed using the SRB assay as described previously in detail (21).

Real-time PCR. Total RNA from U251 cells was obtained using RNA Mini Kit (Qiagen, Inc.). One μg of total RNA was used to perform RT-PCR using RT-PCR kit (PE Biosystems, Foster City, CA). The conditions used for RT-PCR were as follows: 10 min at 25°C, 30 min at 48°C, and 5 min at 95°C. To measure human VEGF, COX-2, GLUT-3, and aldolase expression, real-time PCR was performed using an ABI-Prism 7700 Sequence Detector (Applied Biosystems, Foster City, CA). Typically 5 ng of reverse-transcribed cDNA per sample were used to perform real-time PCR in triplicate samples. Real-time PCR cycles started with 2 min at 50°C, 10 min at 95°C, and then 40 cycles of 15 s at 95°C and 1 min at 60°C. Primers and specific probes were obtained from Applied Biosystems. The following primers and probes were used: human VEGF forward, 5′-TACCTCCACCATGCCAAGTG-3′; human VEGF reverse, 5′-ATGATTCTGCCCTCCTCCTTC-3′; probe, 5′-FAM-TCCCAGGCTGCACCCATGGC-TAMRA-3′; human COX-2 forward, 5′-GAATCATTCACCAGGCAAATTG-3′; human COX-2 reverse, 5′-TCTGTACTGCGGGTGGAACA-3′; probe, 5′-FAM-TGGCAGGGTTGCTGGTGGTAGGA-TAMRA-3′; human GLUT-3 forward, 5′-CGTGGCAGGACTTTTGAGGAT-3′; human GLUT-3 reverse, 5′-AGCAGGCTCGATGCTGTTCAT-3′; human aldolase forward, 5′-GCGCTGTGTGCTGAAAATCAG-3′; and human aldolase reverse, 5′-CCACAATAGGCACAATGCCATT-3′. Detection of 18S rRNA, used as internal control, was preformed using premixed reagents from Applied Biosystems. Detection of VEGF, COX-2, and 18S rRNA was performed using TaqMan Universal PCR Master Mix (Applied

[5] http://dtp.nci.nih.gov.

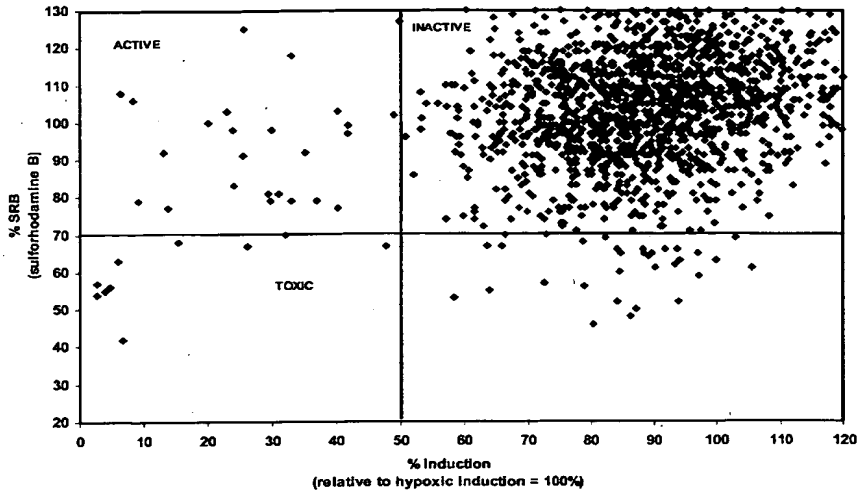

Fig. 1. Results of the diversity set HTS. U251-HRE cells were inoculated into 384-well white flat-bottomed plates at 3000 cells/well in a volume of 25 μl and incubated for 24 h at 37°C, 5% CO_2, and ambient O_2. Experimental agents (1 μM) were added in a volume of 25 μl. After a 20-h incubation in the hypoxia chamber at 37°C, 5% CO_2, and 1% O_2, the plates were removed and incubated at room temperature and ambient O_2 for 1.5 h before luminescence was measured. Compound toxicity was assayed using the SRB assay. Data from the HTS are plotted as percentage induction of luciferase expression (relative to hypoxia alone, equal to 100%) on the *X* axis and percentage toxicity (relative to untreated cells, equal to 100%) on the *Y* axis for each individual compound.

Biosystems), whereas GLUT-3 and aldolase detection was performed using Sybr Green PCR Master Mix (Applied Biosystems).

Relative quantitation values were expressed as follows: $2^{(\Delta Ctr-\Delta Ctt)}$, where *C* is the value measured in each well, *Ct* is the mean of the replicate wells run for each sample, ΔCt is the difference between the mean *Ct* values of the samples in the target wells and those of the endogenous control for the same wells (18S values), $\Delta Ctr-\Delta Ctt$ represents the difference between ΔCt of the reference sample (medium) and ΔCt of the tested samples (treatments). Values are expressed as fold increases relative to the reference sample (medium).

ELISA. Supernatants were collected from U251 cells after 24 h of incubation under the indicated conditions. Total levels of VEGF protein were measured at the Lymphokine Testing Laboratory, Science Applications International Corporation-Frederick, Inc., NCI (Frederick, MD) using human VEGF DuoSet (R&D Systems, Minneapolis, MN).

RESULTS

Development of a HTS Targeting HIF-1 Transcriptional Activity. To engineer human cancer cells to express the luciferase reporter gene under control of a HIF-1-inducible promoter, we cotransfected pGL2-TK-HRE containing three copies of a canonical HRE with a vector containing the neomycin gene for selection in mammalian cells. Surprisingly, we found that hypoxic inducibility of luciferase expression was greatly diminished or totally abrogated in many cell lines upon stable transfection of pGL2-TK-HRE (MCF-7, PC-3, H4-60, OVCAR-3, DU145, A549, MDA-MB-435, and HCT-116) compared with the levels of induction observed in transient transfection experiments (data not shown). In contrast, hypoxic induction of luciferase was largely preserved in U251-HRE cells. In fact, U251-HRE cells expressed low but detectable levels of luciferase in normoxic conditions but expressed significantly higher levels (15 ± 3.1-fold above normoxic control in 10 independent experiments) in cells cultured under hypoxic conditions. DFX also increased luciferase expression to levels comparable with those induced by hypoxia (20 ± 2.8-fold above normoxic control in 10 independent experiments; data not shown).

To identify small molecule inhibitors of HIF-1 transcriptional activity, we developed a HTS using U251-HRE cells. Initial characterization of the assay was achieved by testing the NCI Training Set, a collection of approximately 200 compounds representative of the major mechanistic classes of standard anticancer drugs as well as a variety of specific inhibitors of enzymes or signaling pathways. Results obtained from two independent experiments showed that there was a very high correlation coefficient (0.938; $R^2 = 0.88$), suggesting that results of the HTS were consistent and reproducible. In addition, a statistical parameter developed to evaluate and validate HTS assays (Z-factor) was routinely assessed for quality control purposes (22). Z statistic calculated for the 20 plates of the Diversity Set measuring the "screening window" between normoxic and hypoxic cells was 0.632 ± 0.076, indicative of a statistically significant separation. Based on the consistent performance of U251-HRE cells in HTS, we scaled up to screen a library of approximately 2000 compounds (NCI Diversity Set), which represents a collection of diverse chemical structures available at NCI.

U251-HRE cells were cultured in normoxic or hypoxic conditions for 24 h in the presence or absence of drugs from the NCI Diversity Set at a concentration of 1 μM. Toxicity and inhibition of cell growth were routinely assessed in a parallel SRB assay. In a primary screen, 35 compounds inhibited hypoxic induction of luciferase expression in U251-HRE cells by a factor of ≥50%; 26 of them had little or no toxicity or cell growth inhibition (≤30%) in the SRB assay (Fig. 1). Additional experiments were then aimed at confirming the results of the primary screen and identifying the EC_{50} (the dose at which there was 50% inhibition of hypoxic induction of luciferase) of the 26 positive nontoxic compounds.

Parallel experiments were performed to exclude compounds that inhibited luciferase expression in a nonspecific and/or HIF-1-independent fashion. To this purpose, we developed an engineered cell line (U251-pGL3) in which the luciferase reporter gene is under the control of a constitutively active promoter. U251-pGL3 cells expressed high basal levels of luciferase in normoxic conditions and slightly lower levels in hypoxic conditions (data not shown). We defined the EC_{50} of the 26 compounds identified in the primary screen using U251-HRE and U251-pGL3 cell lines and calculated a SI, obtained by dividing the EC_{50} in U251-pGL3 by the EC_{50} in U251-HRE, which provides an indication of relative specificity toward inhibition of HIF-1-dependent transcription. As shown in Fig. 2, seven compounds had a SI ≥ 10 (chosen as arbitrary threshold), indicating that they had minimal or no activity on the constitutive expression of luciferase in the U251-pGL3 control cell line. Similar results were obtained using a control cell line engineered to express luciferase under control of the minimal TK promoter (U251-TK; data not shown).

In conclusion, 7 compounds out of approximately 2000 compounds

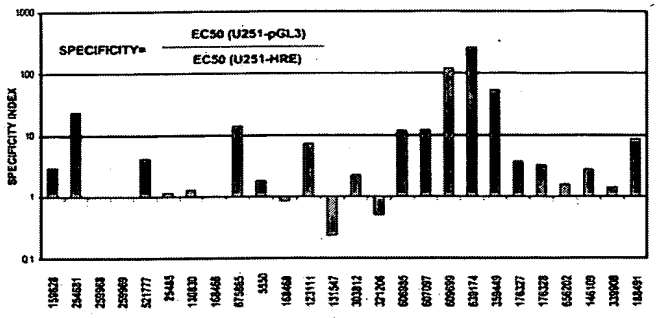

Fig. 2. Summary of the SI of 26 compounds identified in the primary HIF-1 HTS. U251-HRE cells were treated as described in Fig. 1 in the presence of an increasing concentration of the indicated compounds under normoxic or hypoxic conditions. U251-pGL3 cells were treated identically, except that they were treated at 37°C, 5% CO_2, and ambient O_2. EC_{50}s were calculated for each compound, and a SI was determined by dividing EC_{50} U251-pGL3/EC_{50} U251-HRE. Compound toxicity was assayed using the SRB assay.

that compose the NCI Diversity Set preferentially inhibit luciferase expression driven by HIF-1-inducible promoters.

The HIF-1-targeted HTS Coherently Identifies Molecules That Inhibit HIF-1 Transcriptional Activity and VEGF Expression. To test whether the compounds identified in the HTS inhibited the endogenous activity of HIF-1, we incubated U251 cells under normoxic or hypoxic conditions for 8 h in the presence or absence of drugs (0.5 μM) and measured VEGF mRNA expression by real-time PCR. We found that hypoxia induced up to 7-fold higher levels of VEGF mRNA expression in U251 cells relative to normoxic control (Fig. 3). Moreover, hypoxia induced up to ~4-fold higher levels of VEGF protein (2450 pg/ml) above the constitutive levels expressed under normoxic conditions (570 pg/ml). Four of the seven compounds identified in the HTS inhibited hypoxic induction of VEGF mRNA expression by more than 50% relative to hypoxia alone, one showed minimal but not statistically significant inhibition (NSC-254681), and two were inactive. Consistent with these results, hypoxic induction of VEGF protein was inhibited in a similar fashion (data not shown).

Among the four compounds that inhibited hypoxic induction of VEGF mRNA expression in U251 cells, three are CPT analogues and Topo-I inhibitors (NSC-609699, NSC-606985, and NSC-639174) (23), and the remaining one is a quinocarmycin analogue, DX-52-1 (NSC-607097; Ref. 24; Fig. 4). The chemical structure of the remaining three compounds that do not have inhibitory effects on VEGF expression is also shown (Fig. 4).

In conclusion, our results suggest that the HTS coherently identifies molecules that interfere with HIF-1 transcriptional activity and with the hypoxic induction of VEGF expression.

NSC-609699 Specifically Inhibits Hypoxic Induction of VEGF Expression. Of the three CPT analogues identified in the HTS, NSC-609699 (topotecan) is the best characterized for its activities both *in vitro* and in the clinical setting. Therefore, we decided to further investigate the effects of NSC-609699 on hypoxic induction of luciferase expression in U251-HRE cells. As shown in Fig. 5, NSC-609699 inhibited hypoxic induction of luciferase by 79%, 45%, and 27% at 500, 50, and 5 nM, respectively, with an EC_{50} of 71.3 nM. In contrast, NSC-609699 only inhibited constitutive expression of luciferase by 14% in the U251-pGL3 control cell line at the highest concentration used, without reaching an EC_{50}. Parallel SRB analysis showed that NSC-609699 decreased cell viability by only 15% at the higher concentration used, under both normoxic and hypoxic conditions. NSC-609699 also inhibited DFX-dependent induction of luciferase expression in U251-HRE cells in a dose-dependent manner with an EC_{50} of 181 nM (data not shown). The other two CPT analogues identified in the HTS, NSC-606985 and NSC-639174, also inhibited hypoxic induction of luciferase expression in U251-HRE cells with an EC_{50} of 32.7 and 477 nM, respectively (data not shown).

Inhibition of Topo-I activity has been associated with modulation of gene expression and in particular with activation of the ubiquitous transcription factor NF-κB, which plays an important role in the regulation of proinflammatory and antiapoptotic genes. To establish whether NSC-609699 had a differential effect on hypoxic induction of gene expression under our experimental conditions, U251 cells were incubated under normoxic or hypoxic conditions for 8 h in the presence or absence of an increasing concentration of NSC-609699 (from 1 nM to 1 μM), and expression of VEGF mRNA and COX-2 mRNA was evaluated. COX-2 is a hypoxia-inducible proinflammatory gene whose expression is controlled, at least in part, by NF-κB. As shown above, hypoxia induced 6-fold higher levels of VEGF mRNA expression relative to normoxic conditions. NSC-609699 had no effect on accumulation of VEGF mRNA under normoxia at the concentrations tested. In contrast, NSC-609699 had a dramatic inhibitory effect on hypoxic induction of VEGF mRNA expression, with 45% inhibition at 10 nM and 78% inhibition at 1 μM (Fig. 6*A*). Additional experiments also indicated that NSC-609699 inhibits hypoxic induction of other HIF-1-dependent genes in U251 cells, including expression of GLUT-3 and aldolase mRNA by 53% and 60%, respectively (data not shown). Interestingly, we found that NSC-609699 caused a dose-dependent induction of COX-2 mRNA expression under normoxic conditions. In particular, NSC-609699 induced a 2-fold accumulation of COX-2 mRNA at 1 nM and induced up to a 21-fold increase at 1 μM. In addition, hypoxia induced COX-2 mRNA expression (6-fold above baseline), and NSC-609699 had an additive effect when combined with hypoxia, with an 18-fold increase above normoxic levels at 100 nM and up to a 25-fold increase at 1 μM (Fig. 6*B*).

These results demonstrate that NSC-609699 has a differential effect on hypoxic induction of gene expression. Under our experimental conditions, inhibition of Topo-I activity seems to be associated with down-regulation of HIF-1-dependent transcription and activation of NF-κB-dependent responses.

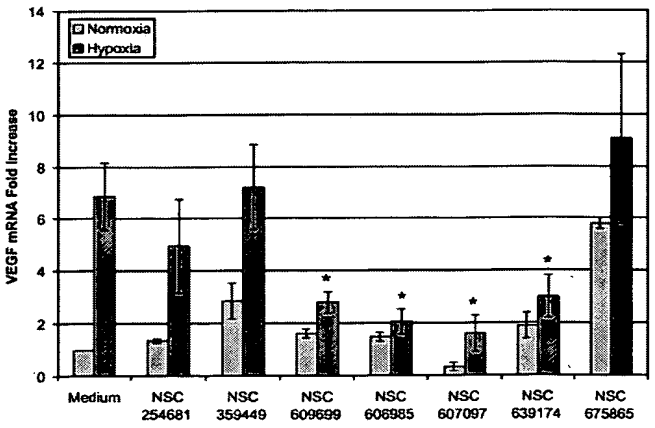

Fig. 3. Inhibition of hypoxic induction of VEGF mRNA expression in U251 cells. U251 cells (2×10^5 cells/well) were seeded in 6-well plates and incubated for 8 h under normoxic or hypoxic conditions, in the presence or absence of the indicated compounds (0.5 μM). Total RNA was harvested and tested for VEGF mRNA expression by real-time PCR, as described in "Materials and Methods." Results are expressed as fold increase relative to VEGF mRNA levels under normoxic conditions (equal to 1) in the absence of drugs. 18S rRNA was tested in parallel as internal control for input RNA. Results are the average ± SE of three independent experiments. Statistical analysis was performed using ANOVA (two-factor with replication) test ($P < 0.05$).

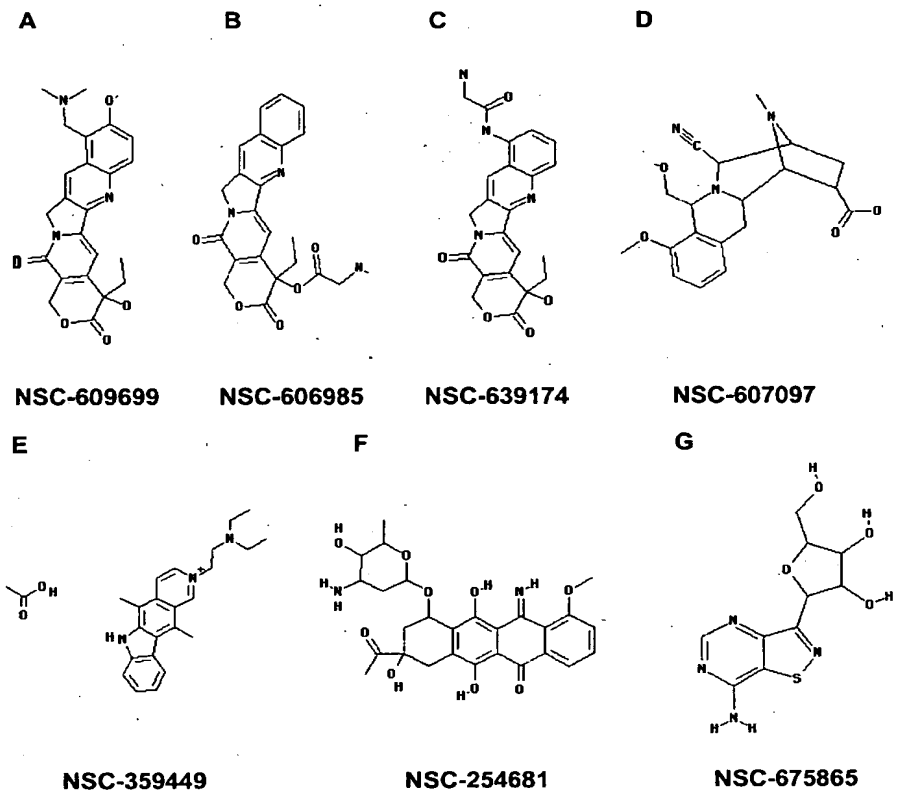

Fig. 4. Chemical structures of positive hits. *A*. NSC-609699, topotecan. *B*, NSC-606985, camptothecin, 20-ester(*S*). *C*, NSC-639174, 9-glycineamido-20(*S*)-camptothecin HCl. *D*, NSC-607097, DX-52-1, quinocarmycin analogue. *E*, NSC-359449, 2-(5,11-dimethyl-6H-2λ^5-pyrido[4,3-b]carbazol-2-yl)-*N*,*N*-diethylethanamine acetate. *F*, NSC-254681, 3-acetyl-3,5,12-trihydroxy-11-imino-10-methoxy-6-oxo-1,2,3,4,6,11-hexahydro-1-naphthacenyl 3-amino-2,3,6-trideoxy-hexopyranoside. *G*, NSC-675865, 1-(7-aminoisothiazolo[4,5-d]pyrimidin-3-yl)-1,4-anhydropentitol.

Inhibition of VEGF Expression by NSC-609699 Is Transcriptional. To assess whether NSC-609699 inhibited VEGF expression at the transcriptional level, we genetically engineered U251 cells to stably express VEGF-p7 containing the luciferase reporter gene under control of a 1.0-kb fragment of the VEGF promoter or VEGF-p11WT, in which the luciferase gene is under the control of a 50-bp oligonucleotide encompassing the active HIF-1 binding site of the VEGF promoter. U251-p7 cells expressed higher levels of luciferase when cultured under hypoxic conditions (2 ± 0.29-fold above normoxic control in five independent experiments) or in the presence of DFX (2.5 ± 0.06-fold above normoxic control; data not shown). U251-p11 cells also expressed higher levels of luciferase either under hypoxic conditions (3.6 ± 0.49-fold above normoxic control) or in the presence of DFX (4.3 ± 0.29-fold; data not shown). U251-p7 and U251-p11 cells were cultured under normoxic or hypoxic conditions in the presence or absence of increasing concentrations of compound NSC-609699. As shown in Fig. 7*A*, NSC-609699 inhibited hypoxic induction of luciferase expression in U251-p7 by 69.7%, 52.3%, and 26.8% at 500, 50, and 5 nM, respectively, with an EC_{50} of 51.2 nM. In addition, NSC-609699 inhibited hypoxia induction of luciferase expression in U251-p11 by 71%, 50.1%, and 30.2% at 500, 50, and 5 nM, respectively, with an EC_{50} of 61.6 nM. NSC-609699 also inhibited DFX-dependent induction of luciferase expression in U251-p7 and U251-p11 cells in a dose-dependent manner with an EC_{50} of 199 and 223 nM, respectively (data not shown). In contrast, experiments performed in the presence or absence of ActD (5 μg/ml) indicated that induction of COX-2 mRNA expression by NSC-609699 is due, at least in part, to transcriptional activation. In fact, NSC-609699 caused a 7-fold increase above basal levels of COX-2 mRNA expression that was completely abrogated by the addition of ActD (Fig. 7*B*).

These data are consistent with inhibition of HIF-1 transcriptional activity and demonstrate that NSC-609699 mediates transcriptional repression of VEGF mRNA expression.

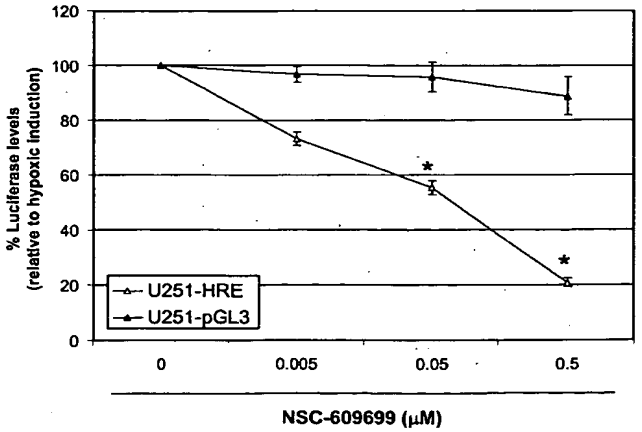

Fig. 5. NSC-609699 specifically inhibits hypoxic induction of luciferase expression in U251-HRE, but not in U251-pGL3. U251-HRE and U251-pGL3 cells (1×10^4 cells/well) were seeded in 96-well optiplates and incubated under normoxic or hypoxic conditions in the presence or absence of the indicated concentration (μM) of NSC-609699. SRB assay was performed on parallel plates to monitor toxicity. Cells were treated for 24 h and then tested for cell viability and luciferase expression. Results are expressed as percentage of luciferase levels (normalized to SRB data) induced under hypoxic conditions (equal to 100%). Data are presented as the average ± SE of six independent experiments. Statistical analysis was performed using ANOVA (two-factor with replication) test ($P < 0.01$). U251-HRE cells, △; U251-pGL3 cells, ▲.

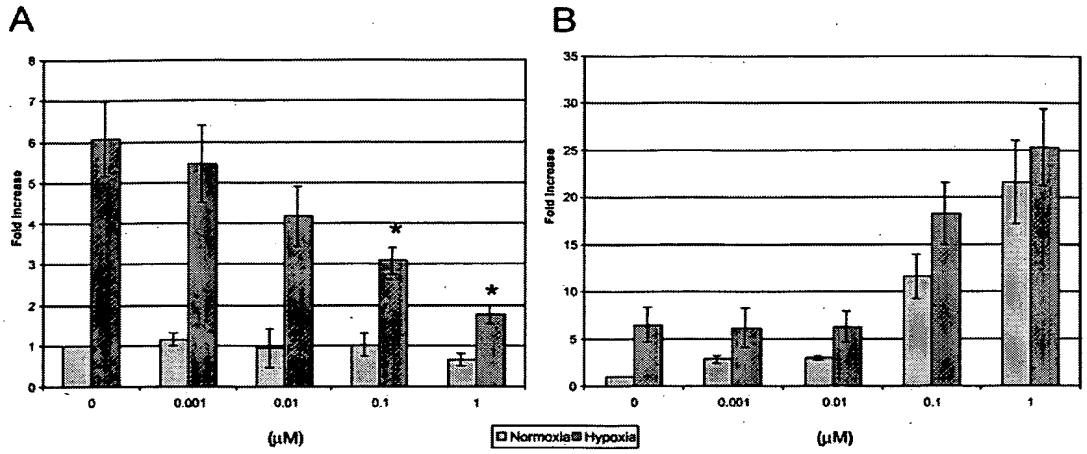

Fig. 6. NSC-609699 differentially regulates VEGF mRNA and COX-2 mRNA expression in U251 cells. U251 cells (2×10^5 cells/well) were seeded in 6-well plates and incubated under normoxic or hypoxic conditions for 8 h, in the presence or absence of increasing concentrations (μM) of NSC-609699 as indicated. Total RNA was harvested and processed for expression of VEGF and COX-2 mRNA by real-time PCR as described. 18S rRNA was tested in parallel to control for input RNA. Results are expressed as fold increase relative to levels of mRNA under normoxic conditions in the absence of drug (equal to 1). Data are presented as the average ± SE of four independent experiments. Statistical analysis was performed using ANOVA (two-factor with replication) test ($P < 0.01$).

NSC-609699 Specifically Inhibits Hypoxic Induction of HIF-1α Protein and DNA Binding Activity. To further investigate the mechanism by which NSC-609699 inhibited HIF-1-dependent transcriptional activation, U251 cells were incubated under normoxic or hypoxic conditions in the presence or absence of NSC-609699 (0.1 μM), and protein levels of HIF-1α and HIF-1β were measured by Western blot. As shown in Fig. 8*A*, we found that U251 cells express low but detectable basal levels of HIF-1α protein at 6 h and slightly higher levels at 24 h, which were substantially increased (up to 6-fold) by incubation under hypoxic conditions at both time points. NSC-609699 decreased the basal levels of HIF-1α protein under normoxic conditions and caused significant inhibition of hypoxic-dependent accumulation of HIF-1α protein by approximately 70% at 6 h and complete abrogation at 24 h. In contrast, HIF-1β was constitutively expressed under nonhypoxic conditions, and its levels were not changed by incubation under hypoxia or by addition of NSC-609699.

In parallel experiments, we examined the effects of NSC-609699 on hypoxic induction of DNA binding activity to an oligonucleotide encompassing a canonical HIF-1 binding site. Nuclear extracts from U251 cells cultured under normoxic conditions have a constitutive binding activity that appears as a doublet (Fig. 8*B*, *lanes 1* and *5*, band C) and a complex of slower mobility (band I) more appreciable at 24 h. Hypoxia increased the appearance of the inducible complex at 6 and 24 h (band I, Fig. 8*B*, *Lanes 3* and *7*). Both binding activities were competed for by an excess of unlabeled specific probe, and the inducible complex was entirely supershifted by the addition of a specific anti-HIF-1α antibody, but not by the addition of an isotype-matched irrelevant antibody (data not shown). NSC-609699 did not affect the constitutive binding activity but significantly decreased at 6 h (Fig. 8*B*, *Lane 4*) and completely abrogated at 24 h (Fig. 8*B*, *Lane 8*) the appearance of the hypoxia-inducible DNA binding complex. Direct addition of up to 1 μM NSC-609699 in the binding reaction did not affect the hypoxia-inducible complex (data not shown), suggesting that NSC-609699 does not directly interfere with the formation of protein-DNA complex.

These results indicate that NSC-609699-dependent inhibition of HIF-1 transcriptional activation is due, at least in part, to a down-regulation of hypoxia-dependent accumulation of HIF-1α protein.

DISCUSSION

HIF-1 is an attractive molecular target for development of novel cancer therapeutics. To identify small molecule inhibitors of HIF-1 transcriptional activation, we have developed a HTS using engineered cell lines that express the luciferase reporter gene in a HIF-1-inducible fashion. Our results using U251-HRE cells to screen the NCI Diversity Set indicate a coherent identification of molecules that inhibit HIF-1 activity and VEGF expression.

HIF-1 activates transcription of target genes by binding to a HRE that contains the HIF-1 core DNA binding site 5′-RCGTG-3′. We have previously demonstrated that a 19-bp element from the inducible nitric oxide synthase promoter containing a canonical HIF-1 binding site (5′-TACGTG-3′) mediates hypoxic and DFX inducibility upon transient transfection in mammalian cells (19, 25). Previous experiments also indicated that a 3-bp mutation of the HIF-1 binding site completely abrogated hypoxic and HIF-1 inducibility of a reporter gene and DNA binding activity (19). We have exploited these characteristics of the HRE to generate engineered human cancer cell lines expressing the luciferase reporter gene in a HIF-1-inducible fashion. Most cell lines lost hypoxic inducibility upon stable transfection of the luciferase reporter vector, despite efforts to identify high-inducible clones by limiting dilution. In contrast, U251-HRE cells express high levels of luciferase consistently and reproducibly upon incubation under hypoxic conditions. Experiments shown in this study were performed with "bulk" transfected U251-HRE cells, which eliminates concerns regarding clonal variability of expression and drug sensitivity. Interestingly, we have tested U251-HRE cells routinely for up to 6 months in culture, and we have observed that hypoxic inducibility was largely preserved, although basal levels of luciferase expression were variable and decreased with higher number of passages in culture (data not shown).

U251 cells have a complex genetic background that may have profound influences on the HIF-1 pathway. In particular, U251 have a mutation of the PTEN tumor suppressor gene (26) and consequent activation of the phosphatidylinositol 3′-kinase/Akt pathway, which is involved in cell survival and regulation of hypoxic responses (9, 27). Recent evidence has indicated that PTEN loss of function increases responsiveness to hypoxic induction of HIF-1 transcriptional activity

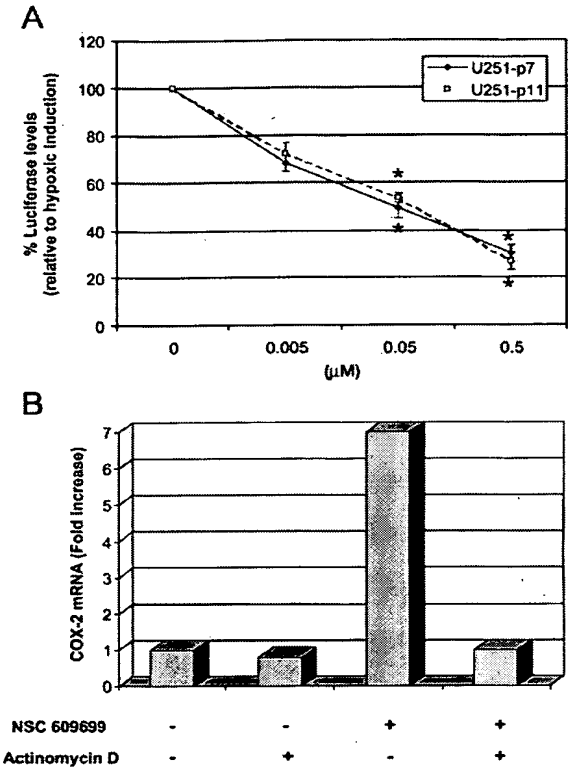

Fig. 7. NSC-609699 specifically inhibits VEGF mRNA expression at the transcriptional level. *A*, U251-p7 and U251-p11 cells (1×10^4 cells/well) were seeded in 96-well optiplates and incubated under normoxic or hypoxic conditions in the presence or absence of the indicated concentration (μM) of NSC-609699. SRB assay was performed on parallel plates to monitor toxicity. Cells were treated for 24 h and then tested for cell viability and luciferase expression. Results are expressed as percentage of luciferase levels (normalized to SRB data) induced under hypoxic conditions (equal to 100%). Data are presented as the average ± SE of four independent experiments. Statistical analysis was performed using ANOVA (two-factor with replication) test ($P < 0.01$). U251-p7 cells, ♦; U251-p11 cells, □. *B*, U251 cells (2×10^5 cells/well) were seeded in 6-well plates and incubated under normoxic conditions for 6 h, in the presence or absence of NSC-609699 (0.1 μM) and ActD (5 μg/ml). Total RNA was harvested and processed for expression of COX-2 mRNA by real-time PCR as described. 18S rRNA was tested in parallel to control for input RNA. Results are expressed as fold increase relative to levels of mRNA present under normoxic conditions in the absence of drugs (equal to 1). Data presented are representative of three independent experiment performed.

with consequent increased expression of genes involved in angiogenesis and survival (7). We found that U251 cells do express low basal levels of HIF-1α protein and DNA binding activity under normoxic conditions. However, U251 cells are very responsive to hypoxic stimulation with induction of HIF-1α protein, DNA binding activity, and luciferase reporter gene expression. Whether the particular genetic make-up makes U251-HRE cells such a suitable model for investigating HIF-1 transcriptional activation remains to be fully determined. The wide window of hypoxic inducibility makes U251-HRE a unique model for drug development applications targeting HIF-1 transcriptional activity. Conversely, these unique features of U251-HRE cells raise the possibility that our screening assay is biased toward identification of agents that act specifically in glioma cells. However, PTEN mutations are common in human cancers, and identification of compounds that act specifically in tumor cells harboring genetic abnormalities would enhance the therapeutic window of HIF-1 inhibitors for clinical development.

The NCI Diversity Set is a collection of approximately 2000 compounds representative of chemical diversity from the larger Developmental Therapeutics Program repository and contains alkylating agents, antimitotic agents, RNA and DNA antimetabolites, Topo-I and Topo-II inhibitors, and DNA-binding and -interacting agents. Because inhibition of transcription is the end point of the HIF-1-targeted HTS, we were particularly concerned of a potential bias of our screen toward preferential identification of compounds that interact with DNA. To minimize this possibility, we have developed control cell lines that express luciferase in a constitutive, HIF-1-independent fashion. In addition, we have selected compounds of interest based on lack of toxicity (as assessed by SRB assay) and high SI (relative ratio of specificity toward inhibition of HIF-1-dependent transcription). Although the compounds identified in the primary screen are known to be DNA-interacting agents when used at high concentrations (28–31), the NCI Diversity Set contains many other DNA-interacting agents that have been rejected from this screen. Therefore, the performance of DNA-interacting agents in our cell-based screen cannot be generalized, and the built-in system of controls is stringent enough to discriminate compounds that act in a nonspecific and/or HIF-1-independent fashion.

We have basically identified two different structures that interfere with HIF-1 transcriptional activity. NSC-607097, known as DX-52-1, is a more stable analogue of quinocarmycin (32). Quinocarmycin and DX-52-1 were evaluated at the NCI in the early 1990s using a disease-oriented drug screen system and were first identified as having melanoma specificity. In particular, seven of eight melanoma lines were more sensitive than average to DX-52-1. In addition, DX-52-1 demonstrated *in vivo* antitumor activity against melanoma using staged s.c. implanted human xenograft models (24). Supported by these data, DX-52-1 was developed to Phase I clinical trials, but its use was discontinued because of unexpected and unpredictable toxicities. Whether inhibition of HIF-1 transcriptional activation played a role in the performance of the drug in the clinical trial is unknown. We have found that NSC-607097 inhibits HIF-1-dependent luciferase expression with an EC_{50} of 170 nM (data not shown) but with a relatively low SI, which raises the possibility that DX-52-1 has

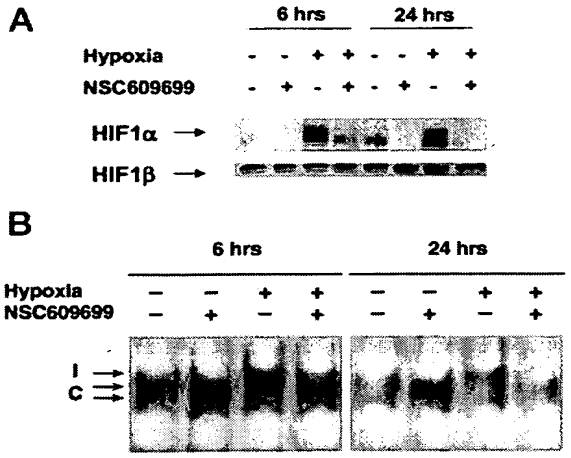

Fig. 8. NSC-609699 specifically inhibits HIF-1α protein accumulation and DNA binding activity. *A*, U251 cells were incubated under normoxic or hypoxic conditions in the presence or absence of NSC-609699 (0.1 μM) for 6 and 24 h, and then nuclear extracts were prepared as described in "Materials and Methods." Fifty μg of protein were separated on an 8% Tris-glycine gel. Specific monoclonal antibodies for detection of HIF-1α and HIF-1β were used as described. Results shown are from one representative experiment of four performed. *B*, U251 cells were cultured under normoxic or hypoxic conditions as described in *A*) for 6 and 24 h, and then nuclear extracts were prepared as described. Electrophoretic mobility shift assay was performed with radiolabeled AB.2 probe as described. Binding activities are labeled as follows: *C*, constitutive; and *I*, inducible. Results shown are from one experiment of at least three performed.

nonspecific effects at higher concentrations and may have a narrow therapeutic window. Interestingly, results of a parallel HTS using U937 cells engineered to express luciferase under the control of a CAAT/enhancer binding protein α-responsive promoter indicated that NSC-607097 (100 nM) induced luciferase expression to levels comparable to retinoic acid, a known activator of this pathway.[6] These data suggest that NSC-607097 has a differential effect on transcription factors, which may have distinct consequences on gene expression.

The second class of compounds identified in the HTS is represented by drugs that inhibit Topo-I activity, topotecan and two CPT analogues. CPTs belong to a class of chemotherapeutic agents that stabilize the complex formed between Topo-I and DNA (33). In the presence of CPTs, Topo-I remains covalently linked to one strand of the DNA and thus leaves the DNA with a protein-linked DNA single-stranded break, which triggers cytotoxic lesions in metabolizing DNA (30, 31). Besides DNA damage, inhibition of Topo-I has been associated with activation of the NF-κB pathway (23, 34) and inhibition of angiogenesis (35, 36). We have found that inhibition of Topo-I activity by topotecan is associated, under our experimental conditions, with HIF-1 transcriptional repression and down-regulation of HIF-1-dependent gene expression, with an EC_{50} in the low nanomolar range. Inhibition of HIF-1 transcriptional activity and VEGF mRNA expression by NSC-609699 was also observed in other human cancer cell lines including MCF-7, P388, CEM, and DU145 (data not shown). Consistent with these results, topotecan also inhibited hypoxic induction of luciferase expression driven by a 1.0-kb fragment of the VEGF promoter that encompasses the HIF-1 binding site, suggesting that topotecan inhibits VEGF transcription. Concomitant with inhibition of VEGF mRNA expression, topotecan independently induced COX-2 mRNA expression and had an additive effect with hypoxia, demonstrating that it mediates a distinct pattern of gene expression. Recently, therapeutic strategies aimed at blocking NF-κB activation associated with Topo-I inhibition have been proposed to decrease NF-κB-dependent antiapoptotic effects (37). Our results raise the possibility that inhibition of COX-2 activity, which has been associated with angiogenic and tumor-promoting effects (38), may become an independent target of therapeutic strategies aimed at improving the clinical efficacy of CPT.

Topo-I inhibitors may have a profound effect on gene expression. It has recently been shown that mRNA levels for particular genes may rise or fall in response to CPT treatment (39). The response of individual genes to CPT analogues may result directly from Topo-I inhibition (such as the immobilization of Topo-I complex on the DNA and sequential DNA damage) or may arise through secondary mechanisms [such as inhibition of direct protein-protein interaction between Topo-I and other transcription factors (40) or recruitment of transcription factors through the immobilization of Topo-I on specific DNA sequences (41)]. We found that inhibition of HIF-1 activity occurs in both transiently and stably transfected cells, suggesting that this activity is independent of DNA conformation (data not shown). More importantly, our results indicate that NSC-609699 selectively inhibits accumulation of HIF-1α protein and consequently the appearance of DNA binding activity, which correlates nicely with inhibition of VEGF mRNA expression. Whether a direct inhibition of Topo-I activity is essential for inhibition of HIF-1α protein accumulation and VEGF expression is currently under investigation in our laboratory. It is conceivable, however, that inhibition of Topo-I activity may be associated with more profound effects on transcription and may not be restricted to HIF-1. In this respect, it may become difficult to discriminate the contribution of HIF-1 inhibition in the clinical setting, and this feature of topotecan or CPT analogues may not be fully exploitable in the clinical setting.

In conclusion, screening of larger chemical libraries using cancer cell lines engineered with HIF-1-inducible promoters may lead to identification of HIF-1 inhibitors that could be developed for clinical application. Accordingly, the DTP has undertaken a HIF-1-targeted HTS campaign of a 140,000-compound library available at the NCI. Although the potential contribution of HIF-1 inhibitors to cancer therapeutics is largely speculative at this time, accumulating information on the involvement of HIF-1 in cancer progression makes HIF-1 an attractive target for development of novel therapeutic strategies.

[6] D. Scudiero, M. Selby, T. Silvers, J. Laudeman, S. Clopper, J. Grams-Fowler, D. Tenen, H. Radomska, E. Sausville, and R. Shoemaker, Development of a cell-based high throughput screen for inducers of C-EBPα, manuscript in preparation.

ACKNOWLEDGMENTS

We thank Shawn Clopper, Julie Grams-Fowler, and Robert Finneyfrock for technical assistance.

REFERENCES

1. Blancher, C., and Harris, A. L. The molecular basis of the hypoxia response pathway: tumour hypoxia as a therapy target. Cancer Metastisis Rev., *17:* 187–194, 1998.
2. Semenza, G. L. Hypoxia-inducible factor 1: oxygen homeostasis and disease pathophysiology. Trends Mol. Med., *7:* 345–350, 2001.
3. Wang, G. L., Jiang, B. H., Rue, E. A., and Semenza, G. L. Hypoxia-inducible factor 1 is a basic-helix-loop-helix-PAS heterodimer regulated by cellular O_2 tension. Proc. Natl. Acad. Sci. USA, *92:* 5510–5514, 1995.
4. Ivan, M., Kondo, K., Yang, H., Kim, W., Valiando, J., Ohh, M., Salic, A., Asara, J. M., Lane, W. S., and Kaelin, W. G., Jr. HIFα targeted for VHL-mediated destruction by proline hydroxylation: implications for O_2 sensing. Science (Wash. DC), *292:* 464–468, 2001.
5. Jaakkola, P., Mole, D. R., Tian, Y. M., Wilson, M. I., Gielbert, J., Gaskell, S. J., Kriegsheim, A., Hebestreit, H. F., Mukherji, M., Schofield, C. J., Maxwell, P. H., Pugh, C. W., and Ratcliffe, P. J. Targeting of HIF-α to the von Hippel-Lindau ubiquitylation complex by O_2-regulated prolyl hydroxylation. Science (Wash. DC), *292:* 468–472, 2001.
6. Ravi, R., Mookerjee, B., Bhujwalla, Z. M., Sutter, C. H., Artemov, D., Zeng, Q., Dillehay, L. E., Madan, A., Semenza, G. L., and Bedi, A. Regulation of tumor angiogenesis by p53-induced degradation of hypoxia-inducible factor 1α. Genes Dev., *14:* 34–44, 2000.
7. Zundel, W., Schindler, C., Haas-Kogan, D., Koong, A., Kaper, F., Chen, E., Gottschalk, A. R., Ryan, H. E., Johnson, R. S., Jefferson, A. B., Stokoe, D., and Giaccia, A. J. Loss of PTEN facilitates HIF-1-mediated gene expression. Genes Dev., *14:* 391–396, 2000.
8. Maxwell, P. H., Wiesener, M. S., Chang, G. W., Clifford, S. C., Vaux, E. C., Cockman, M. E., Wykoff, C. C., Pugh, C. W., Maher, E. R., and Ratcliffe, P. J. The tumour suppressor protein VHL targets hypoxia-inducible factors for oxygen-dependent proteolysis. Nature (Lond.), *399:* 271–275, 1999.
9. Zhong, H., Chiles, K., Feldser, D., Laughner, E., Hanrahan, C., Georgescu, M. M., Simons, J. W., and Semenza, G. L. Modulation of hypoxia-inducible factor 1α expression by the epidermal growth factor/phosphatidylinositol 3-kinase/PTEN/AKT/FRAP pathway in human prostate cancer cells: implications for tumor angiogenesis and therapeutics. Cancer Res., *60:* 1541–1545, 2000.
10. Iyer, N. V., Kotch, L. E., Agani, F., Leung, S. W., Laughner, E., Wenger, R. H., Gassmann, M., Gearhart, J. D., Lawler, A. M., Yu, A. Y., and Semenza, G. L. Cellular and developmental control of O_2 homeostasis by hypoxia-inducible factor 1 α. Genes Dev., *12:* 149–162, 1998.
11. Ryan, H. E., Lo, J., and Johnson, R. S. HIF-1 α is required for solid tumor formation and embryonic vascularization. EMBO J., *17:* 3005–3015, 1998.
12. Carmeliet, P., Dor, Y., Herbert, J. M., Fukumura, D., Brusselmans, K., Dewerchin, M., Neeman, M., Bono, F., Abramovitch, R., Maxwell, P., Koch, C. J., Ratcliffe, P., Moons, L., Jain, R. K., Collen, D., Keshert, E., and Keshet, E. Role of HIF-1α in hypoxia-mediated apoptosis, cell proliferation and tumour angiogenesis. Nature (Lond.), *394:* 485–490, 1998.
13. Maxwell, P. H., Dachs, G. U., Gleadle, J. M., Nicholls, L. G., Harris, A. L., Stratford, I. J., Hankinson, O., Pugh, C. W., and Ratcliffe, P. J. Hypoxia-inducible factor-1 modulates gene expression in solid tumors and influences both angiogenesis and tumor growth. Proc. Natl. Acad. Sci. USA, *94:* 8104–8109, 1997.
14. Ryan, H. E., Poloni, M., McNulty, W., Elson, D., Gassmann, M., Arbeit, J. M., and Johnson, R. S. Hypoxia-inducible factor-1α is a positive factor in solid tumor growth. Cancer Res., *60:* 4010–4015, 2000.
15. Zhong, H., De Marzo, A. M., Laughner, E., Lim, M., Hilton, D. A., Zagzag, D., Buechler, P., Isaacs, W. B., Semenza, G. L., and Simons, J. W. Overexpression of hypoxia-inducible factor 1α in common human cancers and their metastases. Cancer Res., *59:* 5830–5835, 1999.
16. Bos, R., Zhong, H., Hanrahan, C. F., Mommers, E. C., Semenza, G. L., Pinedo, H. M., Abeloff, M. D., Simons, J. W., van Diest, P. J., and Van der Wall, E. Levels of hypoxia-inducible factor-1α during breast carcinogenesis. J. Natl. Cancer Inst. (Bethesda), *93:* 309–314, 2001.

17. Kung, A. L., Wang, S., Klco, J. M., Kaelin, W. G., and Livingston, D. M. Suppression of tumor growth through disruption of hypoxia-inducible transcription. Nat. Med., *6:* 1335–1340, 2000.
18. Shoemaker, R. H., Scudiero, D. A., Melillo, G., Currens, M. J., Monks, A. P., Rabow, A. A., Covell, D. G., and Sausville, E. A. Application of high-throughput, molecular-targeted screening to anticancer drug discovery. Curr. Top. Med. Chem., *2:* 229–246, 2002.
19. Melillo, G., Musso, T., Sica, A., Taylor, L. S., Cox, G. W., and Varesio, L. A hypoxia-responsive element mediates a novel pathway of activation of the inducible nitric oxide synthase promoter. J. Exp. Med., *182:* 1683–1693, 1995.
20. Forsythe, J. A., Jiang, B. H., Iyer, N. V., Agani, F., Leung, S. W., Koos, R. D., and Semenza, G. L. Activation of vascular endothelial growth factor gene transcription by hypoxia-inducible factor 1. Mol. Cell. Biol., *16:* 4604–4613, 1996.
21. Monks, A., Scudiero, D., Skehan, P., Shoemaker, R., Paull, K., Vistica, D., Hose, C., Langley, J., Cronise, P., and Vaigro-Wolff, A. Feasibility of a high-flux anticancer drug screen using a diverse panel of cultured human tumor cell lines. J. Natl. Cancer Inst. (Bethesda), *83:* 757–766, 1991.
22. Zhang, J. H., Chung, T. D., and Oldenburg, K. R. A simple statistical parameter for use in evaluation and validation of high throughput screening assays. J. Biomol. Screen., *4:* 67–73, 1999.
23. Piret, B., and Piette, J. Topoisomerase poisons activate the transcription factor NF-κB in ACH-2 and CEM cells. Nucleic Acids Res., *24:* 4242–4248, 1996.
24. Plowman, J., Dykes, D. J., Narayanan, V. L., Abbott, B. J., Saito, H., Hirata, T., and Grever, M. R. Efficacy of the quinocarmycins KW2152 and DX-52–1 against human melanoma lines growing in culture and in mice. Cancer Res., *55:* 862–867, 1995.
25. Melillo, G., Taylor, L. S., Brooks, A., Musso, T., Cox, G. W., and Varesio, L. Functional requirement of the hypoxia-responsive element in the activation of the inducible nitric oxide synthase promoter by the iron chelator desferrioxamine. J. Biol. Chem., *272:* 12236–12243, 1997.
26. Steck, P. A., Pershouse, M. A., Jasser, S. A., Yung, W. K., Lin, H., Ligon, A. H., Langford, L. A., Baumgard, M. L., Hattier, T., Davis, T., Frye, C., Hu, R., Swedlund, B., Teng, D. H., and Tavtigian, S. V. Identification of a candidate tumour suppressor gene, *MMAC1*, at chromosome 10q23.3 that is mutated in multiple advanced cancers. Nat. Genet., *15* : 356–362, 1997.
27. Mazure, N. M., Chen, E. Y., Laderoute, K. R., and Giaccia, A. J. Induction of vascular endothelial growth factor by hypoxia is modulated by a phosphatidylinositol 3-kinase/Akt signaling pathway in Ha-ras-transformed cells through a hypoxia inducible factor-1 transcriptional element. Blood, *90:* 3322–3331, 1997.
28. Pommier, Y., Schwartz, R. E., Kohn, K. W., and Zwelling, L. A. Formation and rejoining of deoxyribonucleic acid double-strand breaks induced in isolated cell nuclei by antineoplastic intercalating agents. Biochemistry, *23:* 3194–3201, 1984.
29. Hill, G. C., Wunz, T. P., and Remers, W. A. Computer simulation of the binding of quinocarcin to DNA. Prediction of mode of action and absolute configuration. J. Comput. Aided Mol. Des., *2:* 91–106, 1988.
30. Shao, R. G., Cao, C. X., Zhang, H., Kohn, K. W., Wold, M. S., and Pommier, Y. Replication-mediated DNA damage by camptothecin induces phosphorylation of RPA by DNA-dependent protein kinase and dissociates RPA:DNA-PK complexes. EMBO J., *18:* 1397–1406, 1999.
31. Strumberg, D., Pilon, A. A., Smith, M., Hickey, R., Malkas, L., and Pommier, Y. Conversion of topoisomerase I cleavage complexes on the leading strand of ribosomal DNA into 5′-phosphorylated DNA double-strand breaks by replication runoff. Mol. Cell. Biol., *20:* 3977–3987, 2000.
32. Saito, H., Hirata, T., Kasai, M., Fujimoto, K., Ashizawa, T., Morimoto, M., and Sato, A. Synthesis and biological evaluation of quinocarcin derivatives: thioalkyl-substituted quinones and hydroquinones. J. Med. Chem., *34:* 1959–1966, 1991.
33. Hsiang, Y. H., Hertzberg, R., Hecht, S., and Liu, L. F. Camptothecin induces protein-linked DNA breaks via mammalian DNA topoisomerase I. J. Biol. Chem., *260:* 14873–14878, 1985.
34. Huang, T. T., Wuerzberger-Davis, S. M., Seufzer, B. J., Shumway, S. D., Kurama, T., Boothman, D. A., and Miyamoto, S. NF-κB activation by camptothecin. A linkage between nuclear DNA damage and cytoplasmic signaling events. J. Biol. Chem., *275:* 9501–9509, 2000.
35. O'Leary, J. J., Shapiro, R. L., Ren, C. J., Chuang, N., Cohen, H. W., and Potmesil, M. Antiangiogenic effects of camptothecin analogues 9-amino-20(*S*)-camptothecin, topotecan, and CPT-11 studied in the mouse cornea model. Clin. Cancer Res., *5:* 181–187, 1999.
36. Clements, M. K., Jones, C. B., Cumming, M., and Daoud, S. S. Antiangiogenic potential of camptothecin and topotecan. Cancer Chemother. Pharmacol., *44:* 411–416, 1999.
37. Cusack, J. C., Jr., Liu, R., Houston, M., Abendroth, K., Elliott, P. J., Adams, J., and Baldwin, A. S., Jr. Enhanced chemosensitivity to CPT-11 with proteasome inhibitor PS-341: implications for systemic nuclear factor-κB inhibition. Cancer Res., *61:* 3535–3540, 2001.
38. Dubois, R. N. Cyclooxygenase: a target for colon cancer prevention. Aliment. Pharmacol. Ther., *14* (Suppl. 1): 64–67, 2000.
39. Collins, I., Weber, A., and Levens, D. Transcriptional consequences of topoisomerase inhibition. Mol. Cell. Biol., *21:* 8437–8451, 2001.
40. Shaiu, W. L., and Hsieh, T. S. Targeting to transcriptionally active loci by the hydrophilic N-terminal domain of *Drosophila* DNA topoisomerase I. Mol. Cell. Biol., *18:* 4358–4367, 1998.
41. Shykind, B. M., Kim, J., Stewart, L., Champoux, J. J., and Sharp, P. A. Topoisomerase I enhances TFIID-TFIIA complex assembly during activation of transcription. Genes Dev., *11:* 397–407, 1997.